International Journal of Pharmaceutical Research and Applications
Volume 9, Issue 3 May-June 2024, pp: 437-493 www.ijprajournal.com ISSN: 2456-4494

Formulation and Evaluation of Ciprofloxacin-Loaded Silver Nanoparticles with Zinc Oxide as Potent Nano-Antibiotics against Resistant Pathogenic Bacteria

Vikas Thakur
Himalayan Institute of Pharmacy and Research, Rajawala, Dehradun

Date of Submission: 01-05-2024 Date of Acceptance: 10-05-2024

ABSTRACT
In the creation ofciprofloxacin-loaded silver nanoparticles with zinc oxide as potent nano-antibiotics against resistant pathogenic bacteria. These phytochemicals were responsible for triggering an oxidation and reduction reaction during the process. The size of the NPs that were created was measured to be 35 nm on average. The effectiveness of the artificially manufactured ZnO NPs is demonstrated by the increase in plant biomass. We discovered that the incorporation of green-synthesized ZnO NPs into MO led to an increase in shoot production, plant weight, the quantity of photosynthetic pigments, and the amount of total protein present in the plant. These findings point to morpho-physiological alterations occurring in the population. Plant development was inhibited by ZnO NPs concentrations of 10 and 20 mg L-1; nevertheless, these levels stimulated the accumulation of proline and the production of antioxidant enzymes. Despite this, the plant's overall MDA production was decreased.
This research demonstrates that there was a significant improvement in the quality of the in vitro grown plant tissues when ZnO NPs were included in the growing conditions. This study lends credence to the hypothesis that green-synthesized of ciprofloxacin loaded ZnO NPs may have potential applications in a variety of fields, including the medical and agricultural sectors. However, additional research is required to achieve a complete comprehension of the chemical process by which ZnO NPs influence the development of cellular pathways and secondary metabolism.
KEYWORDS:ZNO,CIPROFLOXACIN,NANO-ANTIBIOTICS,METABOLISM,ANTI-OXIDANT.

I. INTRODUCTION

The prefix "nano," which indicates one thousand millionth of a meter (109 m), stems from the Greek word for "dwarf," expressing how very minute this measurement is. It is essential to have a solid understanding of the distinction between nanoscience and nanotechnology. The term "nanotechnology" refers to the application of the discoveries made in the field of "nanoscience," which investigates the atomic, molecule, and atomic-scale properties of many types of matter (1-100 nm)[1]. The application of these discoveries is what is known as nanotechnology. When the radius of the DNA double helix (figure 1.1). is compared to the length of the DNA molecule, it is clear to see that the DNA molecule is incredibly diminutive. Since the fifth century B.C., when the issue was first brought up by the Greeks and Democritus, there has been a heated debate among scientists regarding the nature of matter and whether it is continuous and can be infinitely divided into smaller pieces or whether it is formed of small, indivisible, and indestructible particles, which scientists today call atoms. This debate has been going on for centuries[2]. The Greeks and Democritus were the ones who first brought up this subject, and ever since then, the conversation has carried on about it. Particles that have dimensions on the nanometer scale (less than 100 nm) are referred to as nanoparticles. In recent years, these materials have come to play an increasingly important role in current medicine as, for example, contrast agents in medical imaging and carriers for the transfer of genes into specific cells[3]. These are only two examples of the many applications of these materials. Nanoparticles can be distinguished from bulk materials by a number of distinguishing properties, including their ability to react chemically, absorb energy, and move freely in biological systems[4]. Nanoparticles are also sometimes referred to by the term "zero-dimensional" nanomaterials. Because of this, it is possible to differentiate them from one-dimensional nanomaterials (such as nanowires and

International Journal of Pharmaceutical Research and Applications
Volume 9, Issue 3 May-June 2024, pp: 437-493 www.ijprajournal.com ISSN: 2456-4494

nanotubes) and two-dimensional nanomaterials (such as self-assembled monolayer films), both of which contain at least one or two dimensions that exist outside of the nanoscale[5]. The use of nanoparticles in modern medicine has a wide variety of potential uses. In certain circumstances, the use of nanoparticles makes feasible diagnostic procedures and therapeutic procedures that would not be possible otherwise[6]. Nanoparticles, on the other hand, provide significant challenges for society as well as the environment, particularly in terms of their toxicity. The primary goals of this review are to address the concerns highlighted by social critics and environmentalists, as well as to describe the significant ways in which nanoparticles have advanced modern medicine[7].

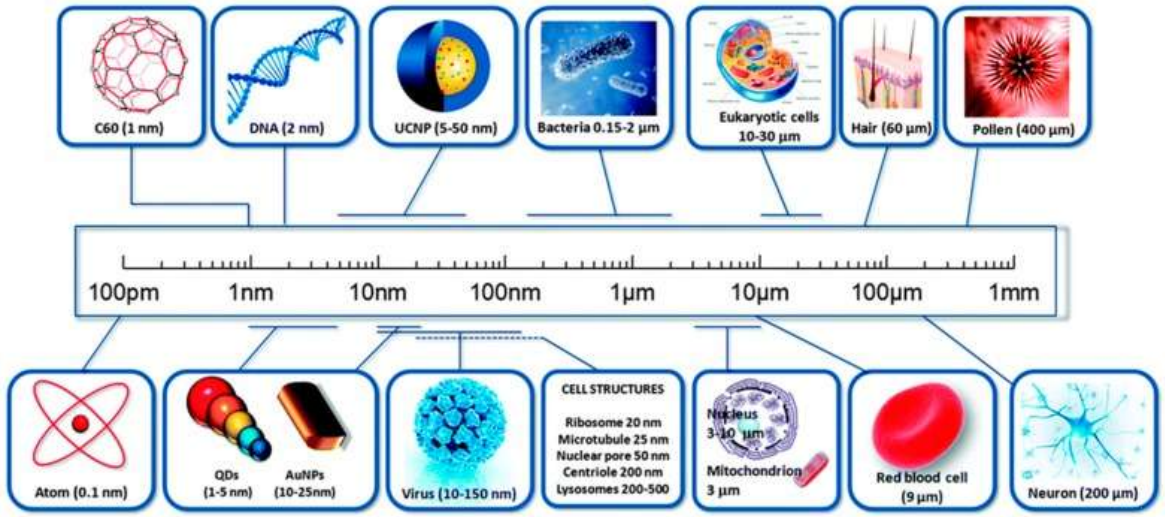

Fig: 1.1 Size of nanomaterial [2]

The field of nanotechnology is one that is on the leading edge and holds a great deal of promise for the future. To put it another way, nanotechnology is one of the most fascinating and potentially game-changing study disciplines of the twenty-first century[8]. This is due to the fact that it is currently considered to be one of the most intriguing fields in scientific research. In the field of nanotechnology, tasks like as research, measurements, manipulations, assembly, and control are all carried out at the nanoscale[9]. Nanotechnology is sometimes referred to as the practise of applying the concepts of nanoscience to real-world settings. According to the National Nanotechnology Initiative of the United States, "nanotechnology is a science, engineering, and technology conducted at the nanoscale (1 to 100 nm), where unique phenomena enable novel applications in a wide range of fields, from chemistry, physics, biology, medicine, engineering, and electronics" [10]. This definition can be found in the United States' National Nanotechnology Initiative. According to this theory, two of the prerequisites for the development of nanotechnology may already have been satisfied. The first issue is one of scale; the primary focus of nanotechnology is the modification of structures at the nanoscale scale for use in practical applications. The second issue is one of scope[11]. The second obstacle is one of creativity; for nanotechnology to be successful, it must be able to exert control over extremely small objects in ways that make advantage of distinctive characteristics that are only accessible at the nanoscale [12]. The subjects of nanoscience and nanotechnology are vastly distinct from one another, and it is essential that the distinction be made between the two. The production and manipulation of extremely small objects, as well as the development of novel tools for understanding and directing the behaviour of these objects, are all components of nanotechnology[13]. The study of ways to exert influence over the atomic and molecular levels of matter is what is known as nanoscience, which is a multidisciplinary field. The study of matter at a microscopic scale, measurement, manipulation, assembly, regulation, and fabrication are all examples of activities that fall under the purview of nanotechnology[14]. In spite of the abundance of publications that chronicle the progression of

International Journal of Pharmaceutical Research and Applications
Volume 9, Issue 3 May-June 2024, pp: 437-493 www.ijprajournal.com ISSN: 2456-4494

nanotechnology, not a single research has presented a thorough review of the area from the time it was first established until the present day[15]. For this reason, a succinct description of the most significant advancements in nanoscience and technology over the course of time is necessary for achieving a comprehensive grasp of the expansion of the subject. The achievements that have been made in nanoscience, which is the study of matter on a size ranging from one to one hundred nanometers, have prepared the way for nanotechnology to produce or improve upon things that were previously unattainable[16]. Because of recent advancements in the manipulation of structures on an atomic scale, it is now possible to create nanomaterials. Materials that possess distinctive optical, electrical, and/or magnetic properties on the nanoscale find use in a wide variety of fields, including medicine and electronics, amongst others. Nanomaterials stand out from other types of substances due to the fact that they possess very enormous surface areas in comparison to their total volumes. The physical and chemical principles that are commonly acknowledged as the basis for the design and functioning of larger-scale structures and systems are referred to as "classical laws," and the phrase "classical laws" is used to characterize those concepts. Yet, the fundamentals of quantum physics, which are in charge of regulating nanomaterials, take precedence over these rules. The study of designing and manufacturing materials and gadgets on an atomic or molecular size is what we mean when we talk about nanotechnology[17]. The numerous advancements that nanotechnology has brought to fields as diverse as medicine, telecommunications, everyday life, agriculture, and the like can be traced back to the widespread effects that nanotechnology has had on nearly every facet of modern life. These advancements include improvements in construction, safety, cleanliness, durability, and intelligence. Because of these advancements, the impact that nanotechnology has on modern life has grown[18]. There are two very different applications for nanoparticles in the things that we use on a daily basis. The addition of nanoparticles to items that currently exist has the potential to improve the functionality of those products. In order to accomplish this objective, the nanomaterials contribute a portion of their distinguishing properties to the composite objects that are generated as a result of the combination. Yet, nanomaterials such as nanocrystals and nanoparticles have the potential to be directly incorporated into the production of cutting-edge technology that is particularly efficient as a result of the one-of-a-kind characteristics that they possess. The advantages of nanoparticles have the potential to influence economic growth across almost all fields[19]. Nanomaterials have various applications and can improve a wide variety of items, including sunscreens, cosmetics, athletic equipment, tires, and electronic devices, to name just a few. The application of nanotechnology in medical research has led to significant advances in a variety of subfields, including diagnostics, imaging, and the delivery of drugs.

The combination of molecular biology with nanotechnology gave rise to the development of brand new academic subfields, such as nanobiotechnology[20]. The study of materials and structures on the nanoscale, as well as the development of such things, can be referred to as "nanotechnology," and it is characterised by the utilisation of both physical and chemical processes in the research and production processes. Due to the one-of-a-kind capabilities of nanomaterials in the areas of chemistry, electricity, optics, biology, and magnetism [21], nanotechnology has emerged as a significant field of study over the course of the past thirty years. Since it is well-established that when combined with biotechnology, nanotechnology creates a platform with tremendous potential and importance with regard to the spectrum of applications [22], there has been a lot of attention paid to nanotechnology. Since that time, nanotechnology has garnered a significant amount of interest, and one of the reasons why is because of this. This is one of the factors that contributed. Creams, cosmetics, athletic wear, fabrics, cleaning the environment, silencing genes, and medical imaging are just a few of the various applications [23]. They are also utilised in the manufacture of a variety of medical imaging modalities. This technique has a wide variety of applications, including but not limited to the following: gene suppression, gene inactivation, diagnostic kits and testing, biological sensors, dental operations, and sterilising the surfaces of medical devices. One such use is the suppression of gene expression. Because of recent developments in nanotechnology, we now have access to effective tools that make it possible to demarcate processes on a magnitude that was unthinkable only a few short years ago [24]. Only a few short years ago,

International Journal of Pharmaceutical Research and Applications
Volume 9, Issue 3 May-June 2024, pp: 437-493 www.ijprajournal.com ISSN: 2456-4494

something of this magnitude was incomprehensible.

Nanotechnology, often known as an enabling technology, focuses on things that are on the nanoscale size or smaller. On various fronts, including the material, device, and system levels, it is anticipated that nanotechnology will improve in the next years. Nanomaterials are at the forefront of development right now, both in terms of theoretical study and actual applications in the real world. A decade ago, the research of nanoparticles was initiated because the size dependency of the nanoparticles' physical and chemical properties [25] inspired the study. They have made it official and begun the initial stages of the commercial exploratory phase. 10 micrometres is the typical length of a cell that is found in a living organism. On the other hand, the components of a cell are on a scale that is sub-micron in size. Proteins, which typically have a size of only 5 nm, are even smaller than the artificial nanoparticles that are currently known to exist. We can get an idea of how nanoparticles might be utilized as extremely small probes to spy on cellular processes without causing too much disruption if we compare the diameters of the particles [26]. The necessity of understanding extremely minute biological processes is a major driving force for the development of nanotechnology.The optical and magnetic effects are the ones that are employed for biological applications the most out of the multitude of size-dependent physical properties that are available to someone interested in the practical side of nanomaterials.

This study intends to do three things: (1) offer readers a historical perspective of the use of nanomaterials to biology and medicine; (2) seek to explain the most recent breakthroughs in this field; and (3) emphasize the difficult path to commercialization. Additionally, hybrid bionanomaterials have the potential to be utilized in the production of state-of-the-art electronics, optoelectronics, and memory devices [27].

Scientists have produced nanoparticles (NPs) in order to take use of the unique properties of nanoparticles. Nanoparticles can be created from a diverse assortment of substances, such as metals, metal oxides, semiconductors, organic molecules, and inorganic chemicals, amongst others. They are able to be produced by processes that range from conventional chemical production to ecologically responsible synthesis. Nanoparticles (NPs) that are created in a laboratory present a number of challenges, the most prominent of which are their toxicity, expense, and inability to perform their intended function. Bio-inspired nanoparticles (NPs) have several advantages over traditionally created NPs, including a low level of toxicity, reduced production costs, and an easier fabrication process [28]. Conventional processes have a number of limitations, some of which are more serious than others. The cost of the raw materials, the medication waste, the potential for chemical and physical incompatibilities, the potential for clinical medicine interactions, and the potential for dose-related side effects are all potential problems.

Nanoparticles that have been designed have a lot of potential in the area of disease diagnosis and therapy that requires a high level of specificity. By cell-specific targeting, molecular transport to specific organelles, and other tactics, nanotechnology offers the ability to avoid the shortcomings of traditional delivery methods, such as biodistribution and intracellular trafficking. This could be accomplished through the use of traditional delivery methods. The National Nanotechnology Initiative (NNI) was announced in the year 2000 by the National Science and Technology Council (NSTC) of the United States of America. This initiative identified well-defined priorities and major difficulties for the area of nanotechnology in order to facilitate the implementation and clinical translation of promising nano-enabled technologies[29]. Recent efforts to investigate and develop nanotechnology have been helped along by these activities; the majority of the study and advancement that has been reported in this subject has centred on nanoparticles (NPs). Because of their ability to increase the stability and solubility of encapsulated cargos, promote transport across membranes, and lengthen circulation times NPs have the potential to improve both the safety and efficacy of a treatment when they are used. Because of these factors, a significant amount of study has been done on NPs, and positive results have been reported in vitro and in animal models involving small animals. Despite this, there is a significant disparity between research conducted on animals and those conducted on humans. indicate that the number of nanomedicines that are genuinely accessible to patients is far lower than what is estimated for the field. This gap in understanding is caused by a lack of information regarding the effects of species-specific changes in physiology and pathology on the behaviour and functionality of nanomedicines

International Journal of Pharmaceutical Research and Applications
Volume 9, Issue 3 May-June 2024, pp: 437-493 www.ijprajournal.com ISSN: 2456-4494

when they are inside the body[30]. In addition to differences between species, there are further obstacles to the translation of therapeutics. Because there is currently a paucity of research on the interactions between nanomedicines and in stratified patient populations, the efficacy of these treatments may be hindered as a result. Because of this, only a select few licensed nanomedicines are recommended as primary treatments, but a few of these drugs have shown to be effective in treating certain patients. This is because the development, shape, and physiology of diseased tissue all have an effect on NP distribution and functionality. This is in part because to the unexplored heterogeneity that exists not only in the molecular underpinnings of diseases but also within patients[31].

However, more recent nanoparticle designs have made use of recent developments in controlled synthesis processes to add more complex structures, bio-responsive moieties, and targeting agents in order to circumvent these biological obstacles to delivery. As a consequence of this, these nanoparticles (NPs) can be utilized as a component of more complex systems, such as nanocarrier-mediated combination therapies, in order to modulate a wide variety of pathways, increase therapeutic efficacy against targeted macromolecules, concentrate on particular stages of the cell cycle, or get around mechanisms of drug resistance. The practice of "precision medicine," sometimes known as "customized medicine," is gaining in popularity, and in 2015, the Precision Medicine Initiative (PMI) was established to assist in advancing this trend. This has led to a refocused effort on the development of NPs as a means of overcoming the biological barriers that are unique to certain patient subsets or disease situations. The goal of precision medicine is to develop individualized treatment plans for patients by analyzing patient data such as their genetic profile, the environmental exposures they've had, and any comorbidities they have. With the help of precision, which lessens the impact of heterogeneity among patients, accurate patient classification, improved drug specificity, and optimal dose or combinatorial strategies are all made feasible. Accurate patient classification is essential for improving patient care[32]. The therapeutic potential of precision medicines is restricted in the same way as that of conventional pharmaceuticals is by the biological obstacles that stand in the way of delivery. Therefore, unique NP designs that are data-informed and constructed to overcome particular constraints in a stratified patient group may be able to significantly improve the administration of precision medicine drugs as well as the responsiveness of patients to these treatments. Although the typical size range for NPs is 1 to 100 nm, there are several that deviate from this norm[10]. For example, the size of some medical NPs may be 5 nm, whereas the size of others may be 250 nm according to. Despite this, nanosystems such as liposomes can have dimensions that are orders of magnitude bigger than a micrometer. There is no way to define or describe NPs that can be considered definitive due to the fact that scientific knowledge is continuously expanding and new discoveries are being made. In light of the scientific and translational information on nanomaterials and nanotechnology provided by the US National Nanotechnology Initiative and the European Commission, the authors believe it is essential to emphasise that the upper size limit of NPs cannot be confined to 100 nm [33]. In addition, the authors believe it is vital to stress that the upper size limit of NPs cannot be confined to 100 nm. The authors arrive at this verdict because they believe it is essential to emphasise that the maximum size of NPs cannot be confined to 100 nm and that this is a vital point to emphasise. Abraxane (130 nm) and Myocet (100 nm) are both instances of nanomedicine products that are larger than 100 nm. These are just two examples. For instance, Abraxane and Myocet are two examples of nanomedicine products that are readily available (180 nm). As a result, the sole factor that can be used to limit or determine the spectrum is the size of the nanomaterials.

Nanoparticles (NPs) and nanodevices both exhibit properties that, due to their microscopic size, are not capable of being seen in their natural environments. Some examples of these characteristics include: NPs are among the most helpful chemicals due to the fact that their diminutive size results in a significant surface area in comparison to their overall volume. This seemingly trivial aspect improves their dependability and reproducibility, thus it shouldn't be neglected because of this fact. In addition to these advantages, their catalytic activity, chemical stability, thermal conductivity, and non-linear optical performance are all improved. The mere fact that something does exist is a pleasant added benefit. To provide just one illustration. It is possible to construct nanosystems out of a wide variety of NPs by manipulating the size, shape, and

International Journal of Pharmaceutical Research and Applications
Volume 9, Issue 3 May-June 2024, pp: 437-493 www.ijprajournal.com ISSN: 2456-4494

surface properties of the NPs in order to increase their performance in imaging, diagnosis, and therapy of potentially fatal diseases. Using nanoparticles that have been functionalized to allow for drug release makes it possible to achieve the controlled release of pharmaceuticals at particular places over an extended period of time [34]. Nanoparticles make it possible for this to take place. To maximise and promote tissue and cell interaction, it is required to effectively manage and analyse aspects such as charge, size, the arrangement of nanoscale medicinal compounds, and form. There are a number of parameters that need to be taken into consideration, some of which include the charge, size, structure, and form of nanoscale pharmaceutical molecules.

1.2 Nanotechnology in Healthcare Sector As a result of the growing application of nanotechnology in the medical field, novel nanosystems for the diagnosis, imaging, and therapy of a wide variety of diseases, such as cancer, cardiovascular illness, ophthalmic disease, and diseases of the central nervous system, have emerged. These nanosystems have the potential to treat cancer, cardiovascular illness, ophthalmic disease, and diseases of the central nervous system. It is quite thrilling to think that these nanosystems may one day be used to treat cancer, cardiovascular disease, ophthalmic disease, and illnesses that affect the central nervous system. Nanomaterials are able to be easily included into biomedical devices due to the fact that their size is comparable to that of the majority of biological systems [35]. In the realm of drug delivery, nanosystems are preferred to more conventional approaches due to the improved retention time and controlled release of pharmaceuticals that they give. This makes the usage of nanosystems an attractive option. One of the most well-known examples of targeted drug delivery, nano-liposomes have demonstrated effectiveness against cardiovascular illness as well as cancer. Nano-liposomes have a high biocompatibility, the ability to manage drug concentrations in the bloodstream, and the ability to deliver drugs to the exact targets for which they were made. These are the primary advantages of using nano-liposomes. Both the current methods of biological imaging, such as fluorescence microscopy, and the existing methods of MRI, such as imaging different parts of the body, have the potential to be vastly improved by the use of nanoparticles. This is because nanoparticles have the ability to encapsulate a large number of different types of information. Nanoparticles are utilised in each of the methods, despite the fact that their chemical make-up is distinct from one another. This article presents a summary of the many different ways in which nanoparticles can be utilised in imaging.

A. **ZnO Nanoparticles :-**

Zinc oxide nanoparticles (also known as ZnONPs) are present in a variety of commercially available goods, including sunscreens, food additives, pigments, and biosensors, to name a few examples. Multiple researchers have utilized a wide variety of cell lines in addition to animal models in order to examine the potentially damaging consequences of these generated ZnONPs. There is evidence that ZnONPs are both genotoxic and cytotoxic when tested in vitro and in vivo, respectively. In further investigations, it was discovered that ZnONPs reduced the amount of viable cells in a manner that was dependent on both the dose and the amount of time[36]. It is believed that ZnONPs cause an increase in the expression of the metallothionein gene, which serves as a biomarker for metal-induced toxicity.According to research, dose-dependent hepatotoxicity is characterized by an increase in malondialdehyde (MDA) level as well as a decrease in superoxide dismutase (SOD) and glutathione peroxidase (GPx) enzyme activity. ZnONPs cause an increase in all three of the aminotransferase levels found in the blood: aspartate aminotransferase (AST), alanine aminotransferase (ALT), and alkaline phosphatase (ALP).

B. **TiO_2 Nanoparticles**

As a pigment, a thickener, and a UV absorber, titanium dioxide (TiO2) is a component that finds widespread application in the cosmetic and skin care sectors. Osseo integration between artificial medical implants comprised of titanium dioxide and natural tissue can now be achieved[37]. To investigate the question of why TiO2NPs pose such a health risk, a number of investigations have been carried out. According to a number of investigations, skin penetration and toxicity of TiO2NPs were seen in hairless mice and pigs after subchronic cutaneous exposure to the particles. However, the vast majority of scientists concur that TiO2NPs from sunscreens pose very little to no damage to human health because it does not appear that these particles permeate the skin to any significant degree. It has been demonstrated that cytotoxicity and genotoxicity can be caused by oral

International Journal of Pharmaceutical Research and Applications
Volume 9, Issue 3 May-June 2024, pp: 437-493 www.ijprajournal.com ISSN: 2456-4494

delivery of TiO2NPs to a variety of cell lines, plants, and mouse brains in vitro. TiO2NPs were found to bioaccumulate, be subacutely poisonous, and be disseminated throughout the tissues of goldfish (Carassius auratus) and C57BL/6 mice. Additionally, it was found that these particles were spread throughout the body[38].

C. Silica Nanoparticles

The food sector has relied heavily on synthetic amorphous silica for the better part of three decades. It has a food additive registration with the European Union under the number E551 and finds widespread application in processed foods. Utilizing SiO_2NP in the food industry's major objective is to achieve the goal of preventing poor flow or "caking" in powdered products. In addition to their employment as a thickening agent in pastes and a flavour carrier, sio_2nps are utilized in the clarification of beverages and the reduction of foaming[39]. Researchers have investigated the effects of SiO_2NP on the cells that line the gastrointestinal tract and discovered that the particles are safe for usage in food. Despite this, the researchers have advocated for additional, thorough research to be conducted in vivo to determine the particles' safety profile. SiO_2NPs are a type of food additive that, as of late, has been found to interact with food matrices in ways that are very component-specific. This discovery came about as a result of new research. In addition, researchers have postulated that the toxicity of SiO_2NPs shifts depending on particle size, concentration, and the origin of the cells being studied. Researchers have demonstrated, through the use of oral and intravenous administration, that the shape of mesoporous SiO_2NPs influences the biodistribution, excretion, and toxicity of the particles[40].

D. Silver Nanoparticles

Diseases of the skin brought on by bacteria and viruses can be treated with AgNPs. These diseases include, but are not limited to, boils, open wounds, chronic ulcers, trophic sores, eczema, and acne. AgNPs have also been reported to be employed as an antimicrobial ingredient in a wide variety of personal care products. These products include soaps, detergents, shampoos, toothpastes, and sprays that clean the air[41]. As a direct consequence of this, AgNPs have become increasingly widespread in the food preservation and packaging industries. Composites of silver-based resin have been used to produce fillings and coatings for use in dentistry and medical devices. Although AgNP have shown promise as a non-toxic preservative in cosmetics, the capacity of AgNP to pass through the protective barrier of the skin is contingent on the barrier's integrity being preserved at all times. This is the case even though AgNP have shown promise. Researchers were able to demonstrate that lower concentrations of AgNPs that were stabilized by ammonia and PVPs did not cause any cytotoxicity in mice. When examined in vitro on human cell lines, however, other studies found that exposure to AgNPs caused DNA damage as well as toxicity and a reduction in the cells' ability to operate normally[42]. In human microvascular endothelial cells, the cytotoxicity and genotoxicity of AgNPs have been investigated in depth, and the results suggest that they may be a useful tool for managing unregulated angiogenesis.

E. Gold Nanoparticles

Before being used in biological applications, gold nanoparticles are frequently coated with biofunctional moieties, such as peptides or sugars, in order to facilitate the regulation of cellular processes. Extensive study has been conducted on gold nanoparticles (AuNPs) to investigate their practicability in medication delivery applications and photothermal therapy. In addition, the co-administration of medications and AuNPs has been shown to increase the therapeutic efficacy of the treatment[43]. AuNPs have use in diagnostics due to the phenomenon of surface plasmon resonance as well as the light-reflecting qualities that they possess. Because of their capacity to form bonds with thiols and amines on their surfaces, gold nanoparticles (AuNPs) have found use as a vector for the delivery of a wide variety of pharmaceutical and biological compounds. Due to the enormous diagnostic and therapeutic potentials of AuNP, the toxicity profiles of these nanoparticles are currently the topic of extensive research. Dendritic cells from the immune systems of mice were grown from bone marrow and then examined for toxicity to gold nanoparticles[44]. According to additional research, citrate-coated AuNPs are genotoxic in human HepG2 cells and have been demonstrated to have this effect. During the biodistribution study, researchers found that the liver of rats contained up to 86% of the peptide-capped AuNPs. According to the findings of research that attempted to deduce the effect that the form of PE-Gylated AuNPs had on the rate of cellular uptake, the endocytosis rate was highest for spherical AuNPs. The rate of

International Journal of Pharmaceutical Research and Applications
Volume 9, Issue 3 May-June 2024, pp: 437-493 www.ijprajournal.com ISSN: 2456-4494

internalization was quickest for spherical AuNP, followed by cubic, rod, and disk-shaped particles. PEG-coated AuNPs accumulated differentially depending on the organ as well, however the toxicity of these particles in vivo was not affected by the particle size at all[45]. Researchers discovered that positively charged AuNPs had a greater influence on cellular toxicity than their counterparts that were negatively charged. This was due to the fact that positively charged AuNPs were more easily transferred across the cell membrane than their counterparts that were negatively charged.

F. Polymeric Nanoparticles In Drug Delivery

These days, biodegradable polymers are the most often used carriers in carefully calibrated pharmaceutical delivery systems. On the other hand, not a lot of research has been done to figure out how biological systems interact with these PNPs. PNPs of a size between 10 and 200 nm use enhanced permeability and retention (EPR) qualities as a defence mechanism to prevent themselves from being filtered out by the kidneys and excreted in the bile. Particles with a size greater than 200 nm are readily identified by the reticuloendothelial system (RES), and the liver is responsible for their elimination from the body. PEGylation is a popular approach that is used to lengthen the amount of time that PNP remains in the circulatory system of the body. After being injected in vivo, cationic PNPs have the potential to interact with nonspecific cells or opsonizing proteins in the blood compartment due to their electrostatic affinity[46]. This can result in cytotoxicity that was not predicted. Tiny, much less negatively charged anionic (almost neutral) PNPs might be utilized in order to offer a wider biological effect while simultaneously decreasing off-target surface reactivity or interactions. This would be possible through the usage of PNPs. Researchers have looked into the relative safety of a number of different biodegradable polymers when used as nanoparticles[47]. The surface charge of Poly(lactic-co-glycolic acid) (PLGA) nanoparticles did not influence the safety of the particles when they were tested on the bronchial epithelium. On the other hand, a number of studies have demonstrated that the toxicity of polymeric PLGA-NP toward humanlike macrophages can be mediated by a surface coating (chitosan [CS], poloxamer 188 [PF68], or poly(vinyl alcohol] [PVA]). Both the hatching rate and the death rate of zebrafish embryos that were treated with CS NP decreased when the concentration of the treatment was increased. Both the nano-sized delivery systems based on the double emulsion approach employing the polymer eudragit®RS+ (DE/RS+) and the double emulsion technique utilizing the polymer poly(-caprolactone)+ (DE/PCL+) were found to be appropriate because of their high encapsulation efficiency and low toxicity, respectively. Oxorubicin (DOX)-loaded poly(-caprolactone) (PCL) nanoparticles were biocompatible and enhanced DOX's anticancer efficacy in human and mouse breast and lung cancer cell lines while simultaneously reduced DOX's toxicity[48]. The enormous body of study on the potentially harmful effects of manufactured substances.

1.3 Optical imaging

While performing conventional imaging of tissue slices or cells, it is common practice to load samples with organic dyes. This is done for a number of reasons. It is common practice to append fluorescent dyes to biomolecules that preferentially attach to cells or components of cells through the use of ligand/receptor interactions. Rhodamine and fluorescein isothiocyanate are examples of dyes that fluoresce when exposed to darkness (FITC). This imaging technique suffers from a number of problems, the most prevalent of which are a lack of fluorescence and photobleaching. The gradual loss of fluorescence over time is referred to as "photobleaching," and there are many different factors that might cause it[49]. Dye molecules are to blame for this since they produce a change in their structure that is irreversible. "Quantum dots" is the colloquial name given to nanoparticles that are composed of inorganic semiconductor molecules (QDs). These nanoparticles, when exposed to ultraviolet (UV) radiation, emit an entrancing fluorescent light, the wavelength (color) of which is significantly dependent on the particle size. These materials are one of a kind due to the fact that their characteristics change depending on their dimensions. The presence of a "band gap" is the defining trait that distinguishes inorganic semiconductor molecules from other kinds of molecules. This characteristic distinguishes inorganic semiconductor molecules from other classes of molecules. The term "band gap" refers to the energy barrier that exists between the valence band (or energy level), which is where electrons typically reside, and the conduction band, which is where electrons can be "advanced" by the input of energy of a specific wavelength (excitation), which

International Journal of Pharmaceutical Research and Applications
Volume 9, Issue 3 May-June 2024, pp: 437-493 www.ijprajournal.com ISSN: 2456-4494

is typically a photon[50]. This barrier prevents electrons from moving from the valence band to the conduction band. Electrons are unable to pass through this barrier and enter the conduction band unless they are assisted in doing so by an excitation particle. Electrons "reside" in the valence band under typical conditions, but under certain conditions, they are able to "advance" into the conduction band. The formation of a hole results from the departure of an electron from the valence band (this is a term given to an energy level lacking an electron, and is not a physical feature). When the excitation is switched off, the electrons that were previously stimulated get de-excited and then return to their original position in the valence band. When subjected to this stimulation, quantum dots (QDs) transform all of their stored infrared energy into visible light. Larger quantum dots, in contrast to their smaller counterparts, are superior devices for the storage and release of energy. This is because larger quantum dots contain a greater number of electron-hole pairs. According to the formula, the length of the wavelength of the light that is produced will get shorter as the size of the QDs gets larger. The light that is produced by QDs is not only more brilliant but also more resistant to being bleached by light in comparison to the light that is released by conventional organic dyes. This is especially helpful in three-dimensional imaging of tissues because the chance of photobleaching increases with each subsequent z-axis acquisition.

Due to the fact that QDs are totally composed of inorganic building units, water is unable to dissolve them. Due of this, in order for QDs to be utilised in biological and medical applications, they are required to have a thin coating of a chemical that is water-soluble applied to them first. Only then will they be usable. The next step, which often entails coating the object with a chemical, is done in order to zero in on a particular cell or cellular component. Typically, this step is done. On the surface of each quantum dot (QD), there is a profusion of binding sites that can be used to attach soluble and/or bioactive substances[51]. These sites can also be used to adhere other molecules. It's possible that the compounds will attach themselves here. The fact that individual QDs are capable of storing a variety of chemicals contributes to the versatility of the material. In a study that used QDs for live cell and in vivo imaging, many different surface modification alternatives were investigated and analysed. We used a variety of methods, including targeted circulation retention and prolonged circulation retention. Oligomeric phosphine-coated quantum dots have been used in more recent research to map lymph nodes in pigs and mice. The findings from these probes are now in your possession. Because of their capacity to release light in response to being activated by near-infrared radiation, CdTe and CdSe were both utilised in the manufacturing process of these QDs[52]. The light that is produced by these QDs has a wide variety of potential applications. Because of this finding, medical professionals are now able to map lymph nodes up to one centimetre below the surface of the skin without having to make any incisions, which is one of the strongest arguments in favour of the importance of the discovery. Because the authors did not conduct toxicity testing on the QDs, they were forced to operate under the assumption that the QD doses they used were not harmful[53]. It is possible to target the QDs to specific organs by coating their surface with chemicals that are absorbed by those tissues. Aiming may now be done with a higher degree of precision. In order to target the lung tissue of mice, we selected a peptide sequence with the name CGFECVRQCPERC. This particular sequence has been demonstrated to bind to endothelial cells in the tissue of the pulmonary artery. The lungs of the mice were the organs that were going to be targeted with the QDs. Quantum dots (QDs) were given to mice tumors in a manner analogous to that described above, either through intravenous or lymphatic injection. Endocytosis, the technique by which the targeted cells took up the QDs, was used both times, however cells in the surrounding tissue were unable to take up the QDs. In order to accomplish this, we have imbedded targeting ligands into the surface of the polymer, and we have encased semiconductor QDs inside of an amphiphilic copolymer. Because of the coordinating ligand, the CdSe-capped ZnS QDs did not combine when they were placed in solution (tri-n-octylphosphine oxide [TOPO]). The butylacrylate, ethylacrylate, and methacrylic acid that make up the segments of the triblock copolymer are methacrylic acid, ethylacrylate, and butylacrylate, respectively[54]. The butylacrylate and ethylacrylate segments are hydrophobic. Figure 2 is a representation of the structure of the copolymer after it is dissolved in solution. It demonstrates how the hydrophobic segment is shifted closer to the TOPO, which results in the carboxylic acid groups of the hydrophilic section being pushed further outward. These hydroxyl

International Journal of Pharmaceutical Research and Applications
Volume 9, Issue 3 May-June 2024, pp: 437-493 www.ijprajournal.com ISSN: 2456-4494

groups have the potential to function as molecular docking stations for affinity ligands and possibly even other substances, such as polymers (ethylene glycol). The composite particles have sizes that range between 20 and 30 nanometers. On the surface of the tumor-targeting particle was an antibody that was specific to prostate specific membrane antigen (PSMA)[55]. When these particles were administered to animals through intravenous injection, they were found to concentrate in the tumors of interest (Figure 1.2). There were no indications of accumulation in the lungs, kidneys, or brain at any point in time. Liposomes are vesicles that are made up of a lipid bilayer on the outside and are full of water on the inside. They come in dimensions ranging from the nanometer to the micrometer, and you can find them. They are capable of grabbing a diverse assortment of molecules, including those that are hydrophilic and those that are lipophilic. As a consequence of this, they have been praised as the most efficient route of medication administration that is currently available[56]. As a result of the compositional similarities between them and the cellular membranes that are found inside the body, they are useful for the in vitro delivery of medications. They are able to carry a significant quantity of medication despite their diminutive size.

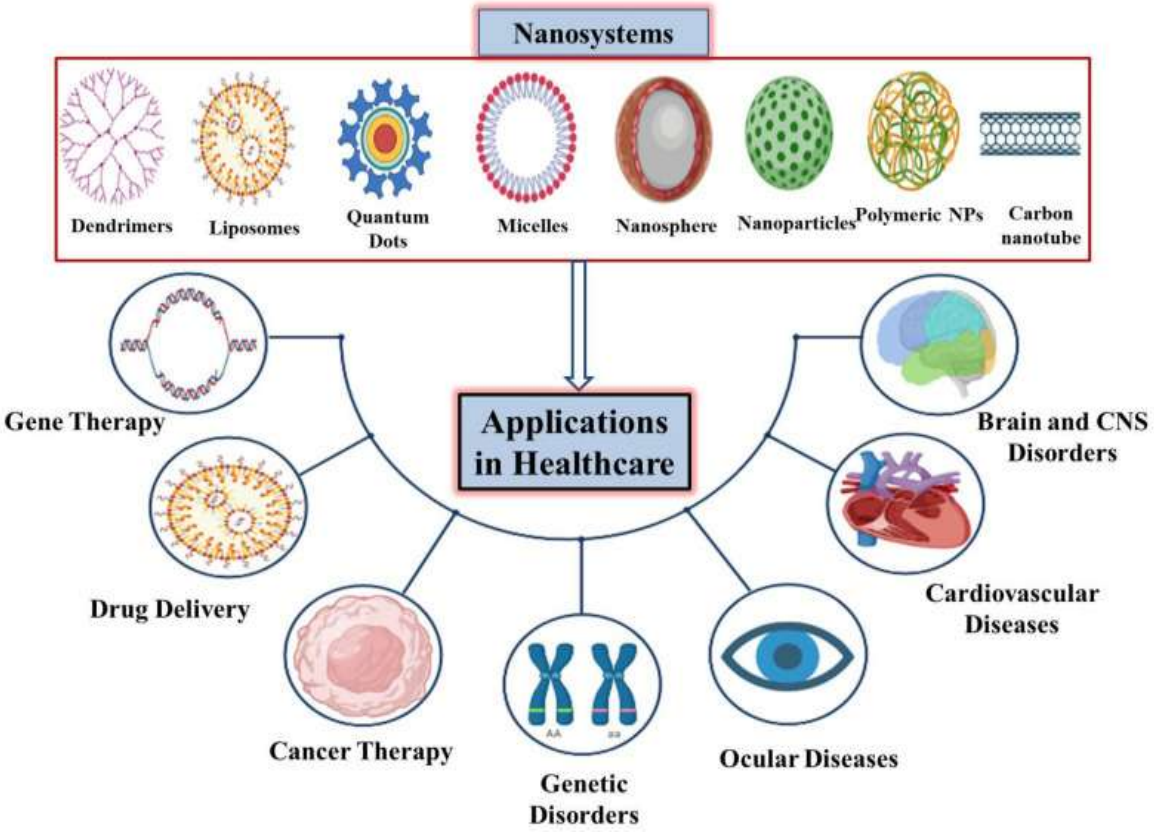

Fig:1.2 Nanotechnology and its applications in medicine: carbon nanotubes, quantum dots, dendrimers, micelles, nanospheres, liposomes, and nanoparticles.

1.4 History of Nanotechnology

One of the most fascinating examples of nanotechnology from antiquity is found in Roman work from the fourth century after the common era. Nanoparticles and nanostructures were both utilized in the researchers' experimental procedures. The Lycurgus cup, widely considered to be one of the finest examples of ancient glasswork, is on display at the British Museum[41]. There has not been any other instance of dichroic glass of this antiquity that has been found up to this point. Dichroic glass is a phrase that is used to describe two unique forms of glass that, depending on the angle at which the light is hitting them,

International Journal of Pharmaceutical Research and Applications
Volume 9, Issue 3 May-June 2024, pp: 437-493 www.ijprajournal.com ISSN: 2456-4494

might appear to be a different hue. These two varieties of glass are known collectively as "dichroic glass." As a result of this, the color of the Cup shifts from green in open air to a bluish-red when observed through glass (Figure 1.3). In 1990, researchers looked into the cup using transmission electron microscopy (TEM) in order to gain further insight into the dichroism phenomenon [42] that they were investigating at the time. It was determined that the presence of nanoparticles with sizes between 50 and 100 nm was responsible for the "two-color effect," also known as diachronism. An X-ray study showed that the nanoparticles are composed of an alloy of silver and gold (Ag-Au) with a 7:3 ratio of Ag to Au and approximately 10% copper (Cu) scattered in a glass matrix [55]. The ratio of Ag to Au in the alloy is 7 to 1, and the glass matrix contains the remaining 10%. The ratio of Ag to Au is 7:3. The color red is produced as a result of the absorption of light with a wavelength of 520 nanometers by gold nanoparticles. Larger particles of silver nanoparticles in colloidal dispersions scatter enough light to give a green hue, whereas smaller particles of silver nanoparticles absorb redder and purpler light, generating a redder and purpler hue. There is a level of agreement that approaches complete unanimity that the cup of Lycurgus is one of the earliest examples of a nanomaterial that was made artificially [31]. The same effect can be seen in the windows of churches built in the late Middle Ages. The stunning red and yellow glow that brightens the space is produced by incorporating gold and silver nanoparticles into the glass, which generates the glass. A wide variety of optical phenomena can be brought about when nanoparticles of differing sizes come into contact with stained glass windows, as can be shown in Figure 4. Ceramics with a lustrous, "lustre" finish were particularly well-liked in Islamic culture, and this aesthetic eventually made its way to Europe. These glazes were produced using a combination of nanoparticles of silver (Ag), copper (Cu), and other elements. Nanoparticles were utilized in the construction of works of art by Italian Renaissance potters working in the 16th century. Cementite nanowires and carbon nanotubes were the primary components used in the production of "Damascus" sabre blades [36] between the 13th and 18th centuries. These blades were renowned for their incredible longevity, tenacity, and ability to keep their edge for an exceptionally long time. Ottoman customs were a major inspiration for this methodological approach. People have endeavored, over the course of many centuries, to bring attention to certain hues and characteristics of the materials they worked with. The medieval artists and forgers who experienced these phenomena did not understand why they were happening.

People's creative fancies and daydreams often serve as the genesis for ground-breaking discoveries in the fields of science and technology. These are the ideals that gave birth to nanotechnology, one of the most promising fields of the 21st century. The word "nanotechnology" refers to the study and manipulation of matter on a scale ranging from one to one hundred nanometers. This is the range in which new phenomena make it feasible to develop novel applications. Nanoparticles have been present in the environment for a significant portion of human history; nevertheless, during the time of the industrial revolution, people's exposure to these particles increased significantly. Research in nanoscience is already well-established as a field. It is commonly believed that Richard Zsigmondy, the recipient of the Nobel Prize in chemistry in 1925, is the person who first conceptualized the "nanometer" notion. He was the first person to use a microscope to measure the size of particles such as gold colloids. In addition, he came up with the term "nanometer" expressly for the purpose of describing particle size. It is generally agreed that the present field of nanotechnology may be traced back to Richard Feynman, who was awarded the Nobel Prize in Physics in 1965. He gave a talk in 1959 titled "There's Plenty of Room at the Bottom" at the American Physical Society conference that was held at Caltech. In this talk, he was the first person to suggest the concept of atomic manipulation[40]. The initial concept proposed by Feynman brought to light novel viewpoints, and subsequent study has shown that his forecasts were accurate. Because of this, he is regarded as the founding father of modern nanotechnology. Nearly 15 years after Feynman's talk, the Japanese scientist Norio Taniguchi was the first to use the term "nanotechnology" to describe semiconductor processes that occurred on the nanoscale scale. He was the first person to adopt the phrase. Using processing, separation, consolidation, and deformation techniques that are enabled by nanotechnology, he contended that it is possible for materials to undergo atomic or molecular level transformations. Eric Drexler, a professor at MIT, wrote "Engines of Creation: The Coming Era of Nanotechnology" in 1986. In this book, he included

International Journal of Pharmaceutical Research and Applications
Volume 9, Issue 3 May-June 2024, pp: 437-493 www.ijprajournal.com ISSN: 2456-4494

concepts from Richard Feynman's "There is Plenty of Room at the Bottom" and used the word "nanotechnology" coined by Taniguchi. This event heralded the start of the most fruitful era in the history of nanotechnology. Drexler proposed the idea of a nanoscale "assembler" that was capable of self-replication and could manufacture structures of any complexity. The form of nanotechnology that Drexler envisioned is usually referred to as "molecular nanotechnology." Another Japanese scientist named Iijima contributed to the advancement of nanotechnology with his discovery of carbon nanotubes.

Around the turn of the 21st century, there was a discernible increase in the amount of attention paid to nanoscience and nanotechnology. It is impossible to overestimate how much of an impact Richard Feynman and his concept of atomic manipulation had on the United States' scientific agenda at the national level. President Bill Clinton made his case for more funding of research into this emerging technology during a speech that he delivered at Caltech on January 21, 2000. In 2008, after being introduced in 2005, the 21st Century Nanotechnology Research and Development Act was finally signed into law by former President George W. Bush. This delayed its implementation by three years. As a direct result of the law, the NNI was founded, and the study into nanotechnology became a priority for the federal government.1 The National Science and Technology Council (NSTC), which is a subcommittee of the President's Cabinet, and the Committee on Technology of the NSTC are currently in responsibility of supervising the National Nanotechnology Initiative (NNI).

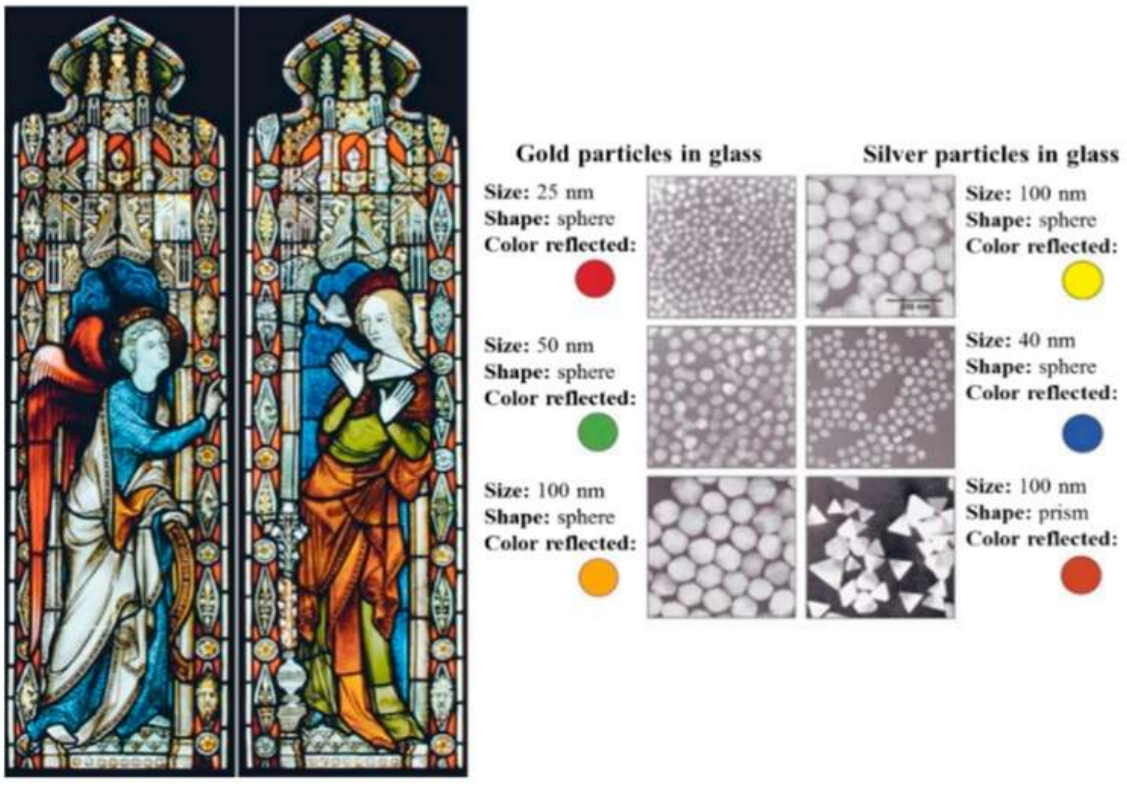

Fig: 1.3 Effect on Nanoparticle color in glass

1.5 Gold Nanoparticles

Gold was one of the first metals discovered, and both its utilization and investigation date back thousands of years. The term "colloidal gold" was initially used for the first time in the fifth and fourth century BC in the writings of intellectuals from China, Arabia, and India. These citations can be located in sources written in Chinese[33]. In the realm of medicine, the population relied on it as a form of treatment available to them (called "golden solution" in China and "liquid gold" in India). In Europe during the Middle Ages, alchemists were interested in and made use of colloidal gold in their work. Paracelsus

International Journal of Pharmaceutical Research and Applications
Volume 9, Issue 3 May-June 2024, pp: 437-493 www.ijprajournal.com ISSN: 2456-4494

wrote about the restorative properties of gold quintessence after he created the substance by reducing gold chloride with vegetable extracts in alcohols or oils. Patients who had been diagnosed with schizophrenia and other mental problems received the so-called "potable gold" from him[34]. His contemporaries, such as the well-known physician Giovanni Andrea, employed " aurum potabile " to treat patients suffering from leprosy, plague, epilepsy, and diarrhea. Giovanni Andrea was a pioneer in the field of medicine. In the year 1583, the French alchemist David de Planis-Campy offered his "longevity elixir" to King Louis XIII of France in his capacity as a physician. This so-called elixir was out to be nothing more than a colloidal solution of gold in water. The philosopher and medical practitioner Francisco Antonii wrote the first known book on colloidal gold in the year 1618 [35-38]. That book is the only one of its kind that we are aware of that has survived to the current era, as far as we are aware. The accessibility of colloidal gold as well as its possible uses in medicine are brought up in this discussion.

In 1971, two British researchers named Faulk and Taylor were the first to disclose antibody conjugation with colloidal gold as a method that made it possible to visualize salmonella surface antigens using direct electron microscopy. This discovery heralded the beginning of what has been called a "revolution in immunochemistry" including the use of gold nanoparticles (GNP) in biological study. Specifically, this finding marked the beginning of the revolution. The utilization of biospecific markers, such as colloidal gold combined with immunoglobulins and other molecules, in various areas of biology and medicine served as the impetus for the investigation. Research on functionalized nanoparticles, also called as conjugates with recognizing biomacromolecules, dates back more than 40 years at this point (such as antibodies, lectins, enzymes, aptamers, and so on). The findings of this study have led to the identification of potential applications for functionalized nanoparticles in a wide variety of various scientific fields. Biochemistry, microbiology, immunology, cytology, plant physiology, and morphology are all subfields that fall under this category[44].

In modern biology and medicine, GNP offers a number of possible uses that may be explored. This involves the identification of bacteria and the destruction of cancer cells through photothermallysis, as well as the application of cutting-edge registration systems for the purpose of monitoring cells and tissues. All four branches of medicine that have been investigated thus far point to the potential benefits of gold nanoparticles (diagnostics, treatment, preventive, and hygiene). Because of its remarkable physical and chemical qualities, GNP can be put to use in a broad number of settings because to its versatility. This is due to the fact that they can be used to a wide variety of uses. Plasmon resonance is responsible for GNP's optical features in particular, and may be traced back to the material. The particular wavelength band in which this resonance occurs can be determined, at least in part, by the size, shape, and structure of the particles [31]. There is a connection between this resonance and the collective excitation of the conduction electrons.

The notion that gold could make a person live longer can be traced all the way back to primordial times [45]. Researchers began investigating gold complexes as a potential treatment for rheumatoid arthritis for the first time in 1925. In recent years, one of the primary focuses of research and development in the field of nanotechnology has been on the transportation of large molecules into cells and tissues [15]. Huge molecules include proteins, peptides, genes, and other large molecules. It is possible that targeted nanoparticle-mediated drug delivery will result in improved oral bioavailability and less unfavorable pharmacokinetics, sustained drug or gene effect in the target tissue, drug solubilization for intravascular delivery, and/or increased stability against decomposition [6-7]. Because of the high glutathione concentrations that can be found inside of cells as well as the relative stability of the ligand-gold association while it is outside of the cell, gold nanoparticles pose a particularly high risk to human health.

An inorganic core is in the center of a nanoparticle, which is then surrounded by an organic monolayer. Nanoparticles are extremely versatile in terms of their size, shape, and chemical composition, which makes them particularly well-suited for use as building blocks in nanobiotechnology. Nanoparticles are extremely malleable, which makes them very promising for use in the emerging field of nanobiotechnology. Nanoparticles like this are formed at the atomic or near-atomic scale, which is a zone in which quantum mechanics reigns supreme. Chemical, electrical, and optical properties can all exhibit significant fluctuation at this size [10], when

International Journal of Pharmaceutical Research and Applications
Volume 9, Issue 3 May-June 2024, pp: 437-493 www.ijprajournal.com ISSN: 2456-4494

compared to the characteristics of the material when it is in its bulk form. The features of nanoparticles are extremely fragile, and they are sensitive to even the smallest changes in particle size. When it comes to influencing a nanoparticle's dynamics, size and shape aren't the only factors that matter; form also has a big impact. An increase in the surface area of the particle in relation to its volume is an indication of the migration of the particle's outermost atoms inside to replace the particle's inside atoms [11]. This migration occurs when the particle's outermost atoms replace the particle's inside atoms. The nanoparticle's physical features are ultimately determined by the manner in which the core material is structured within the nanoparticle.

Although the organic monolayer of the nanoparticle does not significantly contribute to the determination of the core's physical properties, it does play an essential part in the manner in which the nanoparticle interacts with the immediate environment in which it is located. The function of the monolayer is to protect the nanoparticle core from the outside world's impacts and to maintain the core's consistency. Not only that, but the chemical composition of the boundary between the monolayers is what dictates the reactivity and solubility of the nanoparticles. When it comes to addressing the demand for solubility in aquatic environments for biological applications, the formation of a monolayer with biocompatible ligands [12-19] can be of great assistance. The intermolecular interactions of the particle can be altered by adding pendant groups that are more complicated than the monolayer they are attached to. The establishment of a connection between the nanoparticle monolayer and biologically active components such as DNA, peptides, and proteins is of critical importance. The core of the nanoparticle is responsible for dictating how it will behave physically, but the design of the monolayer will define how it will react chemically in a specific environment. Core-gold nanoparticles, which were initially produced in the 1980s [20], have found applications in a wide variety of diverse fields of business. When gold salts are reduced in the presence of a reducing agent, the process of creating nanoparticles is at its most straightforward; nevertheless, there are several additional techniques to accomplish this goal (Figure 4a). It is the very first thing that takes place, and it is what kicks off the process that ultimately results in the formation of nanoparticles made out of gold ions. Stabilizing agents are frequently included in synthesis protocols in order to prevent the formation of aggregates. The method was initially stated by Turkevich [21], and Frens [22] was the one who refined it. First, sodium citrate functions as a reducing agent, and then, once it has been absorbed by the surface, it takes on the role of a stabilizing agent (Figure 4b). Recent developments in nanoparticle synthesis have made it possible to generate stable particles that are both smaller in size (two to six nanometers) and more monodisperse (having the same average size and shape throughout) in size. These particles may now be manufactured. The Brust-Schiffrin technique is widely regarded as the most effective one [23], primarily as a result of its capacity to mass-produce monolayer-protected gold clusters of extremely high quality in very large quantities. Because of this, it stands out as the method that utilizes resources in the best possible way. It is necessary to move gold ions from an aqueous solution of gold salt into the toluene phase, and a phase-transfer agent is required to make this transition as straightforward and uncomplicated as is humanly possible (tetraoctylammonium bromide, TOAB). After a nonpolar organic thiol, which is typically a thiol-terminated long-chain alkane, a reducing agent is next added, but this step typically only takes a very short amount of time to complete (see Figure 4). The capping of the gold cluster by thiols makes it feasible to prevent the formation of a cluster of reduced gold atoms. Because of the incredible strength of the bonds that are formed between gold and sulphur, the monolayer of organic molecules that can be generated by thiol ligands has the potential to be very long-lasting. Its outstanding durability can be due, in a significant part, to the thiol ligands. The principal instrument at one's disposal for modifying the size of gold clusters is a modification to the stoichiometric ratio of ligand to gold.

International Journal of Pharmaceutical Research and Applications
Volume 9, Issue 3 May-June 2024, pp: 437-493 www.ijprajournal.com ISSN: 2456-4494

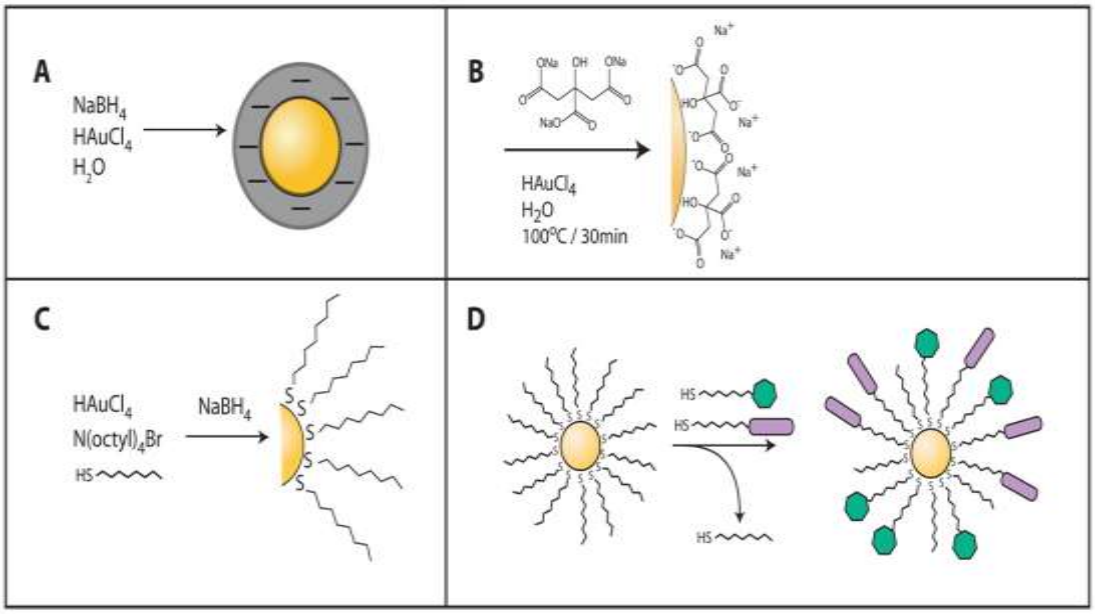

Fig: 1.4 Gold nanoparticle

1.6 Zinc oxide nanoparticles

This substance almost seldom takes the form of a liquid and more frequently than not takes the form of a white powder. Zinc powder is an additive that can be found in a wide variety of products, including plastics, ceramics, glass, cement, rubber (for example, car tyres), lubricants, paints, ointments, adhesives, sealants, pigments, foods (which are a source of the nutrient zinc), batteries, ferrites, and fire retardants, amongst many others. Zinc oxide (also known as ZnO) can be obtained naturally from the mineral zincite; nevertheless, synthetic synthesis accounts for the overwhelming majority of industrial applications of zinc oxide. Zinc oxide (ZnO) is an excellent material to use in the production of clothing and other objects that will come into contact with human flesh since it is non-toxic and does not react negatively with human skin. This makes it an ideal material for use in the production of these types of items[60]. In addition to this, ZnO is an excellent antibacterial agent. Because of the increased surface area, ZnO nanoparticles may be more efficient at performing the function for which they were designed than ZnO in its bulk form.

1.6.1 ZnO nanoparticles importance

1) It is essential to the production of a variety of goods, including cosmetics, paint, plastics, rubber, electronics, and pharmaceuticals, to name just a few of the industries that rely on it.
2) It may also be utilized to treat cancer cells, such as those found in leukemia and carcinoma.
3) In addition, it has potent antimicrobial properties.
4) It's also put to use as a pharmaceutical delivery system.
5) Nanoparticles made of zinc oxide have a wide range of potential uses and are already being put to work in a variety of industries, including those concerned with protecting the environment, manufacturing synthetic textiles, packaging food, working in the pharmaceutical industry, providing medical care, as well as working in construction and interior design.

1.7 Silver Nanoparticles

Silver nanoparticles have established themselves as a leader among the numerous fascinating developments that have occurred in the field of nanotechnology. The vast majority of current research into nanotechnology is focused on developing more efficient manufacturing processes for silver nanoparticles. From this vantage point, it would appear that the "green synthesis" method is one that holds significant promise. Synthesizing silver nanoparticles in the laboratory can be done in a variety of ways, including chemical, biological, and even certain physical approaches. Yet, in recent years, green synthesis has begun to supplant some fast chemical methods due to its lower toxicity and superior quality. This development

International Journal of Pharmaceutical Research and Applications
Volume 9, Issue 3 May-June 2024, pp: 437-493 www.ijprajournal.com ISSN: 2456-4494

came about as a result of increased competition[30].

Nanoparticles' one-of-a-kind characteristics, including their ability to interact with live beings, are determined by the size, shape, and morphology of the particles. Studies both in vitro and in vivo have shown that silver nanoparticles, also known as Ag NPs, possess significant bactericidal activity against a wide range of bacterial species. They are arranged in a number of different configurations so that their morphology as well as their physical properties can be studied. Despite the fact that they were trying to avoid confusion, numerous articles have mixed up the chemical method [28] with green synthesis. Because of their use in electronics, catalysis, medicine, and the regulation of microbial development in biological systems, silver nanoparticles (NPs) have developed a reputation for being environmentally friendly [30]. Biosynthesis of silver nanoparticles can involve a wide variety of organisms, including bacteria, fungi, yeast, actinomycetes, and plant extracts [35]. In recent years, the production of gold and silver nanoparticles has moved beyond the realm of enzymes and into a range of plant parts, such as flowers, leaves, and fruits. Nanoparticles can range in size, shape, and stability depending on a number of factors. Some of these factors include the preparation procedure, the kind of solvent used, the concentration of the reducing agent, and the temperature. Because of their potential to eradicate germs in both their liquid and solid states, silver nanoparticles (NPs) stand out among the other nanoparticles that have been found and described thus far. Although the importance of this material was quickly recognized, it was primarily neglected outside of orientalism and coinage until very recently. Every year, over 320 metric tons of silver nanoparticles (Ag NPs) are manufactured for use in applications such as nanomedical imaging, biosensing, and food items [36]. There are a number of variables that are leading to the growth of bacterial and viral strains that are resistant to several medicines. These factors include mutation, pollution, and change environmental circumstances. In order to find a way out of this stalemate, researchers are hard at work developing anti-microbial drugs for the treatment of disorders caused by microbes. It has been demonstrated that the growth of a wide variety of harmful bacteria can be inhibited by a wide variety of metal salts and metal nanoparticles. Silver and silver nanoparticles have traditionally been recognized as two of the most important antibacterial agents among the large list of metals that have been used [39]. In humans, certain bacteria can be inhibited from spreading through the use of silver salts. They are applied to catheters, incisions, burns, and wounds in order to prevent the spread of infection. According to Das et al.'s research, bacterial growth can be effectively inhibited by using silver nanoparticles of a smaller size. Silk sericin (SS) is a water-soluble protein that is obtained from silk worms at a pH of 11. Ag nanoparticles made from SS, which is isolated from silk worms, contain hydrophilic proteins with highly polar groups like hydroxyl, carboxyl, and amino functional groups. The functional groups on molecules that were discussed previously have the ability to reduce AgNO3 to silver metal. It is believed that the hydroxyl groups of SS create a compound with the silver ions, which stops the silver ions from aggregating or precipitating. The presence of large molecules in the solvent may be sufficient to separate the elemental Ag NPs, but this does not mean that the NPs will be complexed with the large molecules because they are both neutral. It has been determined that SS-capped Ag NPs are effective antibacterial agents against both gram-positive and gram-negative bacteria when put through the appropriate tests.

1.7.1 Silver nanoparticles importance

1) Imaging, biosensing, drug administration, and maintaining high air quality are just a few of the many fields that could benefit from this technology.
2) Silver nanoparticles' biological manufacturing has opened the door to a wide variety of potential applications, including those as optical receptors, catalysts in chemical reactions, biolabels, and antibacterial agents. The preceding are just some examples; there are many more.
3) Silver nanoparticles, while being poisonous to cells, have found significant use in a variety of fields. As some examples, we can look at antimicrobials, treatments, catalysis, microelectronics, and extremely sensitive bimolecular detection and diagnostics.
4) Some examples of medical uses include bandages, birth control tools, surgical instruments, artificial bones, biomedical optical imaging for diagnosis, and biological implants like heart valves.

1.8 Synthesis at Room Temperature

Alternanthera dentata was used in the

International Journal of Pharmaceutical Research and Applications
Volume 9, Issue 3 May-June 2024, pp: 437-493 www.ijprajournal.com ISSN: 2456-4494

synthesis of AgNPs, which took about ten minutes at room temperature and resulted in particles that demonstrated antibacterial activity against E. coli, P. aeruginosa, K. pneumonia, and E. faecalis at a concentration of fifty parts per million [46]. The major ingredients in the formation of AgNPs are flavonoids and proteins derived from the leaf extract of Tephrosia purpurea. The size of the AgNPs was determined to be 16 nm, which is in reasonable accord with the XRD data [47]. In a process that took ten minutes and involved the reduction of silver ion by an aqueous extract of Alternanthera sessilis, researchers observed that proteins and ascorbic acid were responsible for the production of AgNPs with a diameter of thirty nanometers [48].

At room temperature, extracts of the leaves of Mangifera indica, Eucalyptus tereticornis, Carica papaya, and Musa paradisiaca were used to synthesize a variety of sizes and forms of AgNPs. The diameters ranged from 10-50 nm (round and irregular), 25-40 nm (round and ovular), 50-65 nm (ovular), and 60-150 nm (ovular). An aqueous extract of Padina tetrastromatica completely reduced the amount of silver ions that were present in the solution after being shaken for 72 hours at room temperature. Using an environmentally safe aqueous extract of A. dubius, researchers were able to successfully produce silver nanoparticles with sizes ranging from 10 to 70 nm [49]. At normal temperature, a bryophyte called Fissidensminutus was able to rapidly produce silver nanoparticles. Metallic AgNPs (10 nm) can be generated at room temperature in just a few minutes by employing aqueous sorghum extract. Argemone mexicana leaf extract was utilized to form cubic (20 nm) and hexagonal (10-50 nm) shaped AgNPs after being exposed to room temperature for four hours. These shapes were reported to be particularly deadly against pathogenic bacteria and fungus at concentrations of thirty parts per million [50]. The methanolic extract of Eucalyptus hybrida leaves was combined at ambient temperature with an aqueous solution of silver nitrate (AgNO3) to form cuboid AgNPs that ranged in size from 50 to 150 nm. Mentha piperita was able to decrease silver ions and form polydisperse AgNPs (5-30 nm) in as little as 15 minutes at room temperature.

1.9 Synthesis at Higher Temperature

The silver ions were converted into AgNPs by heating a mixture of aqueous Withaniasomnifera root extract and aqueous Ag(NO3)2 at temperatures ranging from 60 to 80 degrees Celsius for twenty minutes [53]. The synthesis of AgNPs from Amaranthus polygonoides can be sped up by making use of a methodology that involves a higher temperature, according to a comparative examination into various different methods [54]. The synthesis of AgNPs from the marine seaweed Gracilariacorticata was seen to take place within 20 minutes at a temperature of 60 degrees Celsius [55]. This was indicated by the appearance of a prominent reddish brown colour. Cacumen platycladi contains reducing sugars and flavonoids, both of which are capable of reducing silver to its nanoparticle form (18.4 nm) when heated to 90 degrees Celsius.

When a solution of Cycas leaf extract was treated with 0.25 M AgNO3 solution and then kept on a steam bath for 10 minutes, AgNPs with a diameter in the range of 2-6 nm were generated [57]. These AgNPs were able to withstand high temperatures and have a high surface area. The growth of E. coli and Salmonella typhimurium was completely inhibited by a silver nitrate solution and an extract of Allium cepa at a concentration of 50 g/mL [58]. Continuous stirring at temperatures between 50 and 60 degrees Celsius was used to make AgNPs of an average size. The production of silver nanoparticles with a diameter of 10-20 nm was accomplished by heating silver nitrate and Jatropha curcas latex in an oil bath that was constantly stirred for a period of four hours [59]. When heated to 95 degrees Celsius, the interaction between the broth made from Magnolia kobus leaf and silver nitrate can produce up to 90 percent AgNPs in about 11 minutes [60].

1.10Synthesis Using Microwave Irradiation

When compared to other extracts, orange peel extract was able to produce silver nanoparticles (nm) in 15 minutes during the microwave-assisted manufacture of AgNPs from citrus fruit peels (orange, grapefruit, tangelo, lemon, and lime) [54]. Spherical AgNPs of 15-20 nm size that were synthesized using the seed extract of Acacia farnesiana (sweet acacia) were microwave-irradiated to increase their antibacterial activity [56]. This activity was demonstrated against Escherichia coli, Staphylococcus aureus, Bacillus subtilis, and Pseudomonas aeruginosa.

An extract of cuminum cyminum seed powder and a solution of silver nitrate were combined in a ratio of 1:10 and irradiated in a

International Journal of Pharmaceutical Research and Applications
Volume 9, Issue 3 May-June 2024, pp: 437-493 www.ijprajournal.com ISSN: 2456-4494

home microwave for a total of one minute and twenty seconds to form AgNPs [57]. Within eight to ten minutes, silver nanoparticles were generated using an extract of Cymbopogon citratus (Lemongrass) with a pH of 8.0 and 90 watts of microwave radiation. Irradiation with microwaves results in the most effective transformation of silver ions into nanoparticles. The use of this method results in particles that have a more uniform shape and a more restricted size range.

1.11 Synthesis by Sonication

When generating silver nanoparticles from Portulaca oleracea, it was demonstrated that sonication was substantially more effective than both the ambient temperature setting and the higher temperature setting [55]. It was determined that the accelerating effect that sonication had on the chemical dynamics and reaction rates was responsible for the homogeneity of the AgNPs that were formed from Pisonia grandis. It is possible that the pathway for chemical synthesis was messed up because ultrasonic radiation causes the creation of free radicals.

1.12 Light Induced Synthesis

Polydispersed silver nanoparticles of size 8-10 nm were swiftly created utilizing a simple procedure employing Cynodondactylon leaf extract under direct sunlight [51]. This process began with aqueous silver nitrate and produced the nanoparticles. It has been shown that adding extract of Solanum trilobatum Linn to shampoo increases the antidandruff effect against fungal infections (Pityrosporumovale and Pityrosporum folliculitis). The extract, when subjected to the irradiation of sunlight, formed AgNPs in the form of cubic and hexagonal structures measuring 15-20 nm. Irradiating a solution containing silver nitrate and Euphorbia milii with a xenon lamp following exposure to ultrashort laser pulses resulted in a significant reduction in the size of the AgNPs, which were reduced to a range of 10-50 nm [55-60].

II. LITERATURE REVIEW

Hao Zhang et.al.,(2022): Many studies have been conducted to learn what kind of ablative qualities epoxy-modified vinyl silicone rubber (EMVSR) composites with hexa phenoxy cyclo tri phosphonitrile have (HPCTP). The studies with oxyacetylene ablation produced a char that was more complete, dense, and thick as a result of the inclusion of HPCTP to the procedure[61].

Quain kang et.al., (2022): We have neglected to recognize the significant part that ice plays in the cooking process. While looking into a local delicacy known as "ice-stewed mutton," we came across the fact that freeze/thaw-induced cavitation can cause negatively charged bulk nanobubbles (BNBs) to be produced in water that has been melted by ice.

Ibraheem et al., (2022): Silver nanoparticles, also known as AgNPs, have been found to contain a wide variety of physicochemical, biological, and functional properties. Two of these properties are the ability to operate as a drug carrier and an antibacterial agent.

Mohsen et al.,(2020): By loading ciprofloxacin (CIP) antibiotic onto silver nanoparticles (AgNPs) made in three different ways, antibacterial activity was improved against Gram-negative (Escherichia coli) and Gram-positive (Staphylococcus aureus) bacteria. A combination of sodium borohydride (NaBH4), lactose, and sodium citrate was utilised, and the mixture was aged for a full year in order to produce AgNPs with a consistent prism form. This was accomplished by using the combination. In the end, a composite material consisting of AgNPs and CIP was created from the AgNPs that were synthesised. For the purpose of characterising the nanocomposites that were formed, various techniques such as transmission electron microscopy (TEM), Fourier transform infrared spectroscopy (FTIR), and ultraviolet-visible (UV-Vis) absorption spectra were all utilised[64].

Anotonionet.al., (2022): In recent years [65], there has been an increased focus placed on the scientific research that underpins the hydrogen evolution process, also known as HER. This process occurs in environments that are alkaline. This is mostly due to the fact that the method can be applied to the achievement of a diverse range of objectives.

Shariati et.al.,(2022): Ciprofloxacin is a fluoroquinolone (FQ) antibiotic that has been on the market for close to thirty years. It has been utilised for the treatment of chronic otorrhea, endocarditis, lower respiratory tract, gastrointestinal, skin and soft tissue, and urinary tract infections[66]. Ciprofloxacin's principal mode of action is to stop the replication of DNA by blocking the A subunit of DNA gyrase.

SamsaulRizamet.al.,(2022): Foods that are individually wrapped in plastic are harmful to both people and the environment[67]. Cinnamon

International Journal of Pharmaceutical Research and Applications
Volume 9, Issue 3 May-June 2024, pp: 437-493 www.ijprajournal.com ISSN: 2456-4494

nanoparticles were created by a process known as solvent casting, and they were subsequently incorporated into biopolymer sheets that were fabricated from red seaweed (Kappaphycusalvarezii). Cinnamon was added to the matrix network of the film at concentrations of 1%, 3%, 5%, and 7% weight-per-weight, and this resulted in an improvement of the film's characteristics.

Sara Oudi et.al., (2022): In the presence of solvothermal conditions, the combination of 1,4-benzenediboronic acid (DBBA) with 5,10,15,20-tetrakis-(3,4-dihydroxyphenyl)porphyrin (DHPP) led to the formation of the porphyrin-based covalent organic framework (COF) known as Porph-UOZ-COF[68]. The complete abbreviation for "University of Zabol," which is commonly referred to simply as "UOZ," is quite a bit longer than its beginnings. Spectroscopy, scanning electron microscopy, and powder X-ray diffraction were some of the techniques that were utilised during the characterization process.

R.suprabhaet.al.,(2022): Because of the specific requirements they have for day-to-day operations, the solar, heat exchanger, and chemical sectors absolutely require high-performance cooling systems. Because they can transfer heat energy more effectively than other fluids, nanofluids based on metal oxides have thermal characteristics that are superior to those of other fluids[69].

Songitasonwalet.al.,(2022): The term "magnetic nanobiochar" refers to a particular type of nanobiochar that possesses heightened magnetic properties (MNBC). For the manufacturing of MNBC, feedstocks such as wood chips, agricultural waste, sewage sludge, animal manure, and other organic waste are required..

L. taryanet.al., (2021): In the 20th and 21st centuries, materials that were heavier, less bendable, and more traditional have been replaced with ones that are lighter and more malleable. There is a very good chance that this pattern will continue on long into the 22nd century[71].

Mostafa et.al., (2021): This topic has been propelled to the top of the list of priorities for the scientific community as a direct result of the development of nanomaterials for use in cutting-edge biomedical applications[72].

Knebel et.al.,(2021): MOFs and COFs, respectively an inorganic-organic hybrid material and a totally organic material, have the potential to drastically alter the landscape of gas separation membranes[73].

III. AIM AND OBJECTIVES

3.1. Aim

Formulation and Evaluation of Ciprofloxacin-loaded Silver nanoparticles with Zinc oxide as potent nano-antibiotics against resistant pathogenic bacteria.

3.2. Objectives

- Recent years have seen an uptick in the usage of zinc oxide nanoparticles (ZnO NPs) in plant science and agricultural studies, making them one of the most widely produced and used nanomaterials worldwide. The purpose of this investigation was to synthesise Ciprofloxacin-loaded Silver nanoparticles with Zinc oxide as potent nano-antibiotics against resistant pathogenic bacteria.
- This method cuts down significantly on the amount of time needed to get the desired size of the nanoparticles. Even though there has been a significant amount of study conducted on the antibacterial effects of zinc oxide and silver nanoparticles (ZnO and Ag NP), there is still opportunity for advancement.
- Green synthesis of silver nanoparticles and ZnO (chemical reduction method) and detailed analysis of both.
- Transmission electron microscopy (TEM), X-ray diffraction (XRD), Fourier transform infrared spectroscopy (FT-IR), and ultraviolet-visible spectroscopy (UV-vis) were used to characteriseZnO NPs.
- It is absolutely necessary to have a comprehensive understanding of the structural and functional repercussions of protein-nanoparticle interactions in vivo. In addition, in order to have a complete understanding of nanoparticle-mediated cell death, one must be aware of the precise effect that NP have on the structure of proteins and the biological activities of cells after they have passed through the cell membrane.
- It is equally important to gain an understanding of the effect that nanoparticles have on the amounts of mRNA expression in live beings. It has been demonstrated that the employment of molecular and chemical chaperones in industrial settings can successfully boost the levels of activity and expression of a wide variety of enzymes that are ordinarily expressed at lower levels.

International Journal of Pharmaceutical Research and Applications
Volume 9, Issue 3 May-June 2024, pp: 437-493 www.ijprajournal.com ISSN: 2456-4494

IV. PLAN OF WORK

A. Literature survey and procurement of materials

B. Pre formulation Studies

- **Identification of Drug**
- ✓ Physical appearance
- ✓ Melting point
- ✓ U V Spectroscopy
- ✓ FTIR Spectroscopy
- ✓ XRD Analysis
- ✓ Electron microscopy

C. Preparation and optimization of the formulation

D. Characterization of formulation.

- Appearance
- pH
- Viscosity
- Syringibility study
- Gelling temperature
- Gelling time
- Total drug content

E. Photosynthetic Pigments and Total Soluble Protein in Response to ZnO Nanoparticles

A. In vitro drug release

B. Stability studies

- Effect of storage temperature on appearance and clarity
- Effect of storage temperature on viscosity

V. DESCRIPTION OF DRUG

- **5.1. Ciprofloxacin**

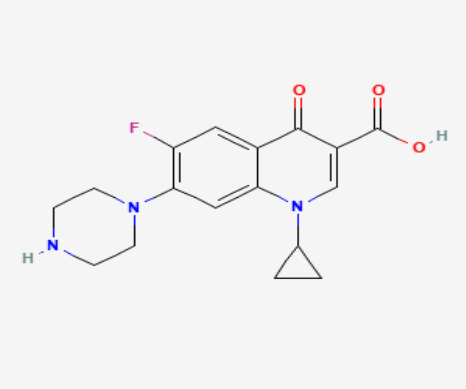

Fig 5.1: Chemical Structure of Ciprofloxacin

- **IUPAC Name:**
- 1-cyclopropyl-6-fluoro-4-oxo-7-(piperazin-1-yl)-1,4-dihydroquinoline-3-carboxylic acid hydrate hydrochloride
- **Chemical Formula:** $C_{17}H_{21}ClFN_3O_4$
- **Synonyms:** Ciprofloxacin hydrochloride, Ciprofloxacin hydrochloride hydrate, Ciprofloxacin hydrochloride monohydrate, Ciprofloxacin HCl
- **Molecular formula:**
- **Molecular weight:** 331.346 g/mol
- **Density:** 1.5 ±0.1 g/cm^3
- **Molecular State:**
- **Melting point:** 581.8^{0}c
- **Colour:** White
- **Partition coefficient:** 1.32± 0.03
- **Drug formulation type: Orally, intravenously and in topical formulations**
- **Solubility:** It is insoluble in water but soluble in 0.1N hydrochloric acid, methanol, and DMSO(<1 mg/ml).
- **Mode of action:** It is a fluoroquinolone of the second generation called ciprofloxacin, and it has the ability to eradicate a wide variety of bacteria, both beneficial and harmful. The action of the medicine is achieved by inhibiting the enzymes DNA gyrase and topoisomerase IV, which are both found in bacteria. Ciprofloxacin has a binding affinity for bacterial DNA gyrase that is one hundred times greater than that for mammalian DNA gyrase.
- **Storage condition:** Keep at a location that is cool, dry, and has enough of ventilation while storing in an airtight container. Protect your body from potential injury.
- **Uses:**Since ciprofloxacin is a broad-spectrum antibiotic, it can be used to treat a wide variety of bacterial infections, including but not limited to the following: Urinary tract infections (UTIs) , Infections of the chest such as pneumonia, Infections of the skin and bones, Diseases spread between sexual partners, Eye infections caused by conjunctivitis, Infections of the ear that have not responded to conventional antibiotics; it is also used to reduce the risk of meningitis in those who have come into close contact with someone who has the disease.

International Journal of Pharmaceutical Research and Applications
Volume 9, Issue 3 May-June 2024, pp: 437-493 www.ijprajournal.com ISSN: 2456-4494

5.2. Zinc oxide

Fig 5.2: Chemical Structure of Zinc Oxide

Chemical name: Zinc oxide
IUPAC Name:oxozinc
Synonyms: Calamine, Chinese white, Zinc white, Philosopher's wool, Flowers of zinc
Molecular formula: ZnO
Molecular weight: 81.38 g/mol
Density: 5.6 g/cm^3
Molecular State: Solid
Melting point: 1975^{0}c
Colour: White

- **Partition coefficient:** Expansion coefficients for volumes are measured and found to increase from near zero in the 10-80 K range to 4.77 x 10-5 K-1 at 298 K, where they essentially plateau.
- **Drug formulation type:** There is a lot of potential for zinc oxide, often known as ZnO, to be used as a preservative in pharmaceutical or cosmetic products. It is possible that the antibacterial actions of ZnO will be altered by the other compounds used in the formulations.
- **Solubility:** It is insoluble in water but soluble in dilute acids and bases.
- **Mode of action:** It is believed that ZnO works by generating reactive oxygen species. These species subsequently promote membrane lipid peroxidation and contribute to the leaking of reducing sugars, DNA, and proteins across the membrane. This results in a decrease in the viability of the cell.
- **Storage condition:** Keep at a location that is cool, dry, and has enough of ventilation while storing in an airtight container. Protect your body from potential injury.

- **Uses:**
- Zinc oxide has anti-inflammatory properties, which means that when it is applied topically, it can both soothe and prevent small skin irritations and abrasions from occurring. When applied directly to the affected area, it has been demonstrated to expedite the healing process of diaper rash as well as other types of dry skin. Zinc oxide is a beneficial substance because it inhibits the growth of microorganisms and has a little astringent quality.
- Zinc oxide is an ingredient used in a number of diaper rash treatments and preventatives. It works to soothe skin irritation caused by contact with the diaper. The majority of the time, modest dosages are utilized for the therapy of diaper rash as well as its control (like 15 percent). Given the possible absorbency of diapers, high concentrations of these solutions (up to 40 percent) are routinely used to treat rashes caused by diapers. This makes perfect sense given the nature of diapers.

VI. MATERIAL & METHODS

Table 6.1: List of Chemicals &Glasswares

Chemical Name	**Company Name**
Zinc nitrate	Himedia, Mumbai, India
Sodium hydroxide	Himedia, Mumbai, India
Silver nitrate	Himedia, Mumbai, India
Peptone	Merck, India
Sodium chloride	Merck, India
Glass ware	**Company Name**
Conical flasks	Borosil, India
Measuring cylinders	Borosil, India
Beakers	Borosil, India
Petri plates	Borosil, India
Test tubes	Borosil, India

International Journal of Pharmaceutical Research and Applications
Volume 9, Issue 3 May-June 2024, pp: 437-493 www.ijprajournal.com ISSN: 2456-4494

6.1. Synthesis of ZnO NPs

The production of zinc oxide nanoparticles was achieved by making some relatively minor adjustments to an established protocol. After mixing in 6.0 grams of zinc acetate dihydrate ($Zn(NO_3)_2$•$2H_2O$) (Sigma-Aldrich) to 100 milliliters of extract and allowing the mixture to settle at 60 degrees Celsius with a magnetic stirrer for two hours, the extraction was completed. After allowing the mixture to cool for ten minutes at a temperature of 25 degrees Celsius, it was centrifuged using a HERMLE Z326K at a rate of 10,000 revolutions per minute in order to separate out any unreacted product. After giving the pellet three washes with distilled water, it was placed on a clean Petri plate, and then it was dried in an oven at 90 degrees Celsius. Following the step of air drying the material, it was next crushed using a mortar and pestle and calcined for two hours at a temperature of 500 degrees Celsius in order to remove any lingering impurities. After being hermetically sealed in an airtight glass container and labeled as ZnO-NPs, the annealed powder was subjected to additional physical characterizations as well as biological applications.

6.1.1. Chemical Synthesis of pure Zinc oxide (ZnO)

ZnO nanoparticles were manufactured by the use of the sol-gel process and zinc acetate (Zn(CH3COO)2. 2H2O, extremely pure AR, grade material from SRL, India) (Figure 6.1). Before adding a (1:1/vol) ammonia solution (Merck India) to the combination in an effort to keep the pH lower than 7.5, the required quantity of zinc acetate was dissolved in triple-distilled water (TDW), which was then used to mix the ingredients together. This was done while maintaining the solution's temperature at room temperature. At first, the zinc was present as zinc hydroxide precipitate. After being recovered using centrifugation, the precipitate was reintroduced into TDW in order to undergo ion removal. At the end, the precipitate was collected once again, and then it was dried at a temperature of 100 degrees Celsius to obtain ZnO.

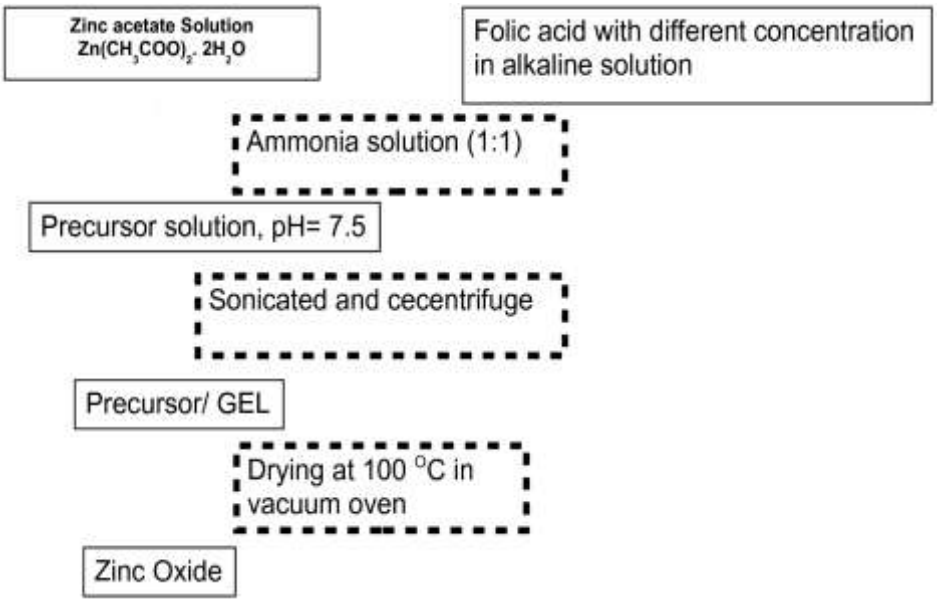

Fig: 6.1 Chemical method for producing ZnO nanoparticles using folic acid as a mold.

6.2. Preparation of ciprofloxacin Ag-NP

Cipro was administered at a dosage of 0.6 grammes per 50 millilitres of water on a regular basis. The Cipro AgNPs nanocomposite was made by combining a Cipro solution with a certain amount of AgNPs (0.1 gm/50 ml), which resulted in the nanocomposite. In order to enhance Cipro absorption, the material was subjected to magnetic agitation for a period of 18 hours. Following centrifugation, the sample was put through a total of five washes in deionized water in order to eliminate any lingering nanocomposites. Cipro AgNPs is the name given to nanocomposites that are composed of Cipro and AgNPs.

International Journal of Pharmaceutical Research and Applications
Volume 9, Issue 3 May-June 2024, pp: 437-493 www.ijprajournal.com ISSN: 2456-4494

6.3. Pre-formulation Studies

During the preformulation phase of drug development, formulation scientists must first characterise the qualities of new medicinal ingredients, including their physical, chemical, and mechanical properties. This is necessary so that they may build dosage forms that are stable, safe, and effective.

6.3.1 Organoleptic Properties

6.3.2 In order to examine the hue, we spread some ciprofloxacin hydrochloride powder that was 100 percent pure across a sheet of white paper and viewed it under adequate illumination. In order to identify the odour and taste of ciprofloxacin hydrochloride on the tongue, extremely small dosages of the drug were consumed.

6.3.2. Solubility test

Experiments on CIP's solubility were carried out in distilled water as well as in PBS (with a pH of 7.4) because CIP is a drug that dissolves very poorly in water and has a U-shaped pH-dependent solubility curve with a pH-dependent minimum around 7.4. The pure drug, the physical combination, and the drug-loaded nanofibrous samples were mixed with 3 mL of distilled water (pH 6.3) or phosphate-buffered saline (pH 7.4) for twenty-four hours at room temperature using a magnetic bar. The solution was either phosphate-buffered saline or phosphate-buffered water. Samples were filtered (0.22 mm, FilterBio PES Syringe Filter; Labex Ltd., Budapest, Hungary), properly diluted, and tested with water and PBS at 275 nm and 271 nm, respectively, before to being measured by UV spectrophotometry (ABL&E-Jasco UV/VIS Spectrophotometer V-730, Budapest, Hungary). This was done before the samples were measured by UV spectrophotometry. The solubility tests were carried out three times on each sample, and the results, including the mean and standard deviation, are reported here

6.3.3. Melting Point

In a capillary apparatus, the melting points of known concentrations of ciprofloxacin hydrochloride were recorded and compared to standards.

6.3.4. Loss on drying

About 5 grammes of each dentifrice were placed in porcelain crucibles and weighed on a precise scale made by BEL Engineering®, which was located in Piracicaba, SP, Brazil. After that, the crucibles that had been filled with dentifrice were placed in an oven (Odontobras®, Ribeiro Preto, SP, Brazil) for twenty-four hours at 105 degrees Celsius. After the period of time that had been given had passed, the samples were reweighed on a precision scale until they were exactly the same as the weight that had been recorded initially. The values for drying loss were determined by applying Eq. (1) to the data.

Loss on drying (LOD) Calculation

$$\% \text{ of Loss on drying} = \frac{\text{Weight loss}}{\text{Weight of sample}} \times 100$$

Where,

Weight of the Sample = (B-A) mg

Weight Loss = (B-C) mg

6.4. Drug Powder Characterisation

Angle of repose:

Calculation of the angle of repose was done with the help of the funnel method. In order to

International Journal of Pharmaceutical Research and Applications
Volume 9, Issue 3 May-June 2024, pp: 437-493 www.ijprajournal.com ISSN: 2456-4494

gather the mixture that had been carefully measured, a funnel was utilised. A modification was made to the height of the funnel such that its spout now just barely brushes the top of the mix mound. We were able to calculate the angle of repose by first measuring the diameter of the powder cone, and then entering those values into the following equation.

Tanθ =h/r

Where,

H= Height

R= Radius

Bulk density

After that, the mixture was put into a graduated cylinder so that the apparent bulk density could be determined. We were able to determine both its mass and its bulk volume (Vb).

Bulk density = M / Vb

Tapped Density

In accordance with USP apparatus-11, a fixed number of taps were made on the measuring cylinder that contained the powder mixture. After the tapping, the volume of the powder was determined to be as little as it could possibly be.

Tapped density = weight/tapped volume

Measurement of powder Compressibility:

The following formula, which took into consideration both the apparent bulk and the tapped density, was used to calculate the percentage compressibility of the mass, which was expressed as a percentage.

$$\text{Compressibility index: } = 100\frac{(V_0 - Vf)}{V_0}$$

➢ Where, Vf = final tapped volume, Vo = initial un tapped volume

6.5. Compatibility studies

Drug excipients compatibility studies by FT-IRFTIR spectroscopy was utilised so that the kinetics of drug-polymer interactions could be investigated. FTIR analyses were carried out on pure drugs, excipients, as well as drug and excipient combinations that were physically mixed. The spectra were acquired by scanning from 400 to 4000 cm-1 using an FTIR spectrophotometer, which stands for a Fourier transform infrared spectrophotometer.

6.6. Preparation of standard curve stock solution & standard solution

The volumetric flask that was used to make the stock solution A held a solution of 0.1 M hydrochloric acid to which 0.050.0001 g of ciprofloxacin hydrochloride had been added. The flask was used to manufacture the stock solution A. In order to produce the standard solutions for the calibration curve, the stock solution A was first quadratically diluted with 0.1 M hydrochloric acid. We tested five different solutions with doses of 2, 4, 6, 8, and 10 g/mL and assessed their absorbance at 278 nm. After ensuring the correctness of each measurement by performing it three times, the data was subjected to statistical analysis.

6.7. Evaluation parameter:

The evaluation parameters are as follows for the purpose of determining the physiochemical properties of the medicament and the excipients.

The thickness of the tablet

Hardness Based on Weight Variation

Evaluation of brittleness

A test of floating

Swelling index

Invitro drug release

Weight variation

The average weight of ten tablets was determined after each tablet was weighed independently and then all of the tablets were weighed together.

Drug content

The medication was extracted in phosphate buffer with a pH of 6.8, and the solution was filtered using Whatman filter paper. Tablets were weighed individually (n = 5 total), and the pH of the buffer was 6.8. After the necessary dilution, absorbance was determined at a wavelength of 227 nm by employing a Shimadzu UV-1601 UV/Vis double-beam spectrophotometer.

Friability

Using a Roche Friabilator, the tablets were broken up to determine their level of friability. In this particular experiment, six tablets were first weighed before being dusted and re-weighed after being put through a combination of abrasion and shock in the plastic chamber of the Friabilator, which rotated at a speed of 25 revolutions per minute (rpm) for a period of four minutes.

International Journal of Pharmaceutical Research and Applications
Volume 9, Issue 3 May-June 2024, pp: 437-493 www.ijprajournal.com ISSN: 2456-4494

Thickness

In order to determine the exact thickness of the buccal tablets, a micrometre screw gauge was utilised. The thickness of ten tablets from each batch was measured to obtain an average value.

Hardness

A Pfizer hardness tester was utilised to ascertain the level of brittleness possessed by the tablets. It is generally agreed that a tablet's hardness of between three and four kilogrammes meets the requirements for appropriate mechanical stability. The evaluations were carried out three times for accuracy.

Dissolution test:

Before the capsule was introduced, the water in each of the six jars that made up the dissolution apparatus had been brought to a temperature of 37 0.5 degrees Celsius. After 5, 10, 20, 30, 40, 60, and 70 minutes had passed, a sample volume of 5 millilitres was drawn from each vessel. In order to maintain the medium's volume at a consistent level, any water that was removed was immediately replaced with an equal quantity of water that was maintained at the same temperature. After filtering the sample solution using whatman filter paper, a volume of 2 millilitres was taken out and diluted to volume with distilled water in a volumetric flask that held 10 millilitres for the purpose of quantitative analysis. The absorbance of the solution was measured using a wavelength of 272 nanometers.

6.8. kinetic Data drug release

Matrix systems are a useful illustration of how critical and difficult it can be to assess the drug release mechanism originating from a pharmaceutical dosage form. In order to find a model-dependent strategy that would best fit the dissolution data, we employed five different release models, the most common of which were zero-order, first-order, diffusion, and exponential equations. Either zero order kinetics or first order kinetics were utilised in the process of describing the dynamics of drug release in matrix systems. We studied the mechanism of drug release from matrix systems by using the Higuchi equation as well as the peppas-Korsmeyer equation.

Zero order kinetics

A linear link between the fractions of drug released and the passage of time is established by this.

Q = kot

Where Q is the amount of medication that has been released at time t and ko is the constant for the zero order release rate.

First order kinetics

The absorption and/or elimination of some medications have also been described using this approach, albeit doing so theoretically is challenging. The equation for the drug's first-order kinetic release is as follows:

logC=logC0ñKt/2.303

(28), in where C0 denotes the concentration of the medication prior to the start of the experiment, k denotes the first order rate constant, and t denotes the passage of time. Plotting the provided data as log cumulative percent-age of medicine remaining versus time will result in the creation of a straight line with a slope of K/2,303. This line can be constructed by plotting the data in a logarithmic format.

Higuchi model:

The first example of a mathematical model aimed to describe drug release from a matrix system was proposed by Huguchi in 1961 (31). Initially conceived for planar systems, it was then extended to different geometrics and porous systems (32).This model is based on the hypotheses that(i) initial drug concentration in the matrix is much higher than drug solubility; (ii) drug diffusion takes place only in one dimension (edge effect must be negligible); (iii) drug particles are much smaller than system thickness; (iv) matrix swelling and dissolution are negligible; (v) drug diffusivity is constant; and (vi)perfect sink conditions are always attained in the release environment .Accordingly, model expression is given by the equation:

$$f_t = Q = A \sqrt{D\,(2C - C_s)\,C_s\,t}$$

where Q is the amount of medication that is released in time t per area unit. The starting concentration of the drug is denoted by the letter C, the solubility of the drug in the matrix medium is denoted by the letter Cs, and the diffusivity of the drug molecules, which is denoted by the letter D, is

International Journal of Pharmaceutical Research and Applications
Volume 9, Issue 3 May-June 2024, pp: 437-493 www.ijprajournal.com ISSN: 2456-4494

found in the matrix substance. This relation holds true at all times, with the sole exception of the point at which the entire supply of the drug in the therapeutic system has been used up.

Korsmeyer -peppas model:

It is used to characterise the release of drugs from polymeric systems when non-fickian mechanisms are taken into consideration. This approach is helpful in situations in which the mechanism responsible for drug release is unknown or in which more than one sort of drug release phenomenon is at play. Even though Peppas (1985) states that this model is only applicable for the first 60% of the release curve, we nonetheless analysed it in both the 60% and 100% drug release profiles. Even so, this model is only applicable for the first 60% of the release curve.

$$\ln(Q_t) = \ln(k_{KP}) + n\ln(t)$$

Where: Qt = percentage of the released drug after time t.
kKP = constant of nanoparticles incorporating geometric characteristic structures.
n = release exponent (related to the drug release mechanism).
t = time.
Weibull: It is an empirical model that serves as a theoretical basis for almost all release kinetics in heterogeneous matrices.
It represents a distribution function describing a phenomenon associated with a finite time

SEM Analysis

An FEI Quanta 600F scanning electron microscope (located in Oregon, United States) was utilised in order to get images of the samples. After affixing the samples to carbon tabs and mounting them on aluminium pins, we used an Emitech K550 to sputter-coat the samples with gold for three minutes while applying 30 milliamps of current. In order to evaluate the particle size and morphology, images were first captured in a high vacuum and then enhanced by making adjustments to the brightness, contrast, and astigmatism.

TEM Analysis

TEM images were used to examine the morphology and size of the silver nanoparticles. Very little amounts of the sample were dropped onto a carbon-coated copper grid, the excess solution was blotted off using paper towels, and the film was dried overnight in a TEM.

Antibacterial activity

For the purpose of determining whether or not AgNPs, CIP, AgNPs-CIP, AgNPs-PEG, and AgNPs-PEG-CIP have a synergistic effect on the growth of S. aureus, A. baumannii, and S. marcescens bacterial suspensions, Mueller-Hinton agar media was utilised. In accordance with the McFarland standard, suspensions were made to have 1.5 108 CFU mL1 in each millilitre. After swabbing each bacterial suspension onto a plate of Mueller-Hinton agar medium, six wells were punched out of each plate using a sterile well cutter. The diameter of each well was 8 millimetres. The plates were then incubated with the bacterial suspensions. In the wells, bacteria were seeded with either 80 litres (L) of AgNPs, CIP, AgNPs-CIP, AgNPs-PEG, or AgNPs-PEG-CIP. Deionized water was utilised so that we could make a comparison. After incubation at 37 °C for 24 hours, the inhibition zones surrounding each well were measured (to the nearest millimetre) in order to assess the antibacterial activity of AgNPs, CIP, AgNPs-CIP, AgNPs-PEG, and AgNPs-PEG-CIP. This was done by viewing and measuring the zones around each well. Before and after the addition of PEG-400 and AgNPs, the diameters of the inhibitory zones were determined, and the findings were compared using the following equation:

$$\text{Fold increase (FI)} = [(b-a)/a] \times 100$$

6.9. Statistical Analysis

The data are presented in such a way as to highlight both the median value and the range of values. A one-way analysis of variance (ANOVA) and duncan's multiple ranges test were each performed on the data sets in order to evaluate whether or not there were statistically significant differences between the treatments (P>0.05 and P>0.01, respectively).

VII. RESULT & DISCUSSION

7.1. Pre-formulation studies

The results of the tests, which were carried out in accordance with the guidelines, are presented in the table 7.1.

7.1.1. Organoleptic property:

International Journal of Pharmaceutical Research and Applications
Volume 9, Issue 3 May-June 2024, pp: 437-493 www.ijprajournal.com ISSN: 2456-4494

Table7.1. Organoleptic qualities assessed through sensory analysis:

Finding	Observation
Color	Pale-yellow
Odor	Odor-less
Taste	Taste-less

7.1.1. Solubility testing:

Ciprofloxacin hydrochloride samples demonstrated solubility in water, soluble in just a little quantity of a solution of and soluble with dimethyl formamide when they were put through the appropriate tests. Additionally, it is soluble in fluids that are slightly alkaline and slightly acidic.

7.1.2. Drug melting point:

The boiling point of ciprofloxacin hydrochloride was determined using the capillary technique. 255 degrees Celsius is the melting point established for ciprofloxacin hydrochloride. The melting point of the pharmaceutical was measured in relation to the USP's standards, proving its purity.

Table-7.2.Observationsforlosson drying

Testing	Lossondrying	Observation
Loss on drying	No more than 0.8%	0.45%

7.1.3. Loss on drying:

Following the steps outlined in 6.2.4, the answer was found. Table 7.2 displays the results.

7.2. **Powder drug characterization:**

7.2.1. Angle of repose:

Values were used to make the calculation; the final tally may be shown in table 7.3.

Table: 7.3. Angle. of repose

Item	Angle of. repose value
CFH	29.09

According to the findings, the raw material possesses superior flow properties.

7.2.2. Flow Property:

It was calculated based on the values, and the outcomes are shown in table 7.4.

Table7.4: The Importance of Pure Drug Flow Properties

Item	Bulk density values	Tapped density values	% Carr's index	Ratio of Hausner %
CFH	0.26	0.48	12.05	1.144

Good flow properties were observed for the ciprofloxacin hydrochloride raw material, as shown by the results.

7.3. Polymer and drug compatibility tests:

FTIR STUDY:

The FTIR spectra of the pure drug, the excipient, and the drug/excipient physical mixture were all obtained between 400 and 4000 wave number (cm-1). There aren't any other peaks that can be seen that could possibly be affecting the primary drug peaks in any way. The IR spectra of the drug and the polymer are presented in the accompanying table and spectrum, along with the

International Journal of Pharmaceutical Research and Applications
Volume 9, Issue 3 May-June 2024, pp: 437-493 www.ijprajournal.com ISSN: 2456-4494

number of waves of their respective characteristic bands.

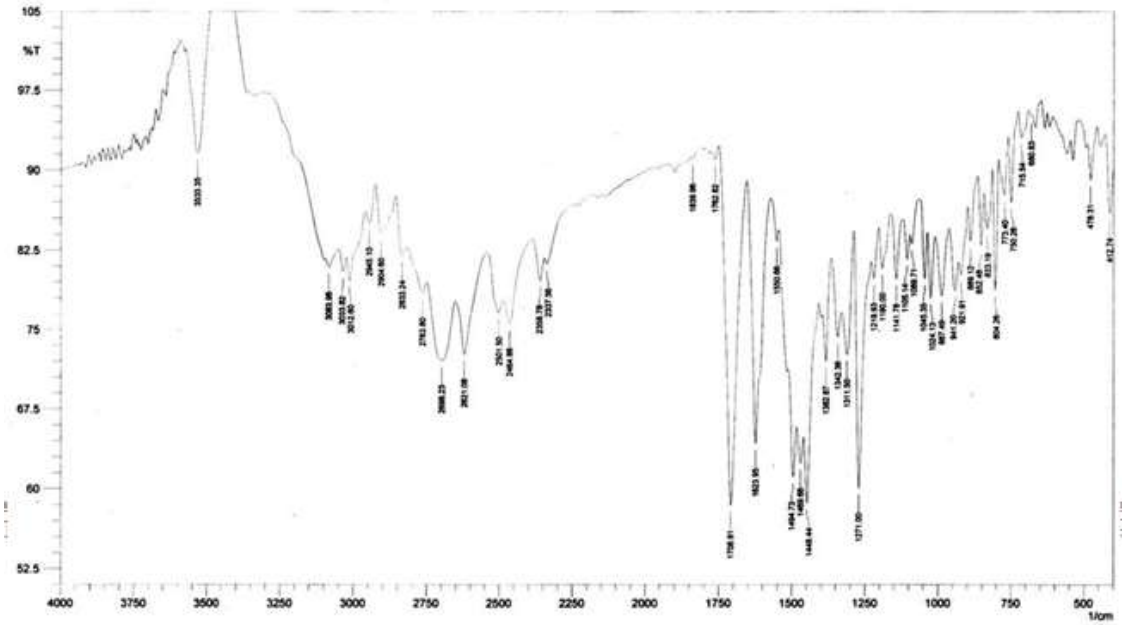

Figure:7.1. The infrared spectrum of a standard for ciprofloxacin hydrochloride

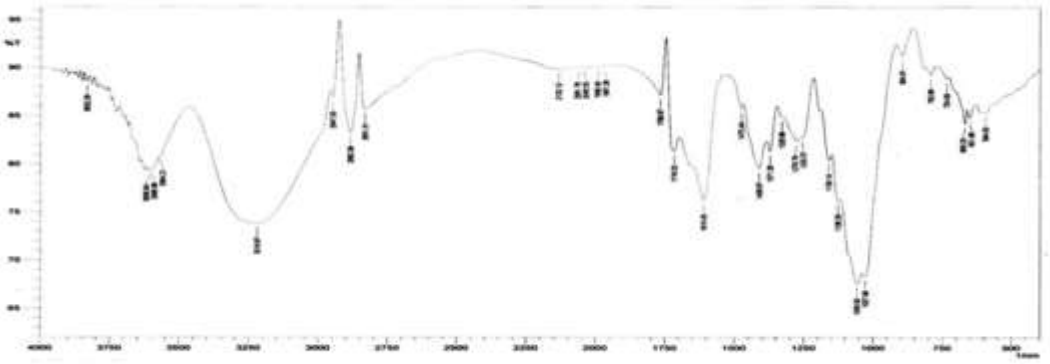

Figure:7.2 Xanthan gum's Infrared Reflectance Spectrum

International Journal of Pharmaceutical Research and Applications
Volume 9, Issue 3 May-June 2024, pp: 437-493 www.ijprajournal.com ISSN: 2456-4494

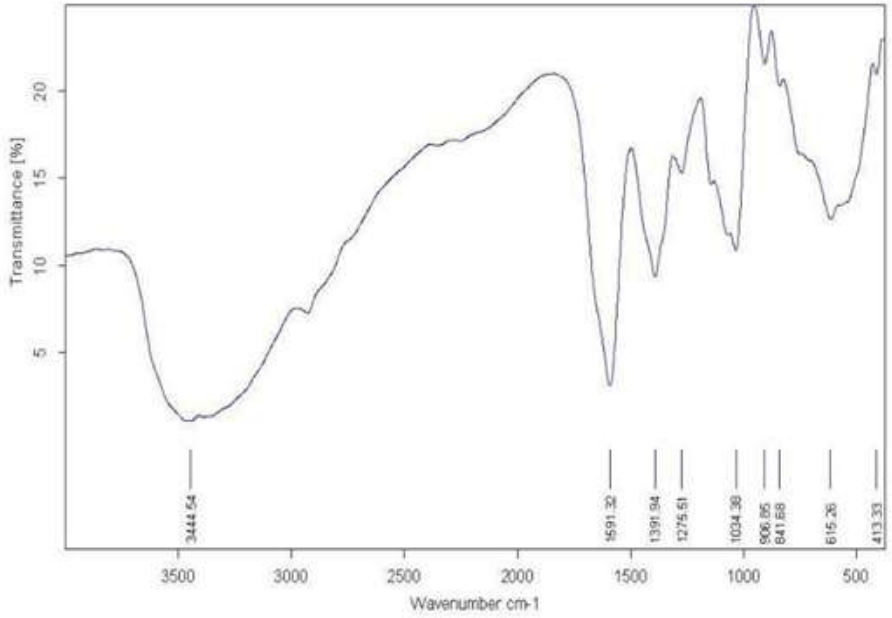

Figure7.3. IRSpectrumofguargum

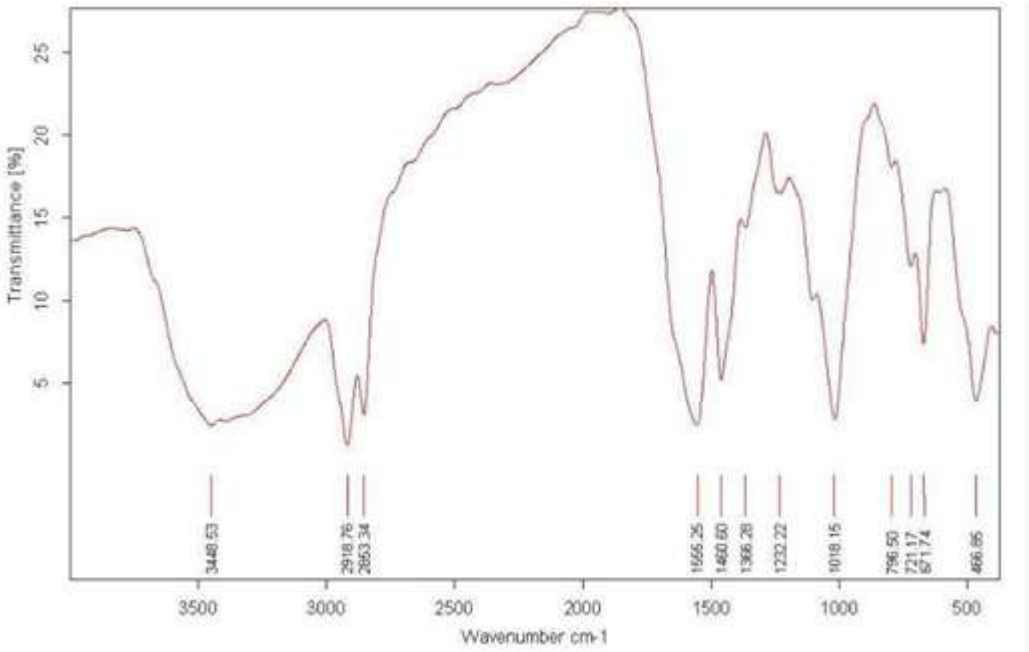

Figure:7.4. Spectra infra-red magnesium stearate

International Journal of Pharmaceutical Research and Applications
Volume 9, Issue 3 May-June 2024, pp: 437-493 www.ijprajournal.com ISSN: 2456-4494

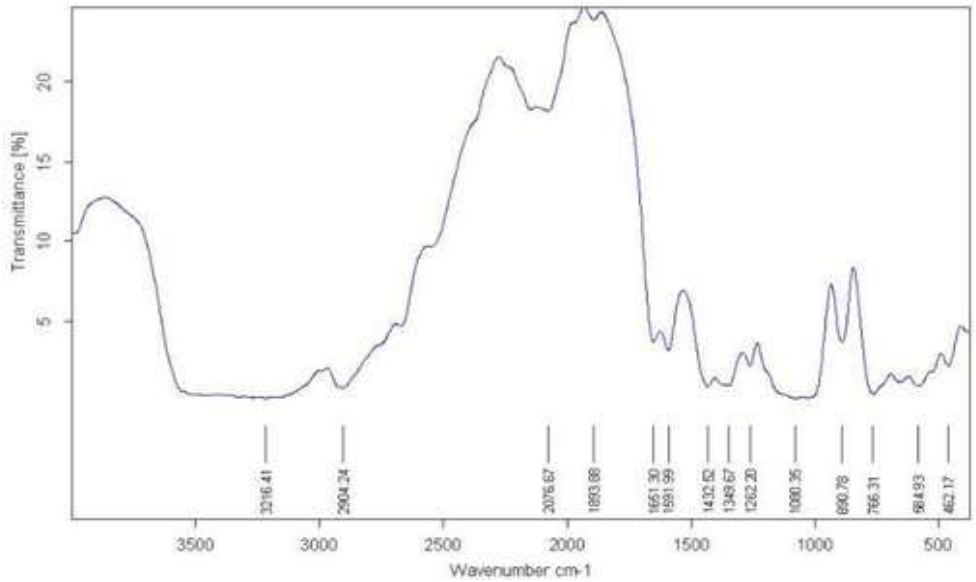

Figure:7.5. Spectra infrared lactose

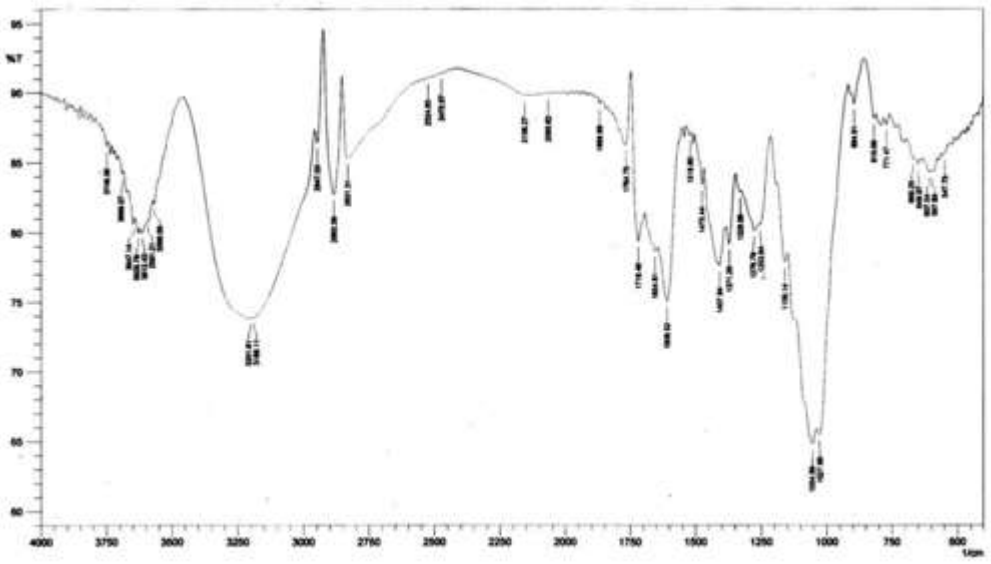

Figure:7.6. A comparison of the infrared spectra of xanthan gum and ciprofloxacin hydrochloride

International Journal of Pharmaceutical Research and Applications
Volume 9, Issue 3 May-June 2024, pp: 437-493 www.ijprajournal.com ISSN: 2456-4494

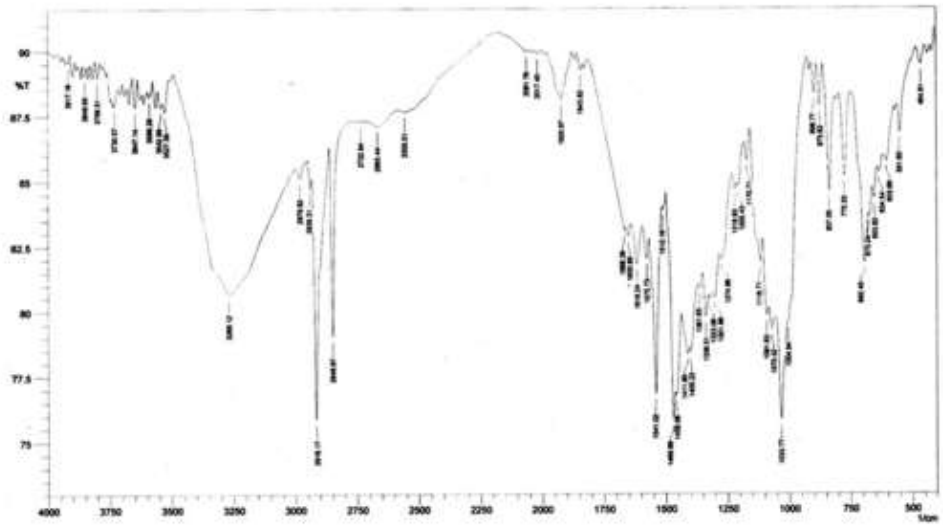

Figure:7.7. Polymers and excipients in the infrared spectrum

Table:7.5. FT-IR Peaks of a Number of Different Components

Pure drug peak (cm^{-1})	Functional groups	Vibration types	Physical mixture peak
3833.25	N-H Group	Medium stretching	3765.14
1809.06	C=O Group	Medium stretching	1808.45
1725.12	C=C Group	Strong stretching	1718.85
1374.00	C-O Group	Low stretching	1350.03

An infrared (IR) spectrophotometer was used for the compatibility study. The infrared spectra of both the unadulterated drug and a physical mixture of the drug and polymer were studied. The types of vibrations identified, together with their corresponding functional classifications, are listed in Table 7.5. The FTIR examination showed that the peaks that had been seen before did not vanish and did not appear. Medication compatibility with excipients was thus established.

7.4. Pure medication Ciprofloxacin standard curve

A calibration curve was developed by establishing a correlation between the absorbance measured at 276 nm and the amount of ciprofloxacin hydrochloride present. These are the results that were discovered.

Table:7.6. Ciprofloxacin hydrochloride standard curve.

Con^c µg/ml	**Absorbance value**
0**Con^c**	0
2**Con^c**	0.175

International Journal of Pharmaceutical Research and Applications
Volume 9, Issue 3 May-June 2024, pp: 437-493 www.ijprajournal.com ISSN: 2456-4494

4**Con**^{c}	0.478
6**Con**^{c}	0.619
8**Con**^{c}	0.800
10**Con**^{c}	0.979

The linear regression analysis used absorbance values as the dependent variable. The following equation provides a description of a straight line that was established as an aid in the process of determining the appropriate dosage of a medication:

$$\mathbf{Y = mx + c}$$

Where Y=absorbance, m=slope, x=concentration

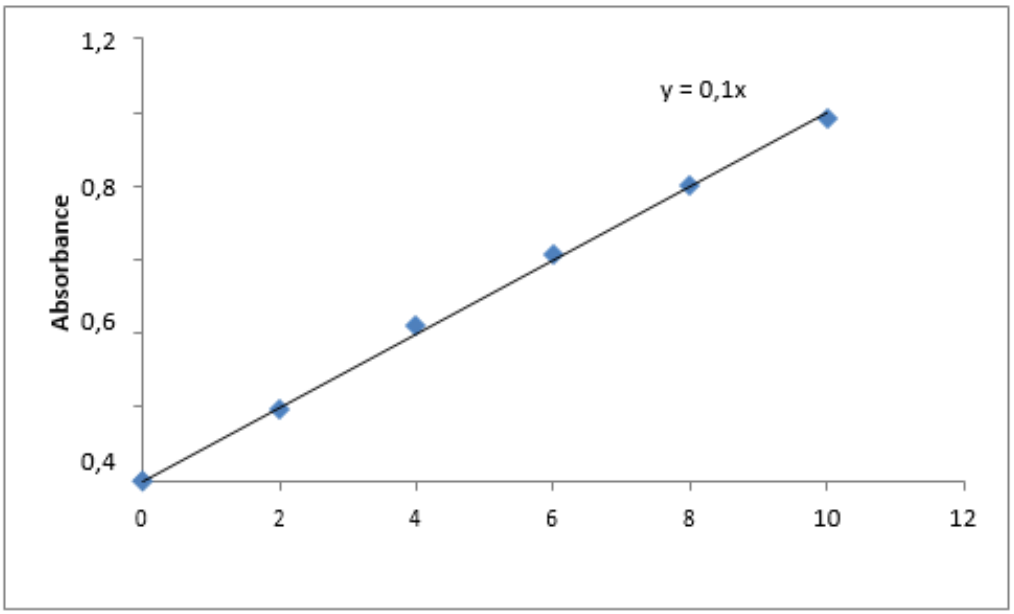

Figure 7.8.Ciprofloxacin, plotted as a normalised concentration vs time curve in 0.1 N HCL

7.5. Analysis of the procedures for development:

Prior to the invention of the floating tablet recipe, pre-compression parameters were looked into. The results of computing the following parameters using the approach outlined in the chapter before this one are displayed in table no.7.7 for your convenience.

International Journal of Pharmaceutical Research and Applications
Volume 9, Issue 3 May-June 2024, pp: 437-493 www.ijprajournal.com ISSN: 2456-4494

Table7.7 An examination of the properties of the powder:

Formulating codes	Angle of repose	Bulk density	Tapped density	Carr's index	Hausner ratio
CFH1	25.95±0.04	0.375±0.01	0.389±0.02	15.12±0.04	1.04±0.02
CFH2	26.98±0.06	0.387±0.02	0.387±0.04	14.87±0.02	1.12±0.01
CHF3	26.08±0.02	0.366±0.05	0.345±0.01	12.47±0.01	1.10±0.04
CHF4	25.02±0.03	0.387±0.03	0.364±0.05	15.45±0.02	1.19±0.04
CHF5	27.01±0.03	0.302±0.04	0.323±0.04	13.39±0.04	1.14±0.12
CHF6	25.38±0.01	0.270±0.06	0.325±0.21	14.51±0.01	1.17±0.45
CHF7	27.09±0.04	0.269±0.07	0.368±0.18	14.20±0.04	1.01±0.12
CHF8	27.15±0.09	0.309±0.05	0.314±0.25	12.16±0.03	1.19±0.14
CHF9	27.14±0.05	0.337±0.06	0.340±0.15	11.32±0.01	1.48±0.05

The angle of repose was determined for each and every formula. In terms of the Swiss Franc, the values were found to fall somewhere in the range of 25.95±0.04 to 27.14±0.05 CHF. This demonstrates that the powder mixture has excellent flow characteristics. Both the bulk density and the tapped density were measured to fall within the range of 0.375±0.01 to 0.337±0.06, with the tapped density falling within the range of 0.389±0.02 to 0.340±0.15. It was discovered that the values for Hausner's ratio fall somewhere in the range of 1.04±0.02 and 1.48±0.05.This is evidence that the powder mixture has very good flow characteristics. Based on the findings, it was determined that the physical combination could be compressed in a straight line. The data from table 7.8 were used to create batches CHF1 through CHF9, which were then saved in that table for further examination at a later time.

7.6. EVALUATION OF ESTIMATED TABLETS:

Table-7.8. Examination of pills that have been formulated

Batch Code	Weight Variation	Hardness	Friability	Drug Content	Thickness
CHF1	319±2.99	4.2±0.24	0.12	95.15±0.12	3.1±0.12
CHF2	316±1.63	4.1±0.54	0.25	96.14±0.21	3.4±0.21
CHF3	315±3.2	4.1±0.20	0.36	96.85±0.42	3.3±0.12
CHF4	310±5.8	4.2±0.15	0.14	96.91±0.21	3.2±0.23
CHF5	315±1.4	4.1±0.21	0.18	9.42±0.29	3.4±0.14
CHF6	316±6.25	4.0±0.38	0.15	93.12±0.14	3.1±0.26
CHF7	317±1.23	4.1±0.06	0.36	98.63±0.36	3.4±0.78
CHF8	314±3.04	4.2±0.56	0.21	91.25±0.89	3.2±0.54
CHF9	321±3.06	4.01±0.26	0.14	98.91±0.54	3.2±0.12

International Journal of Pharmaceutical Research and Applications
Volume 9, Issue 3 May-June 2024, pp: 437-493 www.ijprajournal.com ISSN: 2456-4494

The formulated floating tablets were then evaluated for various physical characteristics like thickness, weight variation, hardness, friability and drug content. The weight variation of tablets was uniform in all formulations and ranged from319±2.99 to 321±3.06. The % deviation is coming within 6% to 8% range for this accepted % deviation should be 6% for 321mg tablet. CHF1-CHF9 batches come with in limit and passed the test. The hardness of the prepared tablets was ranged from 4.2±0.24 to 4.1±0.26, friability values were ranged from 0.12 to 0.14 which falls within the limit of standard (0.1 to0.9%). Drug content of tablets was ranged from 95.15±0.12 to 98.91±0.54. Thickness of tablets was uniform and values are ranged from 3.1±0.12 to 3.2±0.12.

7.5.1. The Floating Test or the Buoyancy Test

When placed in a 0.1 N hydrochloric acid solution at 370 degrees Celsius, the tablets maintained their buoyancy and floated without disintegrating. Table7.9 displays the results of the buoyancy analysis as well as the buoyancy properties of the finished tablet.

The time it took for CHF1–CHF9 to regain their buoyancy varied between fifty and ninety seconds. The batch with xanthan gum and guar gum in it had the best buoyancy lag time (BLT) and total floating time (TFT), as determined by the results.

The CHF4 formulation containing xanthan gum and guar gum had a respectable BLT of 45 seconds, however the CHF4 formulation containing xanthan gum alone and the CHF4 formulation containing guar gum alone demonstrated the highest BLT and TFT of greater than 9 hours, respectively. This could be due to the fact that the gas generating agent and polymer concentrations utilised in this study were kept constant. The difference between BLT and TFT is caused by the release of the generated gas, which cannot be held within the gelatinous layer.

Table7.9: Time employed for floating and buoyancy

Formulation no.	Buoyancylagduration (sec)	Floatingtime hr
CHF1	50	>9hr
CHF2	55	>9hr
CHF3	50	>9hr
CHF4	60	>9hr
CHF5	65	>9hr
CHF6	70	>9hr
CHF7	90	>9hr
CHF8	90	>9hr
CHF9	55	>9hr

International Journal of Pharmaceutical Research and Applications
Volume 9, Issue 3 May-June 2024, pp: 437-493 www.ijprajournal.com ISSN: 2456-4494

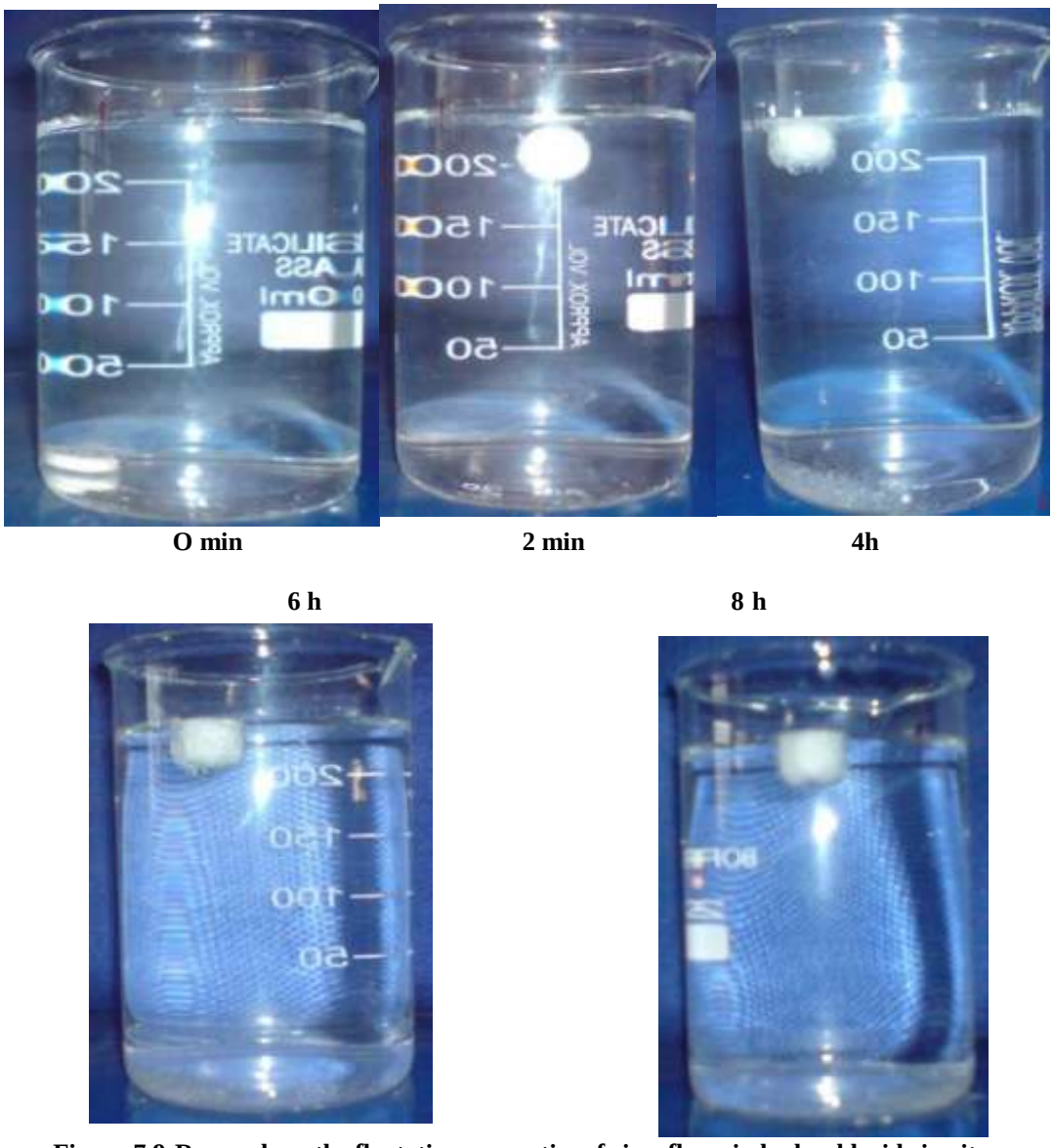

Figure 7.9:Research on the floatation properties of ciprofloxacin hydrochloride in vitro

7.6.1. Swelling. Index:

The results of the research on water consumption by the various formulations are displayed as a percentage in figures 7.10–7.12, which may be seen below. The formulations were improved by the addition of xanthan gum and guar gum, which caused the tablets to swell and remain intact. The change in the concentration of sodium bicarbonate had no effect on the swelling of the pill. After an initial interaction that lasted for six hours, total swelling took place, which was then followed by diffusion and erosion. The formulation containing xanthan gum expands more than the formulations that contain guar gum and xanthan gum individually. The swelling index of the tablets increases in proportion to the increasing polymer viscosity classes.

International Journal of Pharmaceutical Research and Applications
Volume 9, Issue 3 May-June 2024, pp: 437-493 www.ijprajournal.com ISSN: 2456-4494

Table7.10: percentage of swelling index for doses that are formulated to float

TIME(t)	CHF1	CHF2	CHF3	CHF4	CHF5	CHF6	CHF7	CHF8	CHF9
1hr	18.45	24.95	19.25	21.5	20.1	14.6	18.6	17.6	10.15
2hr	30.21	41.99	34.01	29.5	33.4	39.3	17.5	29.5	18.1
3hr	43.98	57.01	47.05	40.1	44.5	42.2	28.8	44.9	22.3
4hr	62.01	69.98	62.98	51.9	58.2	54.4	40.1	52.3	32.1
6hr	70.1	75.14	70.14	64.18	72.3	61.5	45.97	60.1	44.4

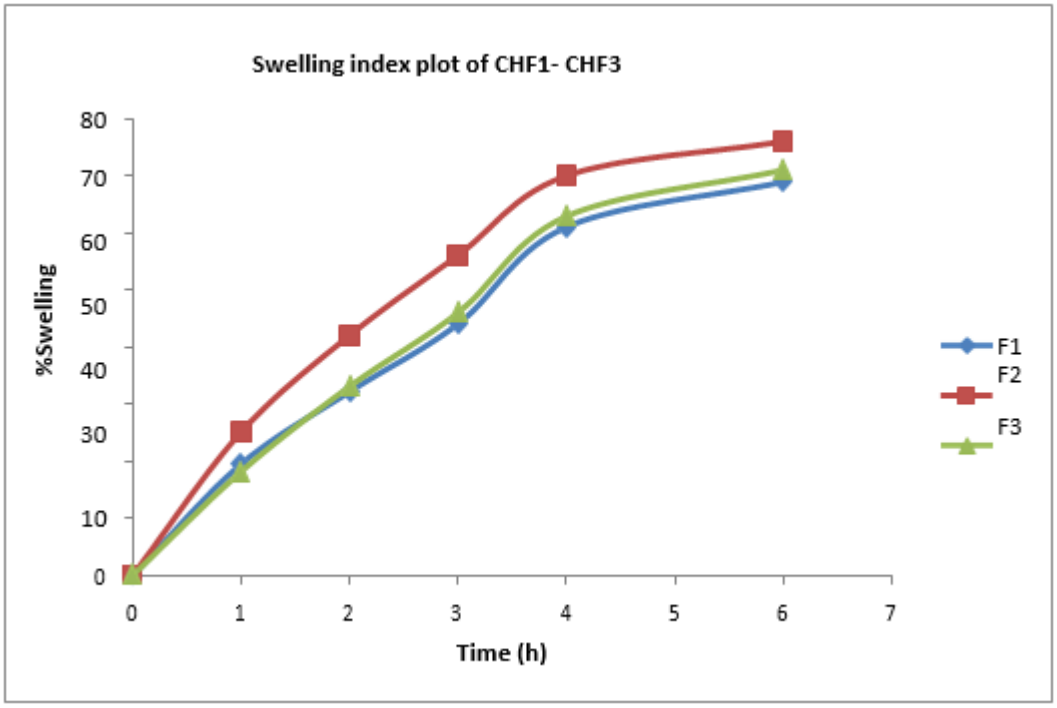

Figure7.10 A plot of the swelling index for CHF1-CHF3

International Journal of Pharmaceutical Research and Applications
Volume 9, Issue 3 May-June 2024, pp: 437-493 www.ijprajournal.com ISSN: 2456-4494

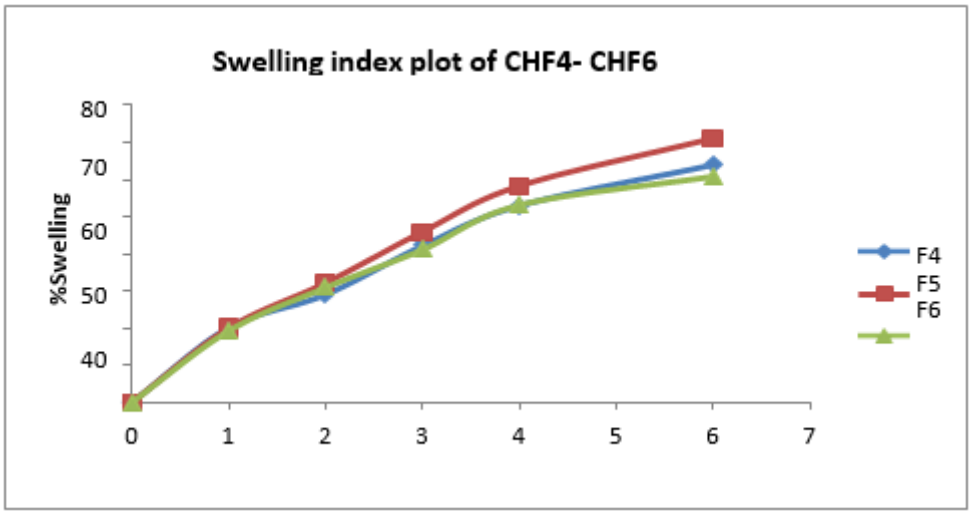

Figure7.11: A plot of the swelling index for CHF4-CHF6

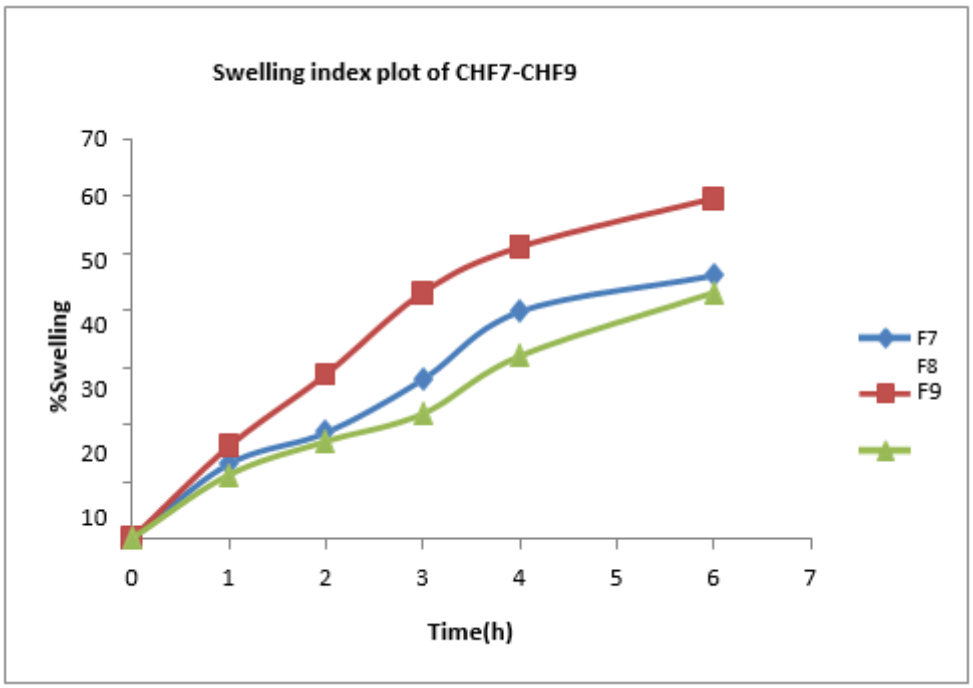

Figure7.12: A plot of the swelling index for CHF7–CHF9

7.5.1. In vitro drug release investigation of prepared floating controlled-dose formulation

Table7.11. Invitro drug release studies

TIME	RELEASE OF DRUGS, Expressed as a Cumulative Percentage (%)								
	CHFl	CHF2	CHF3	CHF4	CHF5	CHF6	CHF7	CHF8	CHF9

International Journal of Pharmaceutical Research and Applications
Volume 9, Issue 3 May-June 2024, pp: 437-493 www.ijprajournal.com ISSN: 2456-4494

0hr	**0**	**0**	**0**	**0**	**0**	**0**	**0**	**0**	**0**
1hr	22.01	22.3	27.18	15.96	22.1	8.62	6.12	4.21	9.21
2hr	32.05	34.2	34.5	26.12	33.5	14.36	14.32	45.32	17.2
3hr	38.7	45.6	46.96	36.25	45.36	24.36	21.32	21.32	25.12
4hr	45.2	56.3	53.6	47.36	52.97	32.14	24.35	25.32	36.15
5hr	54.2	69.2	62.98	55.12	74.21	47.25	36.21	36.14	44.78
6hr	69.3	79.12	75.45	62.54	84.32	54.25	41.21	41.31	54.78
7hr	80.4	96.3	90.3	76.25	95.36	47.25	14.32	55.17	59.8
8hr	98.3	-	95.6	84.32	98.65	14.36	54.21	65.23	66.45
10hr	-	-	-	95.36	-	75.14	63.14	87.21	74.21
12hr	-	-	-	96.23	-	87.52	47.21	96.32	81.21

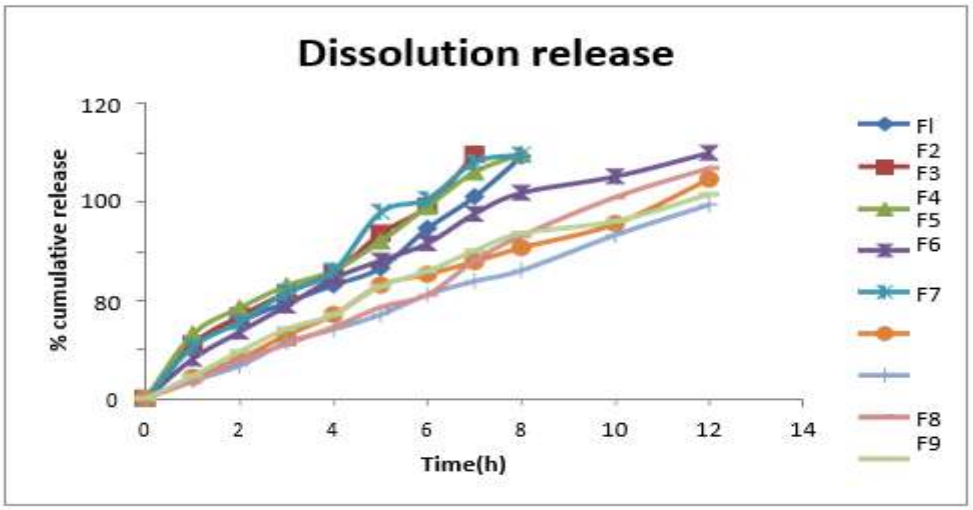

Figure7.13. Invitro drug release studies

International Journal of Pharmaceutical Research and Applications
Volume 9, Issue 3 May-June 2024, pp: 437-493 www.ijprajournal.com ISSN: 2456-4494

An invitro dissolution test was then used to determine how much of the medication was released from the floating controlled release tablets that had been manufactured. In order to replicate the conditions of an in-vivo dissolution setting, the test was carried out in 900 millilitres (cc) of 0.1N hydrochloric acid using a USP-II paddle-type apparatus at a rate of 50 revolutions per minute and a temperature of 370.5 degrees Celsius. The dissolution test produced results that varied greatly depending on the polymer content of the sample. Formulations that employed xanthan gum alone released more quickly than those that contained guar gum alone because of the less binding nature of xanthan gum and the controlled release property that it possessed in comparison to that of guar gum. With the use of Formulation F4, which contained both xanthan gum (15 mg) and guar gum (15 mg), the drug was released at a rate of 99.80% in just 12 hours. The release profiles of the formulations that contained both xanthan gum and guar gum were significantly enhanced in comparison to those that contained either gum utilised on its own.

KINETIC STUDY OF CIPROFLOXACIN SILVER NANOPARTICLES:

Table7.12 An investigation on the kinetics of the optimal formulation

Time hr.	LogTime	√Time	cumulative % drugrelease	Logcumulative %drug release	cumulative %drugremained	Logcumulative %drug remained
0hr	0	0	0	0	99	2.05
1hr	0	1.254	16.4	1.361	84.21	1.96
2hr	0.312	1.345	24.56	1.654	74.21	1.47
3hr	0.624	1.536	36.12	1.475	61.87	1.89
4hr	0.715	2.147	49.14	1.523	54.32	1.58
5hr	0.798	2.561	63.10	1.567	44.16	1.76
6hr	0.945	2.354	14.25	1.491	35.12	1.62
7hr	1.090	2.987	45.36	1.564	20.47	1.54
8hr	1.175	2.141	83.21	1.364	14.44	1.24
10hr	1.345	3.125	96.21	1.564	9.45	0.99
12hr	1.398	3.547	94.15	1.456	0.20	-0.698

International Journal of Pharmaceutical Research and Applications
Volume 9, Issue 3 May-June 2024, pp: 437-493 www.ijprajournal.com ISSN: 2456-4494

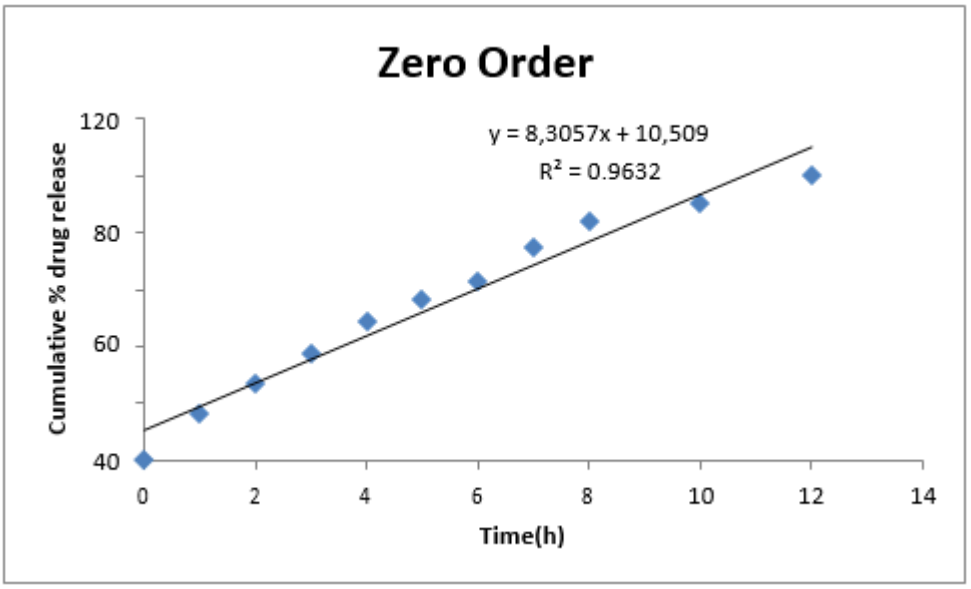

Figure7.14. Zero order graph

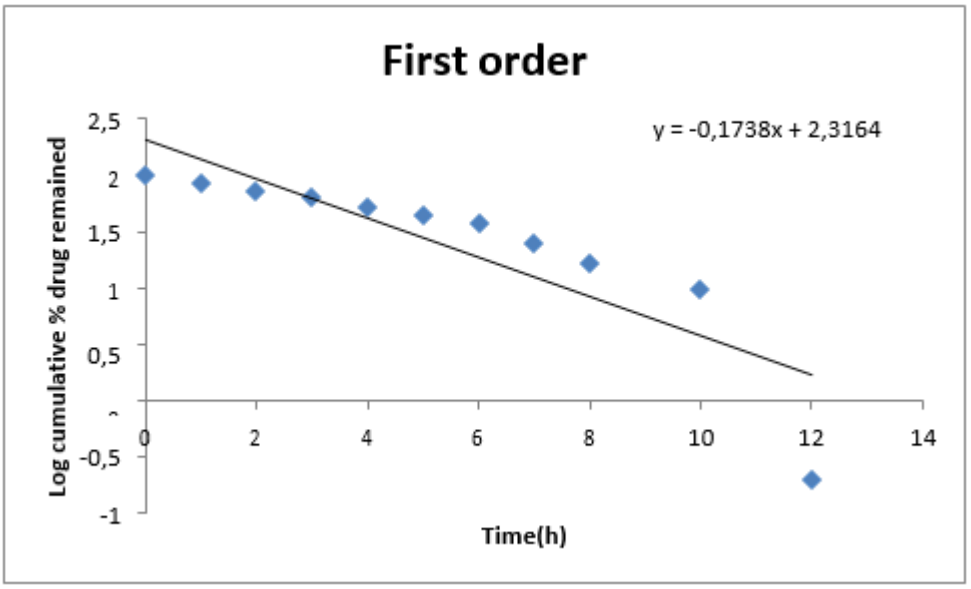

Figure7.15. Firstorder graph

International Journal of Pharmaceutical Research and Applications
Volume 9, Issue 3 May-June 2024, pp: 437-493 www.ijprajournal.com ISSN: 2456-4494

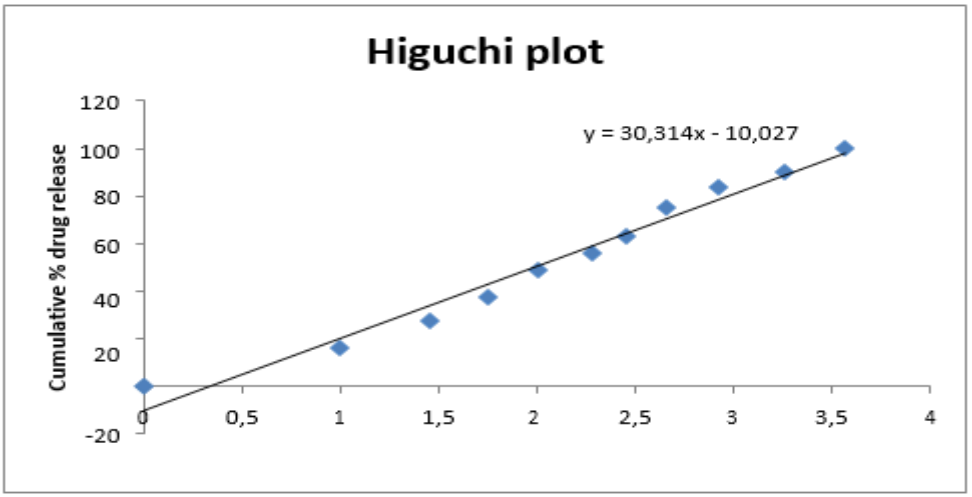

Figure7.16 Higuchigraph

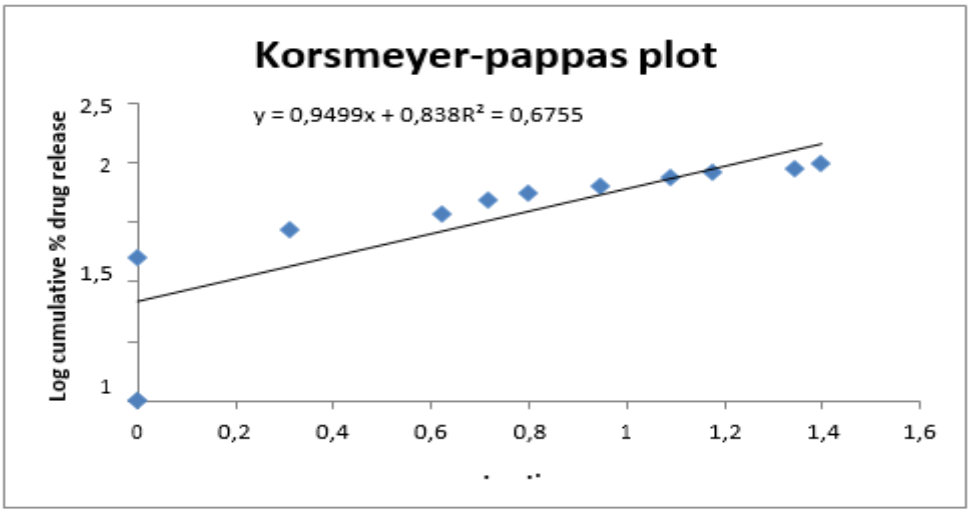

Figure7.17 Korsmeyer Peppasgraph

KINETICS AND DRUGS RELEASE

Table-7.13 Zero order release of Ciprofloxacin

Batch code	Regression coefficient of zero order	Regression coefficient of first order	Order of release
CHF4	0.963	0.741	Zero order release

International Journal of Pharmaceutical Research and Applications
Volume 9, Issue 3 May-June 2024, pp: 437-493 www.ijprajournal.com ISSN: 2456-4494

Table7.14 Higuchi, and korsmeyer-peppas model

Batch code	Higuchi Model	Korsmeyer peppas model
	R^2	R^2
CHF4	0.974	0.675

To investigate the mechanism of drug release from the formulations, the in vitro dissolution data were fitted to zero order, first order, higuchi plot, and korsmeyer-peppas plot. The interpretation of release exponent value (n) was determined, and the findings are displayed in tables 7.13–7.14 and figures 7.14–7.17. R2 values of 0.963 and 0.741, respectively, were determined for the zero and first orders of the expression. After that, we will be in a position to know for certain that the zero-order-release optimisation was carried out in the appropriate manner.

It was discovered that the drug release was controlled by diffusion due to the fact that the regression coefficient in the higuchi plot for the best formulation of CHF4 was 0.974. It was established that the drug's release from the formulation occurred via an anomalous non-fickian transport of diffusion, and a korsmeyer-peppas plot was utilised to determine that the release exponent value n was equal to 0.675.

7.7. STABILITY STUDY:

Three-month stability studies were conducted on the optimal formulation at 40 2 °C and 75% relative humidity 5%.

The following criteria were used to assess the product:

- **Differences in Mass**
- **Hardness**
- **Friability**
- **Substances**
- **Drugs**
- **Analysing dissolution**

1) Temperature range of 40°C 2°C / 75% RH 5%:

Table-7.15: Stability study

TEST	0 days	30 days	60 days	90 days
Weight variation	99±0.87	99±0.55	98±0.84	99±0.76
Hardness	4.5	4.4	4.4	4.3
Friability	0.68	0.69	0.69	0.70
Drug content	99.83±0.04	99.59±0.07	99.39±0.07	99.28±0.06

International Journal of Pharmaceutical Research and Applications
Volume 9, Issue 3 May-June 2024, pp: 437-493 www.ijprajournal.com ISSN: 2456-4494

7.7.1. Formulation CHF4 percent total drug release dissolution data

Table7.16: Stability formulation CHF4 dissolution data

Time (h)	0 days	30 days	60 days	90 days
0	0	0	0	0
1	16.15	16.10	15.57	15.65
2	26.75	25.37	25.12	24.92
3	37.80	36.66	36.70	36.48
4	49.12	48.48	46.54	43.82
5	56.15	54.76	52.62	51.55
6	62.65	62.32	60.85	60.12
7	75.16	74.35	73.45	72.58
8	83.60	82.76	82.32	82.02
10	91.15	91.72	91.32	91.54
12	99.75	99.60	99.44	99.34

International Journal of Pharmaceutical Research and Applications
Volume 9, Issue 3 May-June 2024, pp: 437-493 www.ijprajournal.com ISSN: 2456-4494

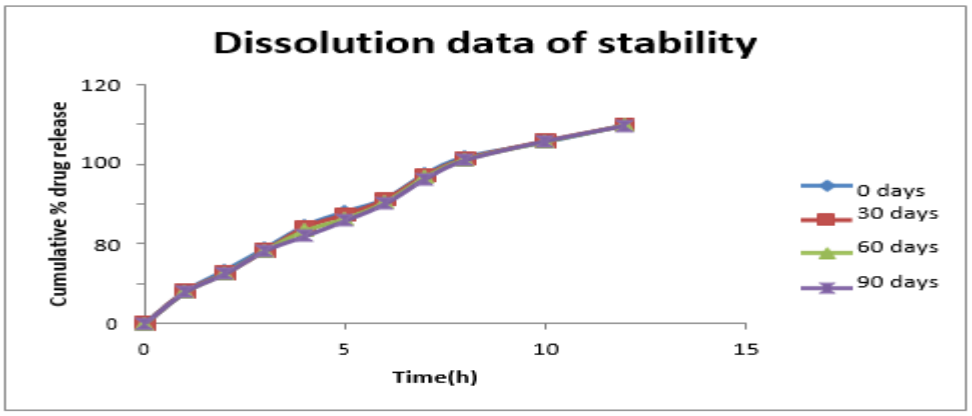

Figure7.18:CHF4 formulation stability dissolution data

The investigations on the most stable formulation's optimal After conducting CHF4 based on accelerated stability conditions and investigating various parameters at 0, 30, 60, and 90 day intervals, it was concluded that the optimised formulation was stable under accelerated settings. This conclusion was reached after conducting the study.

7.8 SEM ANALYSIS

FE-SEM examination was performed on NPs in order to ascertain their size, surface shape, and level of homogeneity. The procedure allowed for the collection of not only quantitative but also qualitative data concerning the NPs' sizes and shapes. At the nanoscale level, particles were synthesised, and the ImageJ software (version 1.8.0, Gaithersburg, Maryland, United States) was used to measure the diameter of the particles[98]. Figure 9A is where agglomeration and aggregation of particles can be seen. This figure also shows that the great majority of AgNPs have spherical forms and smooth surfaces. The results of the XRD analysis demonstrated that the dimensions of the structures ranged between 32.08 and 43.28 nm**.**

The size distribution of the AgNPs-PEG was extended (41.08 to 82.49 nm, 6 B) when the PEG coating was applied, as was anticipated. It appeared that the AgNPs-PEG particles were dispersed, which is consistent with the hypothesis that PEG played a role in preventing the aggregation of the particles[100]. In spite of the PEG and CIP coatings, scanning electron microscopy (SEM) images of AgNPs-PEG-CIP showed particles with sizes ranging from 63.44 to 98.28 nm and with some light aggregation visible. Nevertheless, the size distributions of the NPs that were seen using SEM measurements were significantly more narrow than those that were acquired using the DLS approach. An prior study showed results that were equivalent to those observed in this one. It's probable that the DLS-based results relied on the average hydrodynamic diameter, but the SEM images reflected the metallic core in the centre of the particles. Due to the existence of minute aggregates in the nanosuspensions, the DLS method may have also had an effect on the size distribution of the generated NPs[104].

International Journal of Pharmaceutical Research and Applications
Volume 9, Issue 3 May-June 2024, pp: 437-493 www.ijprajournal.com ISSN: 2456-4494

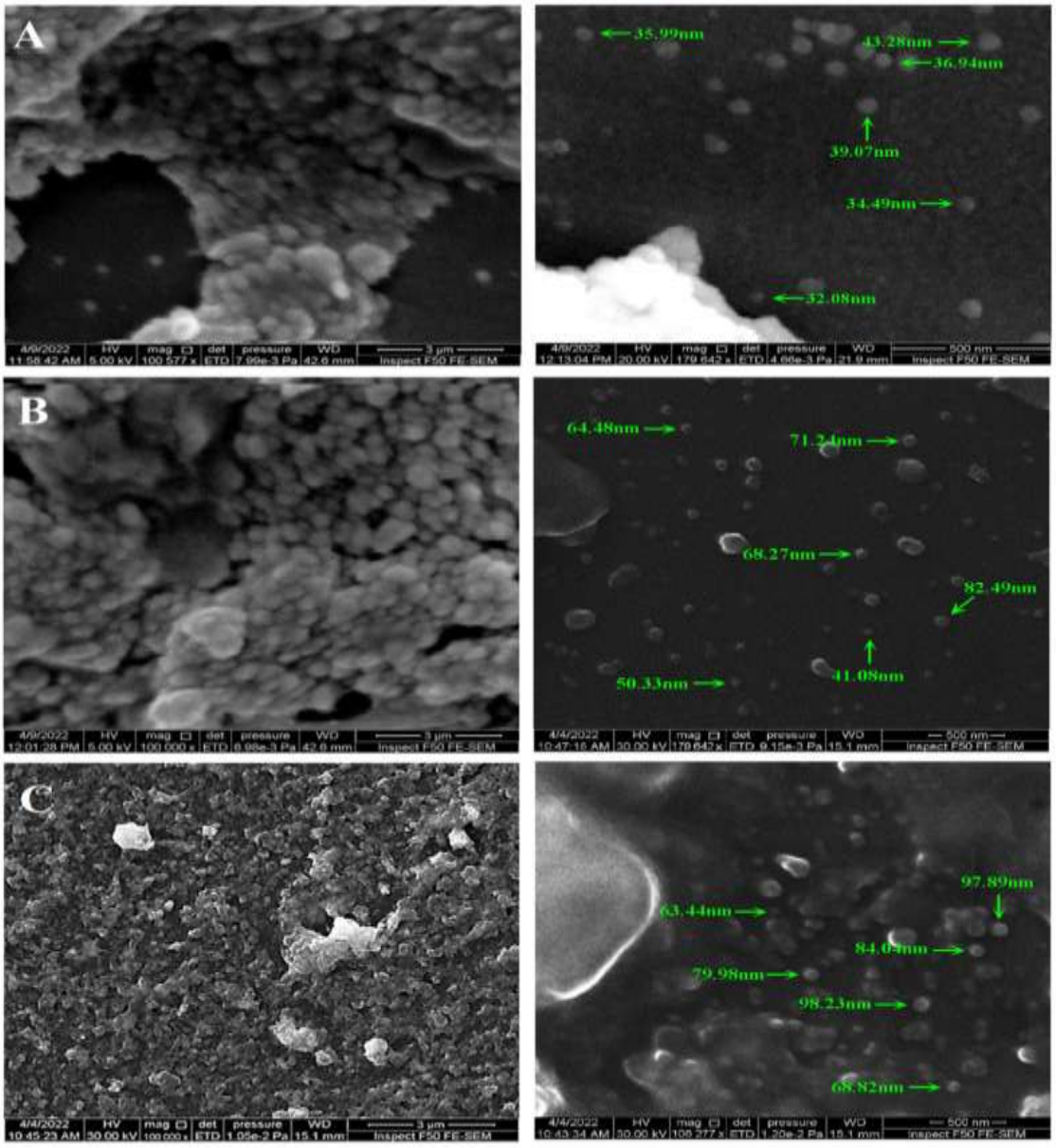

In Figure 7.19, the scale bars represent a distance of 3 metres for the scanning electron micrographs on the left and 500 nanometers for the particle size measurements on the right. Silver nanoparticles in their various forms, including AgNPs-PEG and AgNPs-PEG-CIP.

7.9 TEM ANALYSIS

The shape and size distributions of the synthesisedAgNPs, AgNPs-PEG, and AgNPs-PEG-CIP were investigated by means of transmission electron microscopy (TEM) examination at a magnification of 77.500 kx. The majority of the NPs are round, as shown in Figure7.20, and a histogram of size distribution produced with ImageJ revealed mean sizes of 33.48 nm for AgNPs, 47.35 nm for AgNPs-PEG, and 59.78 nm for AgNPs-PEG-CIP. The results of magnified pictures demonstrated that the majority of the NPs are round. Agglomeration was reduced when polyethylene glycol (PEG) was added to the NPs because PEG prevents the aggregation of particles [98]. PEG molecules that were bound to the AgNPs increased their bulkiness as well as their steric effects and the distance between the particles. The

International Journal of Pharmaceutical Research and Applications
Volume 9, Issue 3 May-June 2024, pp: 437-493 www.ijprajournal.com ISSN: 2456-4494

NPs became less likely to combine as a result of their increased hydrophilicity, which was achieved by establishing hydrogen bonds with the solvent [104]. The AgNPs-PEG-CIP particles are predominantly circular, but there are also some that are triangular and others that are rod-shaped. The size of these particles, which have been given the name AgNPs-PEG-CIP, was determined to be significantly greater than that of both the AgNPs and the AgNPs-PEG. However, throughout the TEM examination and processing of the material, the sample became dehydrated. This may help to explain why the particle sizes were lower than the size indicated by the DLS analysis [105].

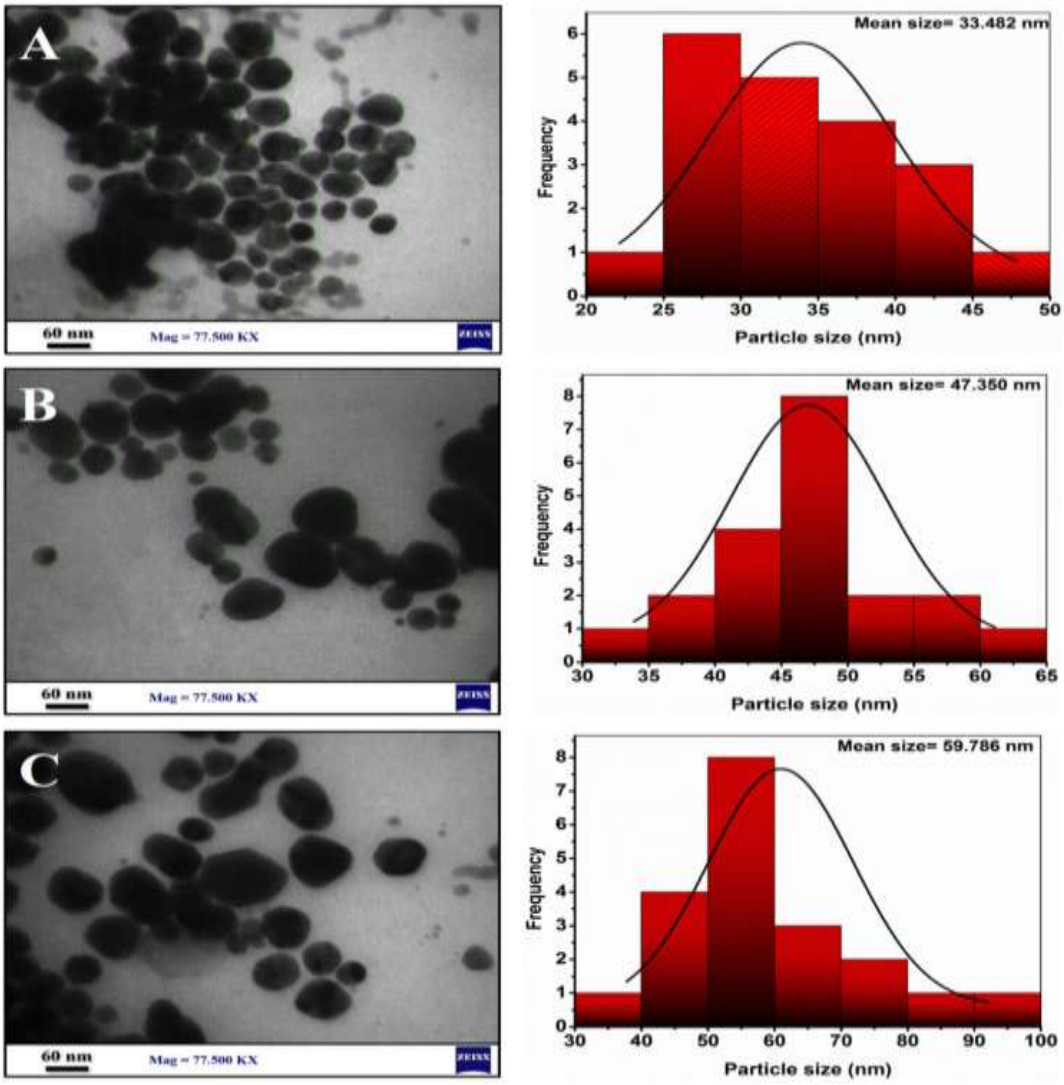

In Figure 7.20, electron micrographs of silver nanoparticles (AgNPs) and their conjugates (AgNPs, B AgNPs-PEG, and C AgNPs-PEG-CIP) can be seen.

7.10 Anti-bacterial Activity

The growth of bacterial isolates was assessed and compared to that of AgNPs and CIP when used alone, as well as to the antibacterial effects of the synergistic combination of AgNPs and CIP, AgNPs and PEG, and AgNPs-PEG-CIP[106]. The studies show that the antibacterial capabilities of CIP were significantly improved when it was conjugated with AgNPs. Figure 13 demonstrates that the AgNPs-PEG-CIP treatment had the most significant effect. AgNPs and CIP demonstrated that the effects of their combined use were synergistic by demonstrating an increase in the diameter of the inhibitory zones produced by

International Journal of Pharmaceutical Research and Applications
Volume 9, Issue 3 May-June 2024, pp: 437-493 www.ijprajournal.com ISSN: 2456-4494

CIP-resistant bacterial strains. The inhibition zones caused by AgNPs alone for S. aureus, A. baumannii, and S. marcescens were respectively 29.33 1.80 mm, 26.66 1.52 mm, and 24.66 2.08 mm, whereas the inhibition zones caused by CIP alone were respectively 16.00 2.12 mm, 13.33 0.57 mm, and 23.33 1.54 mm. The AgNPs-CIP demonstrated the largest inhibition area (35.33 1.52 mm) when tested against S. aureus. This was followed by 32.66 1.15 mm when tested against S. marcescens and 31.00 1.27 mm when tested against A. baumannii. S. marcescens became more susceptible to the antibiotic when CIP was loaded onto the AgNPs. This resulted in a 32-fold increase in inhibition area compared to CIP on its own (which just damaged the bacterial cell wall). The conjugation of AgNPs with CIP promoted antibiotic entrance into bacterial cells, where it inhibited cell division by blocking DNA gyrase enzyme and topoisomerase IV activity [109]. The use of MNPs in conjunction with antibiotics has been shown to reduce antibiotic toxicity as well as the potential for drug-resistant microorganisms [110]. When it came to killing bacteria, the AgNPs-CIP was significantly more efficient against Gram-positive bacteria than it was against Gram-negative bacteria. This is due to the fact that the molecular compositions of different bacterial strains' cell walls are distinct from one another [111]. Because Gram-negative bacteria have a lipopolysaccharide (LPS) layer that is 10 nm thick and covers the outer layer of peptidoglycan, which prevents NPs from penetrating the cell wall [115-120], while Gram-positive bacteria do not.

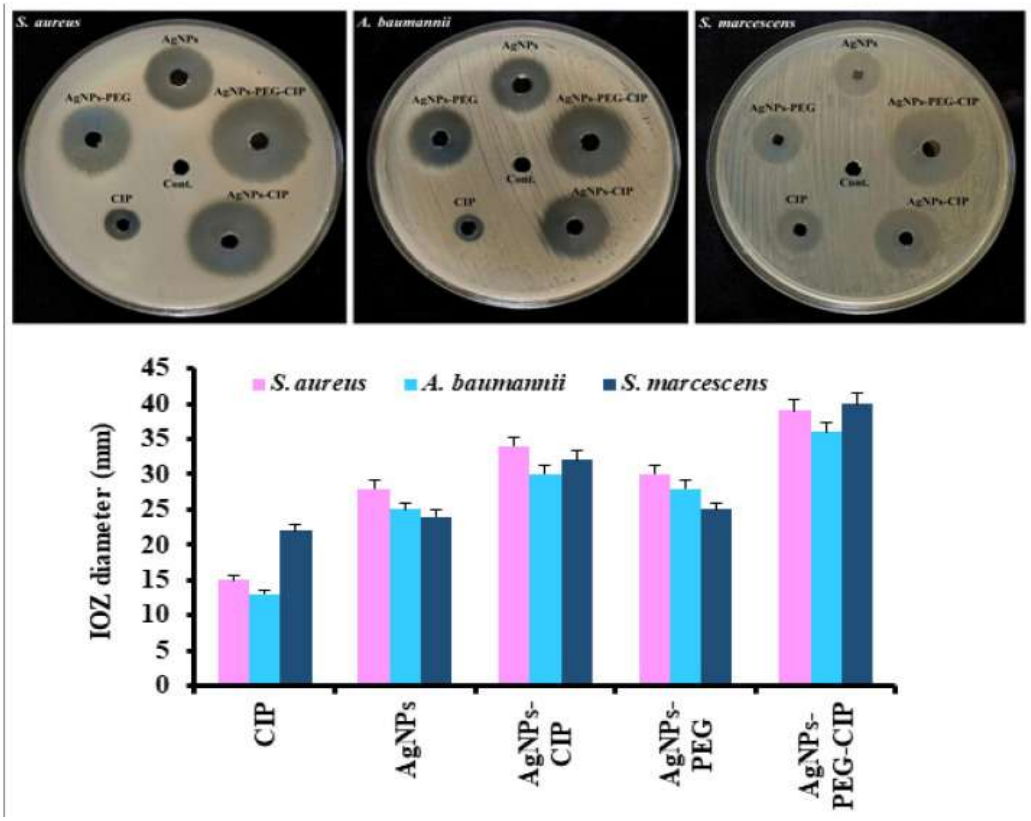

Figure 7.21 illustrates the additive effects of AgNPs-PEG, AgNPs-CIP, and AgNPs-PEG-CIP on the inhibition of the development of harmful bacteria in comparison to the effects of CIP and AgNPs alone.

7.11 DISCUSSION

The results of the experiments, conducted in adherence to the prescribed protocols, are shown in Table 7.1. The solubility of ciprofloxacin hydrochloride samples in water was observed, indicating that they were soluble in a little amount of solution. Additionally, the samples were found to be soluble in dimethyl formamide when subjected to the relevant assays. Moreover, it exhibits solubility in fluids with a mild alkaline or

International Journal of Pharmaceutical Research and Applications
Volume 9, Issue 3 May-June 2024, pp: 437-493 www.ijprajournal.com ISSN: 2456-4494

acidic nature. The capillary technique was employed to ascertain the boiling point of ciprofloxacin hydrochloride. The melting point of ciprofloxacin hydrochloride has been determined to be 255 degrees Celsius. The pharmaceutical's melting point was determined in accordance with the standards set by the United States Pharmacopoeia (USP), thereby confirming its level of purity. The drug's loss on drying was determined to be 0.45, a value deemed acceptable. The results indicate that the ciprofloxacin hydrochloride raw material exhibited favourable flow characteristics. The Fourier Transform Infrared (FTIR) spectra of the individual drug substance, the excipient, and the physical mixture of the drug and excipient were acquired within the wave number range of 400 to 4000 cm-1. There are no observable secondary peaks that might potentially exert any influence on the principal drug peaks. The infrared spectra of the medication and the polymer are displayed in the provided table and spectrum, together with the respective wave counts of their characteristic bands. The compatibility investigation utilised an infrared (IR) spectrophotometer. The infrared spectra of the pure drug and a composite of the drug and polymer were analysed. Table 7.5 presents a comprehensive list of detected vibrations, along with their respective functional classes. The Fourier Transform Infrared (FTIR) analysis revealed that the previously observed peaks remained unchanged and did not exhibit any new appearances. The compatibility of medication with excipients was consequently established. A correlation between the absorbance recorded at a wavelength of 276 nm and the quantity of ciprofloxacin hydrochloride was established in order to build a calibration curve. The following findings were uncovered. The examination of pre-compression parameters was conducted prior to the development of the floating tablet formulation. The outcomes of calculating the specified parameters using the methodology described in the preceding chapter are presented in Table 7.7 for ease of reference. The angle of repose was found for each formula. Regarding the Swiss Franc, it was observed that its values fluctuated between the interval of 25.95±0.04 to 27.14±0.05 CHF. This observation indicates that the powder mixture exhibits exceptional flow properties. Both the bulk density and the tapped density were found to be within the range of 0.375±0.01 to 0.337±0.06, with the tapped density lying within the range of 0.389±0.02 to 0.340±0.15. The investigation revealed that the values pertaining to Hausner's ratio are situated within the interval of 1.04±0.02 and 1.48±0.05.This observation provides empirical support for the notion that the powder mixture has highly favourable flow properties. Based on the results of the study, it was concluded that the physical assemblage could be compressed linearly. Batches CHF1 through CHF9 were created using the data obtained from table 7.8. These batches were subsequently stored in the same table for future analysis. Subsequently, an assessment was conducted on the developed floating tablets to determine their physical attributes, including thickness, weight variation, hardness, friability, and drug content. The weight variation of tablets exhibited uniformity across all formulations, with values ranging from 319±2.99 to 321±3.06. The percentage variance falls within the range of 6% to 8%, which is considered acceptable. However, it is recommended that the permissible percentage deviation for a 321mg pill be limited to 6%. Batches ranging from CHF1 to CHF9 were found to be within the specified limits and successfully passed the test. The tablets exhibited a range of hardness values, specifically ranging from 4.2±0.24 to 4.1±0.26. Additionally, the friability values fell within the acceptable standard range of 0.1 to 0.9%, with a range of 0.12 to 0.14. The drug content of the pills exhibited a range of 95.15±0.12 to 98.91±0.54. The tablets exhibited consistent thickness, with values ranging from 3.1±0.12 to 3.2±0.12. When subjected to a hydrochloric acid solution with a concentration of 0.1 N at a temperature of 370 degrees Celsius, the tablets exhibited the ability to remain buoyant and retain their structural integrity without undergoing disintegration. The findings of the buoyancy analysis and the buoyancy parameters of the completed tablet are presented in Table 7.9. The duration required for CHF1–CHF9 to recover their buoyancy exhibited variability, ranging from fifty to ninety seconds. The batch containing xanthan gum and guar gum exhibited superior buoyancy lag time (BLT) and total floating time (TFT), as indicated by the obtained results. The CHF4 formulation, which consisted of a combination of xanthan gum and guar gum, exhibited a commendable Bottom Loading Time (BLT) of 45 seconds. In contrast, the CHF4 formulation containing only xanthan gum and the CHF4 formulation containing only guar gum displayed the longest BLT and Top Film Thickness (TFT), surpassing 9 hours, respectively. This observation

International Journal of Pharmaceutical Research and Applications
Volume 9, Issue 3 May-June 2024, pp: 437-493 www.ijprajournal.com ISSN: 2456-4494

may be attributed to the consistent maintenance of gas generating agent and polymer concentrations throughout the course of this study. The distinction between BLT and TFT arises from the expulsion of the produced gas, which is unable to be contained within the gelatinous layer. The research findings on water usage for different formulations are presented in figures 7.10-7.12, depicted as percentages. These numbers can be observed below. The formulations were enhanced through the incorporation of xanthan gum and guar gum, resulting in tablet swelling and increased structural integrity. The alteration in the sodium bicarbonate concentration did not yield any discernible impact on the pill's swelling. Following a prolonged first encounter lasting six hours, a subsequent occurrence of overall swelling ensued, subsequently leading to processes of diffusion and erosion. The formulation incorporating xanthan gum exhibits greater expansion compared to formulations comprising either guar gum or xanthan gum alone. The tablets' swelling index demonstrates a positive correlation with the escalating polymer viscosity categories. Subsequently, an in vitro disintegration test was employed to ascertain the extent of drug release from the fabricated floating controlled release tablets. To simulate the circumstances of an in-vivo dissolution environment, the experiment was conducted using a USP-II paddle-type apparatus in 900 millilitres (cc) of 0.1N hydrochloric acid. The apparatus was set to rotate at a speed of 50 revolutions per minute, while maintaining a temperature of 370.5 degrees Celsius. The results obtained from the dissolution test exhibited significant variations, which were contingent upon the polymer content present in the sample. The formulations that only utilised xanthan gum exhibited a faster release rate compared to those using only guar gum. This can be attributed to the lower binding capacity of xanthan gum and its inherent controlled release capability, which surpasses that of guar gum. The medicine was released at a rate of 99.80% within a 12-hour period using Formulation F4, which consisted of a combination of xanthan gum (15 mg) and guar gum (15 mg). The release characteristics of the formulations that comprised both xanthan gum and guar gum were greatly increased in contrast to those that contained either gum employed on its own. The investigations on the most stable formulation's ideal After executing CHF4 based on accelerated stability circumstances and evaluating various parameters at 0, 30, 60, and 90 day intervals, it was established that the optimised formulation was stable under accelerated settings. The form and size distributions of the synthesisedAgNPs, AgNPs-PEG, and AgNPs-PEG-CIP were studied by means of transmission electron microscopy (TEM) examination at a magnification of 77.500 kx. The data presented in Figure 7.20 indicates that a significant proportion of the nanoparticles (NPs) exhibit a spherical shape. Furthermore, an analysis of the size distribution using ImageJ software yielded average sizes of 33.48 nm for AgNPs, 47.35 nm for AgNPs-PEG, and 59.78 nm for AgNPs-PEG-CIP. The findings from the magnified images revealed that a significant proportion of the nanoparticles had a spherical shape. The addition of polyethylene glycol (PEG) to the nanoparticles (NPs) resulted in a decrease in agglomeration, as PEG effectively inhibits particle aggregation. The addition of PEG molecules to the AgNPs resulted in an increase in their overall size, as well as the impact of steric effects and the separation distance between the particles. The combination of the NPs was shown to decrease due to an increase in their hydrophilicity, which was attained through the formation of hydrogen bonds with the solvent. The majority of the AgNPs-PEG-CIP particles exhibit a circular morphology, but a subset of particles display triangular and rod-shaped geometries. The dimensions of the particles, referred to as AgNPs-PEG-CIP, were found to be considerably larger compared to both the AgNPs and the AgNPs-PEG. Nevertheless, during the transmission electron microscopy (TEM) analysis and subsequent material processing, the sample experienced dehydration. This observation may provide an explanation for the discrepancy between the particle sizes obtained from the dynamic light scattering (DLS) study and the expected sizes indicated by the analysis. The assessment of bacterial isolates' growth was conducted and compared to the growth of AgNPs and CIP when utilised individually. Additionally, the antibacterial effects of the combined application of AgNPs and CIP, AgNPs and PEG, and AgNPs-PEG-CIP were also examined. The research findings indicate that the antimicrobial properties of CIP were notably enhanced through its conjugation with AgNPs. Figure 13 illustrates that the therapy using AgNPs-PEG-CIP exhibited the most pronounced impact. The combined utilisation of AgNPs and CIP exhibited a synergistic impact, as evidenced by the

International Journal of Pharmaceutical Research and Applications
Volume 9, Issue 3 May-June 2024, pp: 437-493 www.ijprajournal.com ISSN: 2456-4494

observed augmentation in the diameter of inhibitory zones generated by CIP-resistant bacterial strains. The silver nanoparticles (AgNPs) exhibited inhibition zones of 29.33 ± 1.80 mm, 26.66 ± 1.52 mm, and 24.66 ± 2.08 mm against S. aureus, A. baumannii, and S. marcescens, respectively. In contrast, the inhibition zones generated by ciprofloxacin (CIP) alone were 16.00 ± 2.12 mm, 13.33 ± 0.57 mm, and 23.33 ± 1.54 mm for the same bacterial strains. When tested against S. aureus, the AgNPs-CIP exhibited the highest inhibition area, measuring 35.33 ± 1.52 mm. Subsequently, the recorded measurements were 32.66 ± 1.15 mm for the test conducted with S. marcescens, and 31.00 ± 1.27 mm for the test conducted with A. baumannii. The susceptibility of S. marcescens to the antibiotic increased when CIP was loaded onto the AgNPs. This led to a 32-fold augmentation in the region of inhibition in comparison to the exclusive use of CIP, which just inflicted damage to the bacterial cell wall. The coupling of silver nanoparticles (AgNPs) with ciprofloxacin (CIP) facilitated the uptake of antibiotics into bacterial cells. This led to the inhibition of cell division by interfering with the activity of DNA gyrase enzyme and topoisomerase IV. Research has demonstrated that the utilisation of MNPs in combination with antibiotics can effectively mitigate antibiotic toxicity and minimise the emergence of drug-resistant bacteria. In terms of bactericidal efficacy, the AgNPs-CIP demonstrated a notable superiority over Gram-positive bacteria compared to its effectiveness against Gram-negative bacteria. The distinctiveness of the chemical compositions of cell walls among various bacterial strains accounts for this phenomenon. Gram-negative bacteria possess a lipopolysaccharide (LPS) layer that is approximately 10 nm in thickness and envelops the outer layer of peptidoglycan. This LPS layer acts as a barrier, impeding the penetration of NPs (nanoparticles) through the cell wall. Conversely, Gram-positive bacteria lack this protective feature.

VIII. CONCLUSION

In the creation ofciprofloxacin-loaded silver nanoparticles with zinc oxide as potent nano-antibiotics against resistant pathogenic bacteria. These phytochemicals were responsible for triggering an oxidation and reduction reaction during the process. The size of the NPs that were created was measured to be 35 nm on average. The effectiveness of the artificially manufactured ZnO NPs is demonstrated by the increase in plant biomass. We discovered that the incorporation of green-synthesized ZnO NPs into MO led to an increase in shoot production, plant weight, the quantity of photosynthetic pigments, and the amount of total protein present in the plant. These findings point to morpho-physiological alterations occurring in the population. Plant development was inhibited by ZnO NPs concentrations of 10 and 20 mg L-1; nevertheless, these levels stimulated the accumulation of proline and the production of antioxidant enzymes. Despite this, the plant's overall MDA production was decreased.

This research demonstrates that there was a significant improvement in the quality of the in vitro grown plant tissues when ZnO NPs were included in the growing conditions. This study lends credence to the hypothesis that green-synthesized of ciprofloxacin loaded ZnO NPs may have potential applications in a variety of fields, including the medical and agricultural sectors. However, additional research is required to achieve a complete comprehension of the chemical process by which ZnO NPs influence the development of cellular pathways and secondary metabolism.

REFERENCE

[1]. Morones, J. R. and Elechigerra, J. I. (2005). Interaction of silver nanoparticles with HIV-1. Nanotechnology, 16, 2346.
[2]. Merelo, J.J., M.A. Andrade, A. Prieto and F. Morán. 1994. Proteinotopic Feature Maps. Neurocomputing. 6, 443-454.
[3]. Nair, B. and Pradeep, T. (2002). Coalescence of nanoclusters and formation of submicron crystallites assisted by Lactobacillus strains. Crystal Growth Design. 2, 293–298.
[4]. Nagy, A. and Mestl, G. (1999). High temperature partial oxidation reactions over silver catalysts. Appl Catal A. 188,337.
[5]. Nair.S., Sasidharan. A, Nair .S, and Raina.S. (2008). Role of size scale of ZnO nanoparticles on toxicity toward bacteria and osteoblast cells. J.Mater sci.20, S235-S241.
[6]. Oberdorster, G., Sharp, Z., Atudorei, V., Elder, A., Gelein, R..and Kreyling, W. (2004). Translocation of inhaled ultrafine particles to the brain. Inhal Toxicology. 16,437-440.

[7]. Permyakova , E.A. and Berlinerb, L.J. (2000). α-Lactalbumin: structure and function. FEBS.473, 269-274.
[8]. Pfeil, W. (1998). Is the Molten Globule a Third Thermodynamic State of Protein. The Example of a-Lactalbumin. Proteins Structure, Function and Genetics. 30, 43–48
[9]. Mabrouk, M., Das, D. B., Salem, Z. A., &Beherei, H. H. (2021). Nanomaterials for Biomedical Applications: Production, Characterisations, Recent Trends and Difficulties. Molecules (Basel, Switzerland), 26(4), 1077. https://doi.org/10.3390/molecules26041077
[10]. Paramasivam, G., Palem, V. V., Sundaram, T., Sundaram, V., Kishore, S. C., & Bellucci, S. (2021). Nanomaterials: Synthesis and Applications in Theranostics. Nanomaterials (Basel, Switzerland), 11(12), 3228. https://doi.org/10.3390/nano11123228
[11]. Aflori M. (2021). Smart Nanomaterials for Biomedical Applications-A Review. Nanomaterials (Basel, Switzerland), 11(2), 396. https://doi.org/10.3390/nano11020396
[12]. Albalawi, F., Hussein, M. Z., Fakurazi, S., &Masarudin, M. J. (2021). Engineered Nanomaterials: The Challenges and Opportunities for Nanomedicines. International journal of nanomedicine, 16, 161–184. https://doi.org/10.2147/IJN.S288236
[13]. Rahimi, G., Mohammad, K. S., Zarei, M., Shokoohi, M., Oskoueian, E., Poorbagher, M. R. M., & Karimi, E. (2022). Zinc oxide nanoparticles synthesized using Hyssopus Officinalis L. Extract Induced oxidative stress and changes the expression of key genes involved in inflammatory and antioxidant Systems. Biological research, 55(1), 24. https://doi.org/10.1186/s40659-022-00392-4
[14]. Siddiqi, K. S., Ur Rahman, A., Tajuddin, & Husen, A. (2018). Properties of Zinc Oxide Nanoparticles and Their Activity Against Microbes. Nanoscale research letters, 13(1), 141. https://doi.org/10.1186/s11671-018-2532-3
[15]. Jiang, J., Pi, J., & Cai, J. (2018). The Advancing of Zinc Oxide Nanoparticles for Biomedical Applications. Bioinorganic chemistry and applications, 2018, 1062562. https://doi.org/10.1155/2018/1062562
[16]. Xu, L., Wang, Y. Y., Huang, J., Chen, C. Y., Wang, Z. X., & Xie, H. (2020). Silver nanoparticles: Synthesis, medical applications and biosafety. Theranostics, 10(20), 8996–9031. https://doi.org/10.7150/thno.45413
[17]. Lee, S. H., & Jun, B. H. (2019). Silver Nanoparticles: Synthesis and Application for Nanomedicine. International journal of molecular sciences, 20(4), 865. https://doi.org/10.3390/ijms20040865
[18]. Iravani, S., Korbekandi, H., Mirmohammadi, S. V., & Zolfaghari, B. (2014). Synthesis of silver nanoparticles: chemical, physical and biological methods. Research in pharmaceutical sciences, 9(6), 385–406.
[19]. Kruis F.E., Fissan H., Rellinghaus B. Sintering and evaporation characteristics of gas-phase synthesis of size-selected PbS nanoparticles. Mater. Sci. Eng. B. 2000;69:329–334. doi: 10.1016/S0921-5107(99)00298-6.
[20]. Jung J.H., Oh H.C., Noh H.S., Ji J.H., Kim S.S. Metal nanoparticle generation using a small ceramic heater with a local heating area. J. Aerosol. Sci. 2006;37:1662–1670. doi: 10.1016/j.jaerosci.2006.09.002.
[21]. Chen Y.-H., Yeh C.-S. Laser ablation method: Use of surfactants to form the dispersed Ag nanoparticles. Colloids Surf. A. 2002;197:133–139. doi: 10.1016/S0927-7757(01)00854-8.
[22]. Kinnear C., Moore T.L., Rodriguez-Lorenzo L., Rothen-Rutishauser B., Petri-Fink A. Form follows function: Nanoparticle shape and its implications for nanomedicine. Chem. Rev. 2017;117:11476–11521. doi: 10.1021/acs.chemrev.7b00194.
[23]. Pillai Z.S., Kamat P.V. What factors control the size and shape of silver nanoparticles in the citrate ion reduction method? J. Phys. Chem. B. 2004;108:945–951. doi: 10.1021/jp037018r.
[24]. Turkevich J., Kim G. Palladium: Preparation and catalytic properties of

particles of uniform size. Science. 1970;169:873–879. doi: 10.1126/science.169.3948.873.

[25]. Turkevich J. Colloidal gold. Part I. Gold. Bull. 1985;18:86–91. doi: 10.1007/BF03214690.

[26]. Brust M., Walker M., Bethell D., Schiffrin D.J., Whyman R. Synthesis of thiol-derivatised gold nanoparticles in a two-phase liquid-liquid system. J. Chem. Soc. Chem. Commun. 1994:801–802. doi: 10.1039/C39940000801.

[27]. Dakal T.C., Kumar A., Majumdar R.S., Yadav V. Mechanistic basis of antimicrobial actions of silver nanoparticles. Front. Microbiol. 2016;7:1831. doi: 10.3389/fmicb.2016.01831.

[28]. Evanoff D.D., Jr., Chumanov G. Synthesis and optical properties of silver nanoparticles and arrays. Chem. Phys. Chem. 2005;6:1221–1231. doi: 10.1002/cphc.200500113.

[29]. Goulet P.J.G., Lennox R.B. New insights into Brust−Schiffrin metal nanoparticle synthesis. J. Am. Chem. Soc. 2010;132:9582–9584. doi: 10.1021/ja104011b.

[30]. Dong X., Ji X., Wu H., Zhao L., Li J., Yang W. Shape control of silver nanoparticles by stepwise citrate reduction. J. Phys. Chem. B. 2009;113:6573–6576. doi: 10.1021/jp900775b.

[31]. Bai J., Li Y., Du J., Wang S., Zheng J., Yang Q., Chen X. One-pot synthesis of polyacrylamide-gold nanocomposite. Mater. Chem. Phys. 2007;106:412–415. doi: 10.1016/j.matchemphys.2007.06.021.

[32]. Oliveira M.M., Ugarte D., Zanchet D., Zarbina A.J.G. Influence of synthetic parameters on the size, structure, and stability of dodecanethiol-stabilized silver nanoparticles. J. Colloid Interface Sci. 2005;292:429–435. doi: 10.1016/j.jcis.2005.05.068.

[33]. Xue C., Métraux G.S., Millstone J.E., Mirkin C.A. Mechanistic study of photomediated triangular silver nanoprism growth. J. Am. Chem. Soc. 2008;130:8337–8344. doi: 10.1021/ja8005258.

[34]. Fayaz A.M., Balaji K., Girilal M., Yadav R., Kalaichelvan P.T., Venketesan R. Biogenic synthesis of silver nanoparticles and their synergistic effect with antibiotics: A study against gram-positive and gram-negative bacteria. Nanomedicine. 2010;6:103–109. doi: 10.1016/j.nano.2009.04.006

[35]. Ahmed S., Ikram S. Silver nanoparticles: One pot green synthesis using Terminalia arjuna extract for biological application. J. Nanosci. Nanotechnol. 2015;6:1000309.

[36]. Klaus-Joerger T., Joerger R., Olsson E., Granqvist C.-G. Bacteria as workers in the living factory: Metal-accumulating bacteria and their potential for materials science. Trends. Biotechnol. 2001;19:15–20. doi: 10.1016/S0167-7799(00)01514-6.

[37]. Arokiyaraj S., Vincent S., Saravanan M., Lee Y., Oh Y.K., Kim K.H. Green synthesis of silver nanoparticles using Rheum palmatum root extract and their antibacterial activity against Staphylococcus aureus and Pseudomonas aeruginosa. Artif. Cells Nanomed. Biotechnol. 2016;45:372–379. doi: 10.3109/21691401.2016.1160403.

[38]. Patra S., Mukherjee S., KumarBarui A., Ganguly A., Sreedhar B., Patra C.R. Green synthesis, characterization of gold and silver nanoparticles and their potential application for cancer therapeutics. Mater. Sci. Eng. C. 2015;53:298–309. doi: 10.1016/j.msec.2015.04.048.

[39]. Gajbhiye M., Kesharwani J., Ingle A., Gade A., Rai M. Fungus-mediated synthesis of silver nanoparticles and their activity against pathogenic fungi in combination with fluconazole. Nanomedicine. 2009;5:382–386. doi: 10.1016/j.nano.2009.06.005.

[40]. Mukherjee P., Ahmad A., Mandal D., Senapati S., Sainkar S.R., Khan M.I., Parishcha R., Ajaykumar P.V., Alam M., Kumar R., et al. Fungus-mediated synthesis of silver nanoparticles and their immobilization in the Mycelial matrix: A novel biological approach to nanoparticle synthesis. Nano Lett. 2001;1:515–519. doi: 10.1021/nl0155274.

[41]. Rauwel P., Küünal S., Ferdov S., Rauwel E. A review on the green synthesis of silver nanoparticles and their morphologies studied via TEM. Adv. Mater. Sci. Eng. 2015;2015:682749. doi: 10.1155/2015/682749.

[42]. Lengke M.F., Fleet M.E., Southam G. Biosynthesis of silver nanoparticles by filamentous cyanobacteria from a silver (I) nitrate complex. Langmuir. 2007;27:2694–2699. doi: 10.1021/la0613124.

[43]. Kalimuthu K., Babu R.S., Venkataraman D., Bilal M., Gurunathan S. Biosynthesis of silver nanocrystals by Bacillus licheniformis. Colloids Surf. B Biointerfaces. 2008;65:150–153. doi: 10.1016/j.colsurfb.2008.02.018.

[44]. Kumar S.A., Abyaneh M.K., Gosavi S.W., Kulkarni S.K., Pasricha R., Ahmad A., Khan M.I. Nitrate reductase-mediated synthesis of silver nanoparticles from $AgNO_3$. Biotechnol. Lett. 2007;29:439–445. doi: 10.1007/s10529-006-9256-7.

[45]. Vaidyanathan R., Gopalram S., Kalishwaralal K., Deepak V., Ram S., Pandian K., Gurunathan S. Enhanced silver nanoparticle synthesis by optimization of nitrate reductase activity. Colloids Surf. B Biointerfaces. 2010;75:335–341. doi: 10.1016/j.colsurfb.2009.09.006.

[46]. Li G., He D., Qian Y., Guan B., Gao S., Cui Y., Yokoyama K., Wang L. Fungus-mediated green synthesis of silver nanoparticles using Aspergillus terreus. Int. J. Mol. Sci. 2012;13:466–476. doi: 10.3390/ijms13010466.

[47]. Chen H.-Y., Lin M.-H., Wang C.-Y., Chang Y.-M., Gwo S. Large-scale hot spot engineering for quantitative SERS at the single-molecule scale. J. Am. Chem. Soc. 2015;137:13698–13705. doi: 10.1021/jacs.5b09111.

[48]. Sun H.-B., Fu C., Xia Y.-J., Zhang C.-W., Du J.-H., Yang W.-C., Guo P.-F., Xu J.-Q., Wang C.-L., Jia Y.-L. Enhanced Raman scattering of graphene by silver nanoparticles with different densities and locations. Mater. Res. Express. 2017;4:025012. doi: 10.1088/2053-1591/aa59e5.

[49]. Lai C.-H., Wang G.-A., Ling T.-K., Wang T.-J., Chiu P.-K., Chau C.Y.-F., Huang C.-C., Chiang H.-P. Near infrared surface-enhanced Raman scattering based on starshaped gold/silver nanoparticles and hyperbolic metamaterial. Sci. Rep. 2017;7:5546. doi: 10.1038/s41598-017-05939-0.

[50]. Mulvaney S.P., Musick M.D., Keating C.D., Natan M.J. Glass-coated, analyte-tagged nanoparticles: A new tagging system based on detection with surface-enhanced raman scattering. Langmuir. 2003;19:4784–4790. doi: 10.1021/la026706j.

[51]. Doering W.E., Piotti M.E., Natan M.J., Freeman R.G. SERS as a foundation for nanoscale, optically detected biological labels. Adv. Mater. 2007;19:3100–3108. doi: 10.1002/adma.200701984.

[52]. Loo C., Lowery A., Halas N., West J., Drezek R. Immunotargetednanoshells for integrated cancer imaging and therapy. Nano Lett. 2005;5:709–711. doi: 10.1021/nl050127s.

[53]. Kang H., Jeong S., Park Y., Yim J., Jun B.-H., Kyeong S., Yang J.-K., Kim G., Hong S., Lee L.P., et al. Near-infrared SERS nanoprobes with plasmonic Au/Ag hollow-shell assemblies for in vivo multiplex detection. Adv. Funct. Mater. 2013;23:3719–3727. doi: 10.1002/adfm.201203726.

[54]. Kelkar S.S., Reineke T.M. Theranostics: Combining imaging and therapy. Bioconjug. Chem. 2011;22:1879–1903. doi: 10.1021/bc200151q. 102. Jun B.H., Noh M.S., Kim J., Kim G., Kang H., Kim M.S., Seo Y.T., Baek J., Kim J.H., Park J., et al. Multifunctional silver-embedded magnetic nanoparticles as SERS nanoprobes and their applications. Small. 2010;6:119–125. doi: 10.1002/smll.200901459.

[55]. Hu M., Ghoshal A., Marquez M., Kik P.G. Single particle spectroscopy study of metal-film-induced tuning of silver nanoparticle plasmon resonances. J. Phys. Chem. C. 2010;114:7509–7514. doi: 10.1021/jp911416a.

[56]. Ardini M., Huang J.-A., Sánchez C.S., Mousavi M.Z., Caprettini V., Maccaferri N., Melle G., Bruno G., Pasquale L.,

International Journal of Pharmaceutical Research and Applications
Volume 9, Issue 3 May-June 2024, pp: 437-493 www.ijprajournal.com ISSN: 2456-4494

Garoli D., et al. Live intracellular biorthogonal imaging by surface enhanced raman spectroscopy. Sci. Rep. 2018;8:12652.

[57]. Yen C.-W., de Puig H., Tam J., Gómez-Márquez J., Bosch I., Hamad-Schifferli K., Gehrkea L. Multicolored silver nanoparticles for multiplexed disease diagnostics: Distinguishing dengue, yellow fever, and ebola viruses. Lab Chip. 2015;15:1638–1641. doi: 10.1039/C5LC00055F.

[58]. Liu J., Wang Z., Liu F.D., Kane A.B., Hurt R.H. Chemical transformations of nanosilver in biological environment. ACS Nano. 2012;6:9887–9899. doi: 10.1021/nn303449n.

[59]. Zhou W., Ma Y., Yang H., Ding Y., Luo X. A label-free biosensor based on silver nanoparticles array for clinical detection of serum p53 in head and neck squamous cell carcinoma. Int. J. Nanomed. 2011;6:381–386. doi: 10.2147/IJN.S13249.

[60]. Zhang F., Braun G.B., Shi Y., Zhang Y., Sun X., Reich N.O., Zhao D., Stucky G. Fabrication of Ag@SiO2@Y_2O_3:Er nanostructures for bioimaging: Tuning of the upconversion fluorescence with silver nanoparticles. J. Am. Chem. Soc. 2010;132:2850–2851. doi: 10.1021/ja909108x.

[61]. Zhang H, Tian J, Yan L, Zhou S, Liang M, Zou H. Improving the Ablation Properties of Liquid Silicone Rubber Composites by Incorporating Hexaphenoxycyclotriphosphonitrile. Nano materials. 2023; 13(3):563. https://doi.org/10.3390/nano13030563

[62]. Jian Li, Ning Li, Yuanyuan Zheng, Dongyang Lou, Yue Jiang, Jiaxi Jiang, Qunhui Xu, Jing Yang, Yujing Sun, Chuxuan Pan, Jianlan Wang, Zhengchun Peng, Zhikun Zheng, Wei Liu, Interfacially Locked Metal Aerogel Inside Porous Polymer Composite for Sensitive and Durable Flexible Piezoresistive Sensors, Advanced Science, 10.1002/advs.202201912, 9, 23, (2022).

[63]. Ibraheem, D. R., Hussein, N. N., Sulaiman, G. M., Mohammed, H. A., Khan, R. A., & Al Rugaie, O. (2022). Ciprofloxacin-Loaded Silver Nanoparticles as Potent Nano-Antibiotics against Resistant Pathogenic Bacteria. Nanomaterials (Basel, Switzerland), 12(16), 2808. https://doi.org/10.3390/nano12162808

[64]. Mohsen, E., El-Borady, O. M., Mohamed, M. B., & Fahim, I. S. (2020). Synthesis and characterization of ciprofloxacin loaded silver nanoparticles and investigation of their antibacterial effect. Journal of Radiation Research and Applied Sciences, 13(1), 416-425.

[65]. Ma, J., Huang, D., Tian, Y., Yang, H., Chen, X., Xu, B., ... & Li, Y. (2022). Separation and recovery of tin and copper from tin refining sulfur slag using a new process of airtight sulfuration–Vacuum distillation. Journal of Cleaner Production, 378, 134553.

[66]. Shariati, A., Arshadi, M., Khosrojerdi, M. A., Abedinzadeh, M., Ganjalishahi, M., Maleki, A., ... &Khoshnood, S. (2022). The resistance mechanisms of bacteria against ciprofloxacin and new approaches for enhancing the efficacy of this antibiotic. Frontiers in Public Health, 10, 1025633.

[67]. Khalil, H. A., Yahya, E. B., Jummaat, F., Adnan, A. S., Olaiya, N. G., Rizal, S., ... & Thomas, S. (2022). Biopolymers based aerogels: A review on revolutionary solutions for smart therapeutics delivery. Progress in Materials Science, 101014.

[68]. Oudi, S., Oveisi, A. R., Daliran, S., Khajeh, M., &Teymoori, E. (2020). Brønsted-Lewis dual acid sites in a chromium-based metal-organic framework for cooperative catalysis: Highly efficient synthesis of quinazolin-(4H)-1-one derivatives. Journal of colloid and interface science, 561, 782-792.

[69]. Mahesha, C. R., Suprabha, R., Harne, M. S., Galme, S. G., Thorat, S. G., Nagabhooshanam, N., ... & Markos, M. (2022). Nanotitanium Oxide Particles and Jute-Hemp Fiber Hybrid Composites: Evaluate the Mechanical, Water Absorptions, and Morphological Behaviors. Journal of Nanomaterials, 2022.

[70]. Sonowal, S., JOSHI, S. J., BORAH, S. N., ISLAM, N. F., PANDIT, S., PRASAD, R., & SARMA, H. (2022). Biosurfactant-assisted phytoremediation of potentially toxic elements in soil: Green technology for meeting the United Nations Sustainable Development Goals. Pedosphere, 32(1), 198-210.

[71]. Harrop, E. N., Mensinger, J. L., Moore, M., & Lindhorst, T. (2021). Restrictive eating disorders in higher weight persons: A systematic review of atypical anorexia nervosa prevalence and consecutive admission literature. International Journal of Eating Disorders, 54(8), 1328-1357.

[72]. Issa, S. A., Zakaly, H. M., Pyshkina, M., Mostafa, M. Y., Rashad, M., & Soliman, T. S. (2021). Structure, optical, and radiation shielding properties of PVA–BaTiO3 nanocomposite films: An experimental investigation. Radiation Physics and Chemistry, 180, 109281.

[73]. Hosseini Monjezi, B., Kutonova, K., Tsotsalas, M., Henke, S., & Knebel, A. (2021). Current trends in metal–organic and covalent organic framework membrane materials. AngewandteChemie International Edition, 60(28), 15153-15164.

[74]. Zhu, N., Li, G., Zhou, J., Zhang, Y., Kang, K., Ying, B., ... & Wu, Y. (2021). A light-up fluorescence resonance energy transfer magnetic aptamer-sensor for ultra-sensitive lung cancer exosome detection. Journal of Materials Chemistry B, 9(10), 2483-2493.

[75]. Vanchinathan, K., Valluvan, K. R., Gnanavel, C., Gokul, C., & Albert, J. R. (2021). An improved incipient whale optimization algorithm based robust fault detection and diagnosis for sensorless brushless DC motor drive under external disturbances. International Transactions on Electrical Energy Systems, 31(12), e13251.

[76]. Gradinaru, L. M., BarbalataMandru, M., Drobota, M., Aflori, M., Butnaru, M., Spiridon, M., ... & Vlad, S. (2021). Composite materials based on iron oxide nanoparticles and polyurethane for improving the quality of MRI. Polymers, 13(24), 4316.

[77]. Albalawi, F., Hussein, M. Z., Fakurazi, S., &Masarudin, M. J. (2021). Engineered nanomaterials: The challenges and opportunities for nanomedicines. International Journal of Nanomedicine, 16, 161.

[78]. Guermazi, A., Tannoury, C., Kompel, A. J., Murakami, A. M., Ducarouge, A., Gillibert, A., ... & Hayashi, D. (2022). Improving radiographic fracture recognition performance and efficiency using artificial intelligence. Radiology, 302(3), 627-636.

[79]. Siddiqi, K. S., Husen, A., & Rao, R. A. (2018). A review on biosynthesis of silver nanoparticles and their biocidal properties. Journal of nanobiotechnology, 16(1), 1-28.

[80]. Chen, S., Huang, D., Zeng, G., Xue, W., Lei, L., Xu, P., ... & Cheng, M. (2020). In-situ synthesis of facet-dependent BiVO4/Ag3PO4/PANI photocatalyst with enhanced visible-light-induced photocatalytic degradation performance: synergism of interfacial coupling and hole-transfer. Chemical Engineering Journal, 382, 122840.

[81]. Oh, D. K., Lee, S., Lee, S. H., Lee, W., Yeon, G., Lee, N., ... & Ok, J. G. (2019). Tailored nanopatterning by controlled continuous nanoinscribing with tunable shape, depth, and dimension. ACS nano, 13(10), 11194-11202.

[82]. Iravani, S. (2014). Bacteria in nanoparticle synthesis: current status and future prospects. International scholarly research notices, 2014.

[83]. Quéré, C., Andrew, R. M., Friedlingstein, P., Sitch, S., Hauck, J., Pongratz, J., ... & Zheng, B. (2018). Global carbon budget 2018. Earth System Science Data.

[84]. Cho, K. M., & Khaing, A. T. BIOSYNTHESIS OF ZINC OXIDE NANOPARTICLESUSING CALOTROPIS GIGANTEAL.(MA-YO-GYI), CHARACTERIZATION AND ANTIMICROBIAL ACTIVITIES.

[85]. Han, X. D., Tian, X. L., Yu, W. H., Xiang, S. K., Hu, P., Wang, B. Q., ... & Feng, C. (2017). Influence of peripheral alkyl chain length on the mesomorphic behaviours of hexasubstituted triphenylene 2, 3-

dicarboxylic esters. Liquid Crystals, 44(11), 1727-1738.

[86]. Ayon, S. A., Hasan, S., Billah, M. M., Nishat, S. S., & Kabir, A. (2022). Improved luminescence and photocatalytic properties of Sm3+-doped ZnO nanoparticles via modified sol–gel route: A unified experimental and DFT+ U approach. Journal of Rare Earths.

[87]. Rehman, R., Raza, A., Noor, W., Batool, A., & Maryem, H. (2021). Photocatalytic degradation of alizarin red S, amaranth, Congo red, and rhodamine B dyes using UV light modified reactor and ZnO, TiO2, and SnO2 as catalyst. Journal of Chemistry, 2021, 1-9.

[88]. Yayehrad, A. T., Wondie, G. B., & Marew, T. (2022). Different nanotechnology approaches for ciprofloxacin delivery against multidrug-resistant microbes. Infection and Drug Resistance, 413-426.

[89]. Fonseca, B. B., Silva, P. L. A. P. A., Silva, A. C. A., Dantas, N. O., De Paula, A. T., Olivieri, O. C. L., ... & Goulart, L. R. (2019). Nanocomposite of Ag-Doped ZnO and AgO nanocrystals as a preventive measure to control biofilm formation in eggshell and salmonella spp. Entry into eggs. Frontiers in microbiology, 10, 217.

[90]. Kruawan K, Kangsadalampai K. Antioxidant activity, phenolic compound contents and antimutagenic activity of some water extract of herbs. Thai J Pharm Sci. 2006;30:28–35.

[91]. Shinwari ZK, Qaiser M. Efforts on conservation and sustainable use of medicinal plants of Pakistan. Pak. J. Bot. 43(1), 5–10 (2011).

[92]. Li R-J, Gao C-Y, Guo C, Zhou M-M, Luo J, Kong L-Y. The anti-inflammatory activities of two major withanolides from Physalis minima via acting on NF-κB, STAT3, and HO-1 in LPS-stimulated RAW264.7 cells. Inflammation 40(2), 401–413 (2017).

[93]. Süntar I. Importance of ethnopharmacological studies in drug discovery: role of medicinal plants. Phytochem. Rev. 19(5), 1199–1209 (2020).

[94]. Katiyar C, Kanjilal S, Gupta A, Katiyar S. Drug discovery from plant sources: an integrated approach. AYU (An Int. Q. J. Res. Ayurveda) 33(1), 10 (2012).

[95]. Lahlou M. The success of natural products in drug discovery. Pharmacol. Pharm. 4(3A), 15 (2013).

[96]. Vuorela P, Leinonen M, Saikku P et al. Natural Products in the Process of Finding New Drug Candidates. Curr. Med. Chem. 11(11), 1375–1389 (2004).

[97]. Rates SM. Plants as source of drugs. Toxicon 39(5), 603–613 (2001).

[98]. Appelhans MS, Bayly MJ, Heslewood MM et al. A new subfamily classification of the Citrus family (Rutaceae) based on six nuclear and plastid markers. Taxon 70(5), 1035–1061 (2021).

[99]. Gupta AK, Tandon N. Reviews on Indian medicinal plants. Indian Council of Medical Research, New Delhi, India: 1, 312 (2004).

[100]. Badal S, Delgoda R. Pharmacognosy fundamentals, applications and statergy. Academic Press, London, UK: (2016).

[101]. Boy HIA, Rutilla AJH, Santos KA et al. Recommended medicinal plants as source of natural products: a Review. Digit. Chinese Med. 1(2), 131–142 (2018).

[102]. Soumya Prakash Rout, Choudary KA, Kar DM, Das L, Jain A. Plants in traditional medicinal system - future source of new drugs. International J. Pharm. Pharm. Sci. 1(1), 1–23 (2009).

[103]. Gerardo Aguirre, Araceli Salgado-Rodríguez, Lucía Z Flores-López, MP-H y Ratnasamy Somanathan. Asymmetric Synthesis of Naturally Occurring β-Hydroxyamides (R)-Tembamide and (R)-Aegeline. J Mex. Chem Soc. 45, 21–24 (2001).

[104]. Kaur, A.; Preet, S.; Kumar, V.; Kumar, R.; Kumar, R. Synergetic effect of vancomycin-loaded silver nanoparticles for enhanced antibacterial activity. Colloids Surf. B Biointerfaces 2019, 176, 62–69.

[105]. Deng, H.; McShan, D.; Zhang, Y.; Sinha, S.S.; Arslan, Z.; Ray, P.C.; Yu, H. Mechanistic study of the synergistic antibacterial activity of combined silver nanoparticles and common

antibiotics. Environ. Sci. Technol. 2016, 50, 8840–8848.
[106]. Aisida, S.O.; Ugwu, K.; Akpa, P.A.; Nwanya, A.C.; Nwankwo, U.; Botha, S.S.; Ezema, F.I. Biosynthesis of silver nanoparticles using bitter leave (Veronica amygdalina) for antibacterial activities. Surf. Interfaces 2019, 17, 100359.
[107]. Shevtsova, T.; Cavallaro, G.; Lazzara, G.; Milioto, S.; Donchak, V.; Harhay, K.; Korolko, S.; Budkowski, A.; Stetsyshyn, Y. Temperature-responsive hybrid nanomaterials based on modified halloysite nanotubes uploaded with silver nanoparticles. Colloids Surf. A Physicochem. Eng. Asp. 2022, 641, 128525.
[108]. Thomas, R.; Jishma, P.; Snigdha, S.; Soumya, K.R.; Mathew, J.; Radhakrishnan, E.K. Enhanced antimicrobial efficacy of biosynthesized silver nanoparticle-based antibiotic conjugates. Inorg. Chem. Commun. 2020, 117, 107978.
[109]. Pellegrino, D. Antioxidants and cardiovascular risk factors. Diseases 2016, 4, 11.
[110]. Mohanta, Y.K.; Nayak, D.; Biswas, K.; Singdevsachan, S.K.; Abd_Allah, E.F.; Hashem, A.; Mohanta, T.K. Silver nanoparticles synthesized using wild mushroom show potential antimicrobial activities against food borne pathogens. Molecules 2018, 23, 655.
[111]. Reidy, B.; Haase, A.; Luch, A.; Dawson, K.A.; Lynch, I. Mechanisms of silver nanoparticle release, transformation and toxicity: A critical review of current knowledge and recommendations for future studies and applications. Materials 2013, 6, 2295–2350.
[112]. Prakash, N.; Sadaf, M.; Salomi, A.; Daniel, E.C. Cytotoxicity of functionalized iron oxide nanoparticles coated with rifampicin and tetracycline hydrochloride on Escherichia coli and Staphylococcus aureus. Appl. Nanosci. 2019, 9, 1353–1366.
[113]. Abbara, W.K.; Ramadan, W.H.; Rahbany, P.; Al-Natour, S. Evaluation of the appropriate use of commonly prescribed fluoroquinolones and the risk of dysglycemia. Ther. Clin. Risk Manag. 2015, 11, 639–647.
[114]. Rezvanian, M.; Tan, C.K.; Ng, S.F. Simvastatin-loaded lyophilized wafers as a potential dressing for chronic wounds. Drug Dev. Ind. Pharm. 2016, 42, 2055–2062.
[115]. Giguère, S.; Dowling, P.M. Fluoroquinolones. In Antimicrobial Therapy in Veterinary Medicine; John Wiley & Sons, Inc.: Hoboken, NJ, USA, 2013; pp. 295–314.
[116]. Naqvi, S.Z.H.; Kiran, U.; Ali, M.I.; Jamal, A.; Hameed, A.; Ahmed, S.; Ali, N. Combined efficacy of biologically synthesized silver nanoparticles and different antibiotics against multidrug-resistant bacteria. Int. J. Nanomed. 2013, 8, 3187.
[117]. Huang, L.; Liu, M.; Huang, H.; Wen, Y.; Zhang, X.; Wei, Y. Recent advances and progress on melanin-like materials and their biomedical applications. Biomacromolecules 2018, 19 , 1858–1868.
[118]. Kuskov, A.N.; Kulikov, P.P.; Goryachaya, A.V.; Tzatzarakis, M.N.; Docea, A.O.; Velonia, K.; Tsatsakis, A.M. Amphiphilic poly-N-vinylpyrrolidone nanoparticles as carriers for non-steroidal, anti-inflammatory drugs: In vitro cytotoxicity and in vivo acute toxicity study. Nanomed. Nanotechnol. Biol. Med. 2017, 13, 1021–1030.
[119]. Mandal, A.; Meda, V.; Zhang, W.J.; Farhan, K.M.; Gnanamani, A. Synthesis, characterization and comparison of antimicrobial activity of PEG/TritonX-100 capped silver nanoparticles on collagen scaffold. Colloids Surf. B Biointerfaces 2012, 90, 191–196.
[120]. Mohsen, E.; El-Borady, O.M.; Mohamed, M.B.; Fahim, I.S. Synthesis and characterization of ciprofloxacin-loaded silver nanoparticles and investigation of their antibacterial effect. J. Radiat. Res. Appl. Sci.